UNIVERSIDADE FEDERAL DO PARÁ
CENTRO DE GEOCIÊNCIAS
CURSO DE PÓS-GRADUAÇÃO EM GEOLOGIA E GEOQUÍMICA

FÁCIES, PETROGRAFIA E GEOQUÍMICA DA FORMAÇÃO CODÓ, NEO-APTIANO, BACIA DE SÃO LUÍS-GRAJAÚ

TESE APRESENTADA POR

JACKSON DOUGLAS SILVA DA PAZ

Como requisito parcial à obtenção do Grau de Doutor em Ciências na área de GEOLOGIA

DATA DA APROVAÇÃO:
COMITÊ DE TESE:

____
DILCE DE FÁTIMA ROSSETTI
(ORIENTADORA)

____
MOACIR JOSÉ BUENANO MACAMBIRA
(CO-ORIENTADOR)

____
ALCIDES NÓBREGA SIAL

____
ANA MARIA GÓES

____
VIRGÍNIO NEUMANN

____
WERNER TRUCKENBRODT

Belém - 2005

À Nazaré

AGRADECIMENTOS

À Dilce de Fátima Rossetti, para quem eu não tenho palavras suficientes para expressar toda a minha gratidão, afeto e admiração;

Ao Prof. Moacir Macambira, pela amizade e pela co-orientação em todas as etapas dentro do Laboratório de Geocronologia da UFPA;

Ao CNPq pela concessão da bolsa de estudo;

Ao Grupo Itapicuru Agro-Industrial S/A pela colaboração e pela liberdade que nos foi concedida de acessar as minas exploradas por esta companhia nos arredores do Município de Codó;

Ao Grupo Mineradora Vale do Grajaú S/A pela atenção e pela liberdade concedidas para observar as minas exploradas por esta empresa na região do Município de Grajaú;

À hospitalidade do povo tanto de Codó quanto de Grajaú, onde sempre fomos bem recebidos. Em especial, às Sras. D. Gonçala e D. Edite, donas das pousadas que nos receberam muito cordialmente neste trabalho durante as etapas de campo, e à D. Fátima, cuja comida foi um alento durante estas etapas;

Ao Museu Paraense Emílio Goeldi pela infra-estrutura concedida durante os vários anos deste trabalho;

À Universidade Federal do Pará, ao Centro de Geociências e ao Curso de Pós-Graduação em Geologia e Geoquímica, pela infra-estrutura, pelo pessoal e pela organização que me auxiliaram muito neste trabalho;

À Coordenação do Curso de Pós-Graduação em Geologia e Geoquímica, nas pessoas do seu atual coordenador Prof. Dr. Cândido Veloso, do antigo coordenador Prof. Dr. Paulo Gorayeb e das secretarias Gladys Pimentel e Cleidiane Caldeira, pela atenção e competência que dispensaram a mim em todas as etapas deste trabalho;

À comissão que formou a banca examinadora desta tese: à Dra. Ana Maria Góes, amiga de todos, membro do nosso grupo de pesquisa em geologia histórica e sedimentar (GSED) e por quem nossa admiração vai além da geologia; ao Dr. Werner Truckenbrodt, pela paciência com que tentou melhorar cada aspecto dos mais variados textos relacionados com este trabalho, durante os anos em que trabalhei ao seu lado; ao Dr. Alcides Nóbrega Sial, cujo apoio foi fundamental na execução da parte deste trabalho relacionada aos isótopos estáveis; e ao Dr. Virgínio Neumann, que acreditou neste trabalho de imediato, sabendo que seria difícil mas executável no prazo exigido;

Ao Grupo de Geologia Histórica e Sedimentar (GSED) do Museu Goeldi e Universidade Federal do Pará, em especial aos estudantes do grupo que sempre estiveram um ao lado do outro a fim de ajudar da melhor forma possível: Emídio, Carol Miranda, Daniele, Marivaldo, Anderson, Leandro, Hebérton, Cristovam, Leonardo, Denis, Sue Anne, Samanta e Paulinha;

Ao Laboratório de Isótopos Estáveis do Núcleo de Estudos de Granitos da Universidade Federal de Pernambuco (LABISE/NEG/UFPE), nas pessoas da Profa. Dra. Valderez Ferreira, que além disso foi extremamente atenciosa com este trabalho quando da minha estadia no LABISE, auxiliando-me totalmente na parte de análise elementar com fluorescência de raios-X; à Silvana Diene Barros, pela amizade, pelo amor e pelo carinho mútuos; Roberta Brasilino, pela amizade e carinho recebidos na sua casa e de Xuxxu; à Gilsa, pela experiência compartilhada na separação química de C e O; e, de novo, ao Prof. Sial, pela paciência e atenção com que me recebeu em seu laboratório.

Ao Laboratório de Geocronologia e Isótopos Estáveis da Universidade Federal do Pará (Pará-Iso/UFPA), nas pessoas do Prof. Dr. Moacir Macambira, das Químicas Rose Brabo, Roberta e da estudante Gilmara, pela atenção despendida com meu trabalho e pelo auxílio na execução das etapas mais difíceis;

Ao Laboratório de Geoquímica Orgânica da Universidade Estadual do Rio de Janeiro, nas pessoas do Prof. Dr. René Rodrigues, do Químico Luis Freixo e da secretária Sra. Rosalva, pela ajuda dispensada durante a minha estadia naquele laboratório;

Ao pessoal técnico do Laboratório de Laminação do Centro de Geociências, cujos técnicos Sra. Shirley Tavares, Sr. Eduardo Soares e Sr. Israel Tavares, eu sou muito grato pela franca amizade, e ao Laboratório de Sedimentologia do Centro de Geociências, na pessoa do Sr. Antônio Lopes, pela amizade e paciência. Todos com atenção e cuidado no trato deste trabalho;

Ao pessoal da Coordenação de Ciências da Terra do Museu Paraense Emílio Goeldi, nas pessoas do Chico, Cristina, Márcia, Cléia, Paulo, Hudson, Maria Tereza, Amílcar, Josué e D. Maria, pelo companheirismo compartilhado nestes anos;

Ao pessoal de transporte do Museu Goeldi, pela amizade nas duras etapas de campo:

Aos meus amigos Braga e Paulo Benevides e suas famílias pela amizade e cordialidade em me receber durante a minha estadia na sua cidade, realizando etapas deste trabalho;

Aos amigos mais de perto, daqui de Belém, Leonilde, D. Siroca e Seu Joca, Leonete, Leonora, Vante, Paulinho, Veruska, Angelina e a toda a família Aviz, pelo bem-querer como a de um membro da família;

Ao amigos próximos Erimar, Vanderlei, Cláudia e Heloísa, que são amigos de todas as horas;

E aos amigos distantes Eisner, Elias, Izaías, Naná, Roseane, Douglas e Ana Maria, que são amigos para sempre.

À minha família, mais perto, Naíde, Élson, Everton, Felipe, Chico e todos os outros mais longe;

À minha mãe...

Aos meus irmãos Jailton, Derimar e Janderson ...

À Leninha...

MUITO OBRIGADO!

O Lago

Eu não vi o mar.
Não sei se o mar é bonito,
não sei se ele é bravo.
O mar não me importa.

Eu vi o lago.
O lago, sim.
O lago é grande
E calmo também.

Na chuva de cores
da tarde que explode
o lago brilha
o lago se pinta
de todas as cores.
Eu não vi o mar. Eu vi o lago...

(Corrompido a partir de Carlos Drummond de Andrade... no original “A lagoa”).

SUMÁRIO

LISTA DE FIGURAS

RESUMO

A Formação Codó, objeto deste estudo, corresponde a uma unidade geológica neoaptiana bem conhecida por ser o único registro exposto de rochas desta idade na margem equatorial brasileira. Esta formação, constituída de folhelhos betuminosos, calcários e evaporitos, é particularmente bem exposta nas bordas sul e leste da Bacia de São Luís-Grajaú, MA, áreas aqui investigadas com o intuito: 1. de aprimorar o entendimento do sistema deposicional, discutindo-se a hipótese de formação em ambientes lacustres; e 2. reconstituir as condições paleohidrológicas com base na integração de dados faciológicos, estratigráficos, petrográficos e isotópicos (C, O, Sr e S). Os dados de campo confirmaram sistema lacustre para a área de Codó, onde se desenvolveram lagos salinos, estáveis, bem estratificados, e com períodos de fechamento, quando prevaleceram condições anóxicas acompanhadas pela precipitação de sais em subambientes de lago central. Na região de Grajaú, por outro lado, prevaleceram condições mais efêmeras, com desenvolvimento de complexo de *sabkha*/*saline pan*, e precipitação de evaporitos principalmente nas margens do sistema, sob condições de salinas marginais e de planícies lamosas.

Os estudos faciológico e estratigráfico mostraram, também, que a Formação Codó em ambas as áreas estudadas está organizada em ciclos de arrasamento ascendente, que registram a progradação de depósitos de lago marginal sobre os de lago central. Três categorias de ciclos foram distinguidos, designados aqui de inferior, intermediário, e superior. Os ciclos de ordem inferior, de espessuras variando entre milímetros a poucos centímetros, são formados por depósitos com acamamentos constituídos de um dos seguintes arranjos litológicos: a) folhelho negro betuminoso e evaporito; b) folhelho negro betuminoso e *calcimudstone*; c) folhelho negro betuminoso e *packstone*-*wackestone* peloidal; d) folhelho cinza-esverdeado e *calcimudstone*; e) folhelho cinza-esverdeado e *packstone*-*wackestone* peloidal; f) folhelho cinza-esverdeado e *packstone*-*wackestone* ostracodal; ou g) g*rainstone*-*wackestone* ostracodal e/ou *calcimudstone* com tapetes criptomicrobiais e *packstone* ooidal-pisoidal. Estes ciclos são atribuídos a depósitos sazonais, tendo em vista as suas espessuras regulares na escala milimétrica, típicas de depósitos climaticamente controlados.

Os ciclos de ordem intermediária têm, em média, 1,7 m de espessura e são subdivididos por ciclos completos e incompletos. Ciclos completos são compostos de

depósitos de lago central, que gradam para acima a depósitos de lago intermediário e marginal, sendo representados por dois tipos: ciclos com depósitos de lago central, constituídos por folhelhos e evaporitos (C1); e ciclos com depósitos de lago central, constituídos por folhelho cinza esverdeado (C2). Ciclos incompletos são formados por sucessões faciológicas onde pelo menos uma das associações de fácies está ausente. São também de dois tipos: ciclos com depósitos de lago central e intermediário (I1); e ciclos com depósitos de fácies de lago intermediário e central (I2).

Os ciclos de ordem superior medem, em média, 5,2 m de espessura e consistem em quatro unidades deposicionais, limitadas por superfícies de descontinuidade, sendo internamente constituídas por ciclos intermediários, tanto completos quanto incompletos, e de distribuição variável em direção ao topo das seções. A unidade 1, mais inferior, está apenas parcialmente exposta, com 2,7 m de espessura em média, sendo formada por um intervalo constituído por ciclos I1 delgados. A unidade 2 tem, em média, 5,2 m de espessura e contem todos os tipos de ciclos, principalmente ciclos completos. A unidade 3, com 2,6 m de espessura em média, é constituída por quase 80% de ciclos I2. A unidade 4 apresenta 2,2 m de espessura média, inclui exclusivamente ciclos incompletos, embora a maior parte desta unidade tenha sido destruída pela formação do limite da seqüência aptiana.

A caracterização sedimentar detalhada e o padrão de empilhamento dos ciclos de ordens intermediária e superior suportam gênese ligada à atividade tectônica sin-sedimentar. Isto é particularmente sugerido pela alta variabilidade de fácies, pela extensão lateral limitada, e por mudanças aleatórias na espessura e freqüência dos ciclos de ordem intermediária. Além disto, os quatro ciclos de ordem superior são correlacionáveis com zonas estratigráficas apresentando diferentes estilos de estruturas de deformação sin-sedimentar, atribuídos em trabalhos anteriores a atividades sísmicas sin-deposicionais. Portanto, os vários episódios de arrasamento do lago, registrados na Formação Codó pelos ciclos de ordem intermediária e superior, são atribuídos a flutuações no nível de água do lago promovidas por pulsos sísmicos contemporâneos à sedimentação.

A análise petrográfica dos evaporitos da Formação Codó permitiu que se definissem melhor as histórias tanto deposicional do sistema lago-*sabkha-saline pan,* quanto pós-deposicional. Sete morfologias de evaporitos foram reconhecidas: 1. gipso *en chevron*; 2. gipso/anidrita nodular/lenticular; 3. gipso acicular; 4. gipso em mosaico; 5. gipso brechóide/gipsarenito; 6. gipso/anidrita pseudo-nodular; e 7. gipso em roseta. A despeito desta ampla variedade de fases, a abundância de gipso *en chevron*, gipso/anidrita nodular/lenticular e gipso brechóide/gipsarenito, registra a boa preservação de formas primárias. Esta interpretação é suportada pela associação destas morfologias de gipso com depósitos mostrando acamamento horizontal de natureza cíclica, que são atribuídos a flutuações do nível de base do lago, eventualmente culminadas com períodos de exposição subaérea. Mesmo o gipso acicular e o gipso em mosaico, interpretados como produtos de substituição do gipso *en chevron* e do gipso brechóide/gipsarenito, mostram características de formação autigência ainda sob influência do ambiente deposicional. Fases de formação de gipso sob condições diagenéticas mais profundas são registradas somente no gipso/anidrita pseudo-nodular, atribuídos a mobilizações durante halocinese. Além disto, gipso em rosetas, que interceptam todas as outras fases evaporíticas, têm também origem diagenética ligada a processos tardios por interação com água subterrânea e/ou intemperismo superficial.

A constatação de forte influência deposicional registrada em, pelo menos, grande parte das morfologias dos evaporitos da Formação Codó (i.e., gipso primário ou eodiagenético), além da constatação de microfácies carbonáticas com poucas modificações diagenéticas, motivaram a aplicação de métodos isotópicos com propósitos de reconstituição paleoambiental. Os resultados obtidos mostram que ciclos de expansão/contração do sistema deposicional em ambas as áreas estudadas são acompanhadas por variações significativas nos valores isotópicos. A ampla dispersão de valores dos isótopos de Sr e S dentro de cada ciclo deposicional reforça a interpretação petrográfica de que a diagênese não modificou a assinatura geoquímica deposicional dos evaporitos, confirmando seu valor como ferramenta paleoambiental. Além disto, origem não marinha para os evaporitos é sugerida pelas razões $^{87}Sr/^{86}Sr$, que variaram de 0,70782 a 0,70928, consideradas mais altas do que aquelas esperadas para evaporitos oriundos da água do mar no Neo-Aptiano (entre 0,70720 e 0,70735). O $\delta^{34}S$ variou nas amostras estudadas de 16.12‰ to 17.89 ‰ $_{(V\text{-}CDT)}$ na região de Codó, mostrando-se também em total desarmonia com valores marinhos do Neo-Aptiano (i.e., entre 13‰ e 16‰ $_{(V\text{-}CDT)}$). Tanto Sr quanto S foram influenciados pelas características das fácies deposicionais, de tal forma que, durante a expansão do sistema deposicional, os valores de $^{87}Sr/^{86}Sr$ decresceram devido à inibição do ^{87}Sr liberado a partir de argilominerais pela drenagem interna de planícies lamosas. Nos picos de expansão, os valores de $^{87}Sr/^{86}Sr$ eram os mais baixos, o que é relacionado à submergência de planícies lamosas e introdução de águas depletadas em ^{87}Sr oriundo do intemperismo de calcários e evaporitos marinhos permianos a neocomianos, tanto quanto basaltos triássicos a neocomianos.

Enquanto o estudo dos isótopos de Sr e S observou o comportamento destes nos evaporitos da Formação Codó, análises de isótopos de C e O foram realizadas nos carbonatos e também revelaram uma ampla distribuição isotópica, com valores exclusivamente baixos de $\delta^{13}C$ e $\delta^{18}O$, ou seja , entre –5.69‰ e –13.02‰ $_{(PDB)}$ e –2.71‰ e –10.80‰ $_{(PDB)}$, respectivamente. Adicionalmente, estas razões variam de acordo com ciclos de arrasamento considerados neste trabalho como de origem tectônica e que, em geral, mostram razões de $\delta^{13}C$ e $\delta^{18}O$ mais leves na base, onde predominam depósitos de lago central, e progressivamente mais pesados em direção ao topo, onde depósitos de lago marginal são mais expressivos. Também confirmando a assinatura deposicional, este comportamento leva a propor um modelo isotópico controlado por eventos de sismicidade sin-sedimentar. Assim, razões isotópicas com valores mais leves parecem estar relacionados com eventos de inundação promovidos por subsidência, que resultou no desenvolvimento de um sistema de lago perene. Razões isotópicas com valores mais pesados estariam relacionados a fases de lago efêmero e seriam favorecidas pelo soerguimento e/ou aumento da estabilidade tectônica. Além disso, os resultados mostram que sistemas de lagos fechados predominaram em pelo menos parte do tempo de evolução desses depósitos, o que é indicado pela boa covariância positiva (i.e., +0,42 e +0,43) entre o carbono e o oxigênio, embora fases de lago aberto também sejam registradas pelos valores de covariância negativa (i.e., –0,36).

ABSTRACT

The Codó Formation is an important geological unit in Brazil, representing the only record of Neoaptian rocks exposed along the Brazilian equatorial margin. This unit consists of bituminous black shales, limestones and evaporites, which are particularly well represented in the south and east margins of the São Luís-Grajaú Basin, around the towns of Codó and Grajaú, State of Maranhão. These areas were investigated in order to: 1. improve the depositional system, discussing the hypothesis that the Codó Formation was produced in a lacustrine setting; and 2. reconstruct the paleohydrological conditions with basis on the integration of facies, stratigraphy, petrography and isotope (C, O,Sr and S) data. Hence, the field data presented herein confirmed a lacustrine system for the Codó area, where prevailed stable, well-stratified, saline lakes characterized by periods of closure, anoxia and salt precipitation in the central saline lakes. On the other hand, ephemeral conditions with development of a *sabkha*/saline pan complex prevailed in the Grajaú area, where salts precipitated mostly in the marginal portions of the system (i.e., marginal saline pans and mudflats).

Studies focusing facies and stratigraphy also revealed that in both areas the Codó Formation is arranged into several shallowing-upward cycles formed by progradation of marginal into central lake deposits. Three types of cycles were distinguished, referred to here as lower, intermediate and higher rank cycles. The lower rank cycles correspond to millimetric interbeddings of: a) bituminous black shale and evaporite; b) bituminous black shale and calcimudstone; c) bituminous black shale and peloidal wackestone-packstone; d) grey/green shale and calcimudstone; e) grey/green shale and peloidal wackestone-packstone; f) grey/green shale and ostracodal wackestone/grainstone; h) ostracodal wackestone/grainstone and/or calcimudstone with cryptomicrobial mats and ooidal/pisoidal packstone. These are attributed to seasonal deposition with basis on their regular nature forming very thin cycles resembling varves.

The intermediate rank cycles average 1.7 m thick and are formed by complete and incomplete cycles. Complete cycles show an upward transition from central to intermediate and then marginal facies associations, and include two types: C1 cycles with central lake deposits consisting of evaporites and black shales; and C2 cycles with central lake deposits

formed by gray/green shale. Incomplete cycles are those formed by successions lacking at least one of the facies associations, consisting of either central and intermediate lake deposits (cycles I1) or intermediate and marginal lake deposits (cycles I2).

The higher rank cycles average 5.2 m thick and consist of four depositional units, which display shallowing-upward successions formed by both complete and incomplete, intermediate rank cycles that vary their distribution upward in the section, and are bounded by sharp surfaces. Unit 1, the lowermost one, averages 2.7 m in thickness, being entirely composed by thin I1 cycles. Unit 2 averages 5.2 m thick, and displays all of the aforementioned intermediate cycles, especially complete ones. Unit 3, averaging 2.6 m thick, consists of 80% of cycles I2. Finally, unit 4, which averages 2.2 m in thickness, displays only incomplete cycles, though its uppermost part was not preserved due to erosion during the development of the Aptian sequence boundary.

The detailed sedimentological characterization and the stratal stacking patterns of the intermediate and higher rank cycles support a genesis linked to syn-sedimentary tectonic activity, particularly suggested by high facies variability, limited lateral extension, as well as frequent and random thickness changes of the intermediate-rank cycles. Additionally, the matching between the four higher rank cycles with four stratigraphic zones having different styles of soft-sediment deformation structures previously described in the literature as resulting from seismic activities, is a further argument to corroborate this interpretation. Therefore, the several episodes of lake shallowing recorded in the intermediate and higher rank cycles of the Codó Formation are attributed to fluctuations in the lake water level, triggered by seismic pulses alternating with sediment deposition.

The petrographic analysis of the evaporites from the Codó Formation allowed to better defining both the lake-*sabkha-saline pan* depositional system and the post-depostional histories. Seven evaporite morphologies were recognized: 1. chevron (selenite) gypsum; 2. nodular/lensoidal gypsum/anhydrite; 3. acicular gypsum; 4. mosaic gypsum; 5. brecciated gypsum/gypsarenite; 6. pseudo-nodular anhydrite/gypsum; and 7. rosettes of gypsum. Despite of this large variety of evaporite phases, the chevron gypsum, the nodular/lensoidal gypsum/anhydrite and the brecciated gypsum/gypsarenite record the preservation of primary features. The association of these morphologies with deposits displaying cyclic horizontal bedding, attributed to lake level fluctuations eventually culminated with subaerial exposure, reinforces this interpretation. Even acicular gypsum and mosaic gypsum, which replaced the chevron and brecciated gypsum/gypsarenite, respectively, formed under the influence of the depositional surface. Burial phases of gypsum are only recorded in the pseudo-nodular anhydrite/gypsum, attributed to salt mobilization induced by halokinesis. In addition, rosettes of gypsum, which crosscut the other evaporite morphologies, diagenetic in origin, have probably formed as the latest evaporite phase of the study area, under the influence groundwater and/or surface weathering.

In the present research, isotope studies aiming paleoenvironmental purposes were motivated by both confirmation of strong depositional influence for at least great part of the evaporites from the Codó Formation (i.e., primary and eodiagenetic gypsum), and the low diagenetic modification recorded for the limestones. Results of these approaches show that expansion/contraction cycles in both studied areas were accompanied by significant changes in isotope values. The wide dispersion of Sr and S isotope data within individual depositional cycles reinforces the lack of significant diagenetic modification as suggested by the petrographic analysis, and confirms the utility of these isotopes as environmental tools. Additionally, a non-marine brine source is suggested by $^{87}Sr/^{86}Sr$ ratios ranging from 0.707824 to 0.709280, which are higher than those from late Aptian seawater (i.e., between 0.70720 and 0.70735). The $\delta^{34}S$ varies from 16.12 to 17.89 ‰$_{(V\text{-}CDT)}$ in the Codó area, which is also in disagreement with late Aptian marine values (ranging from 13 to 16 ‰$_{(V\text{-}CDT)}$). Both geochemical tracers were influenced by facies characteristics, and thus a model is provided where expansion of saline pan/lake systems led to decreasing $^{87}Sr/^{86}Sr$ values due to the inhibition of the ^{87}Sr from clay minerals originated during the internal draining of mudflats. During expansion peaks, the $^{87}Sr/^{86}Sr$ values were lower due to submergence of mud flats and introduction of external ^{87}Sr-depleted waters related to weathering of Permian to Neocomian marine limestones and evaporites, as well as Triassic to Neocomian basaltic rocks. Furthermore, the sulphur isotope values decrease in the southern margin of the basin from 14.79 to 15.60 ‰$_{(V\text{-}CDT)}$ probably due to increased evaporation in shallower water settings.

While the studies of Sr and S isotopes emphasized the evaporites of the Codó Formation, the analysis of C and O isotopes were carried out on the carbonates. The data revealed a wide distribution of dominantly low $\delta^{13}C$ and $\delta^{18}O$ values, ranging from –5.69‰ to

–13.02‰ and from –2.71‰ to –10.80‰, respectively. It was also observed that these ratios vary according to seismically-induced shallowing-upward cycles, in general becoming lighter in their bases, where central lake deposits dominate, and progressively heavier upward, where marginal lake deposits are more widespread. In addition to confirm a depositional signature for the analysed samples, this behavior led to introduce a seismic-induced isotope model. Hence, lighter isotope ratios appear to be related with flooding events promoted by subsidence, which resulted in the development of a perennial lake system, while heavier isotope values are related to ephemeral lake phases favored through uplift and/or increased stability. Furthermore, the results show that a closed lake system dominated, as indicated by the overall good positive covariance (i.e., +0.42 to +0.43) between the carbon and oxygen isotopes, though open phases are also recorded by negative covariance values of –0.36.

APRESENTAÇÃO

Esta tese acha-se organizada sob a forma de quatro artigos, já submetidos ou aprovados em periódicos científicos indexados na categoria internacional A ou B. Adicionam-se a estes, um capítulo introdutório de integração e um capítulo final com uma síntese das principais conclusões advindas desta pesquisa.

O capítulo 1 tem por meta fazer uma introdução, com a apresentação da área de estudo, problemática que motivou a pesquisa, objetivos, métodos, bem como um breve sumário dos princípios teóricos relacionados com a aplicabilidade da geoquímica isotópica na reconstrução paleohidrológica de sistemas lacustres, tema de abordagem de dois dos capítulos desta tese. O capítulo 2 trata da descrição litológica e caracterização das diferentes categorias de ciclos sedimentares reconhecidos na Formação Codó, com discussão dos possíveis fatores causadores. O capítulo 3 contém a descrição petrográfica dos evaporitos da unidade investigada, com o objetivo de: 1. reconstituir sua paragênese; e 2. distingüir entre fases evaporíticas formadas sob influência do ambiente deposicional e aquelas geradas por processos diagenéticos, possibilitando a escolha de amostras com melhor potencial para os estudos isotópicos de Sr e S. O capítulo 4 apresenta os resultados da análise isotópica de Sr e S dos evaporitos da Formação Codó, com o objetivo de fornecer elementos adicionais que contribuam na determinação da origem da salmora. O capítulo 5 contém os resultados dos estudos isotópicos de C e O das rochas calcáreas intercaladas aos evaporitos e folhelhos da unidade estudada, tendo por objetivo de contribuir para no melhor entendimento do regime hidrológico vigente durante a deposição. Por fim, o capítulo 6 compreende as principais conclusões sintetizadas neste estudo.

A grande contribuição desta tese foi a consolidação do conhecimento a respeito da Formação Codó, fazendo uso do estudo integrado combinando análise faciológica com estudos petrográficos e métodos isotópicas enfocando Sr, S, C e O, como ferramenta chave para a caracterização mais precisa de sistemas deposicionais lacustres e entendimento de sua paleohidrologia.

1. INTRODUÇÃO

1.1. ARCABOUÇO GEOLÓGICO E PROBLEMÁTICA

A configuração atual da costa brasileira e as principais feições estruturais que controlam a dinâmica geológica da margem continental brasileira começaram a ser estabelecidos durante o Mesozóico, ao mesmo tempo em que as principais reservas de petróleo do mundo se formavam. No Eocretáceo, a região nordeste do Brasil formava o último elo de ligação entre a América do Sul e África, o que se estendeu até o período Aptiano, o qual marca, assim, a separação definitiva entre estes dois continentes e a livre circulação das águas entre o Atlântico Norte e Sul (Szatmari *et al*., 1987; Zanotto & Szatmari, 1987; Feijó, 1996). Este processo de separação foi desencadeado por um complexo sistema de rifteamento, marcado inicialmente pela implantação de diversos sistemas deposicionais lacustres ao longo de toda margem continental brasileira (inclusive continente adentro), e que culminou com transgressão marinha. A implantação dos lagos foi assíncrona ao longo da margem continental brasileira, ocorrendo genericamente de sul para norte. Desta forma, as bacias das regiões sul e sudeste brasileiras começaram a apresentar lagos representativos da fase pré-rifte ainda no Neocomiano, enquanto que nas bacias da região equatorial, os lagos são registrados apenas a partir do Aptiano.

Na Bacia de São Luís-Grajaú, localizada em grande parte do Estado do Maranhão, a sedimentação aptiana é bastante expressiva, merecendo destaque por ser a única bacia da margem equatorial onde a sucessão aptiana pode ser investigada na escala de afloramentos. Esta bacia foi formada durante a separação dos continentes sul-americano e africano, nos últimos estágios da fragmentação do *Gondwana*, no Cretáceo Inferior, por processos transtensivos associados com o estabelecimento do Sistema de Gráben Gurupi (Góes & Rossetti, 2001). Este sistema interliga as sub-bacias de Grajaú, São Luís e Caetés numa única feição estrutural tipo rift (Fig. 1-1A). A Bacia do Grajaú, por si só, abrange uma área de aproximadamente 130.000 km^2 e atinge espessuras de até 900 m, e, como continuidade ao sul da Bacia de São Luís, tem sido redenominada por Bacia de São Luís-Grajaú (Góes & Rossetti 2001).

O embasamento da Bacia de São Luís-Grajaú é composto de rochas da Bacia do Parnaíba, de cinturão de dobramentos Gurupi e Tocantins-Araguaia e do Cráton São Luís (Góes, 1995). O preenchimento sedimentar é representado por três megasseqüências deposicionais, designadas S1, S2 e S3 (cf. Rossetti, 2001; Fig. 1-1B). A seqüência S1 tem idade aptiana superior a albiana inferior e inclui as formações Grajaú e Codó em sua porção basal. A Formação Grajaú consiste de arenitos esbranquiçados, quartzosos, com granulação fina, e conglomerados quartzosos de origem flúvio-deltaica com contribuição eólica (e.g., Rezende, 1997). A Formação Codó constitui-se em folhelhos betuminosos, anidritas, calcários e arenitos lacustres (Campbell *et al.*, 1949; Aranha *et al.*, 1991). A seqüência S2 depositou-se durante o Eo/Mesoalbiano, correspondendo à Unidade Indiferenciada descrita na Bacia de São Luís (cf. Rossetti & Truckenbrodt, 1997), cujas características faciológicas são inferidas principalmente a partir de dados de subsuperfície e que levam a interpretá-la como registro de ambientes fluvio-deltaico a marinho marginal (Rossetti, 2001). A seqüência S3 depositou-se entre o Neoalbiano e um tempo incerto no Cretáceo Superior/Terciário, sendo representada por sucessões sedimentares atribuídas a sistemas estuarinos de vales incisos, cujas duas sucessões mais superiores desta seqüência acham-se bem expostas na Bacia de São Luís e correspondem às formações Alcântara e Cujupe (Rossetti, 2001). A Formação Alcântara (Albiano superior a Cenomaniano) constitui-se de arenitos bem estruturados, de coloração característica marrom-chocolate, granulometria fina a média e cimentação de calcita. Subordinadamente, ocorrem pelitos, conglomerados e calcários. Estes depósitos foram gerados principalmente em ambiente de ilha-barreira sujeito à ação de ondas de tempestade (Rossetti, 1998). A Formação Cujupe (Neocretáceo ?) é constituída por arenitos cauliníticos, de granulometria fina a muito fina, bem selecionados, cores branca, rósea ou amarelada, com estruturas geradas dominantemente por correntes de maré (Rossetti, 1998). Sobrepostos a estas unidades, ocorrem depósitos terciários atribuídos às formações Pirabas, Barreiras e depósitos Pós-Barreiras (Rossetti & Truckenbrodt, 1997).

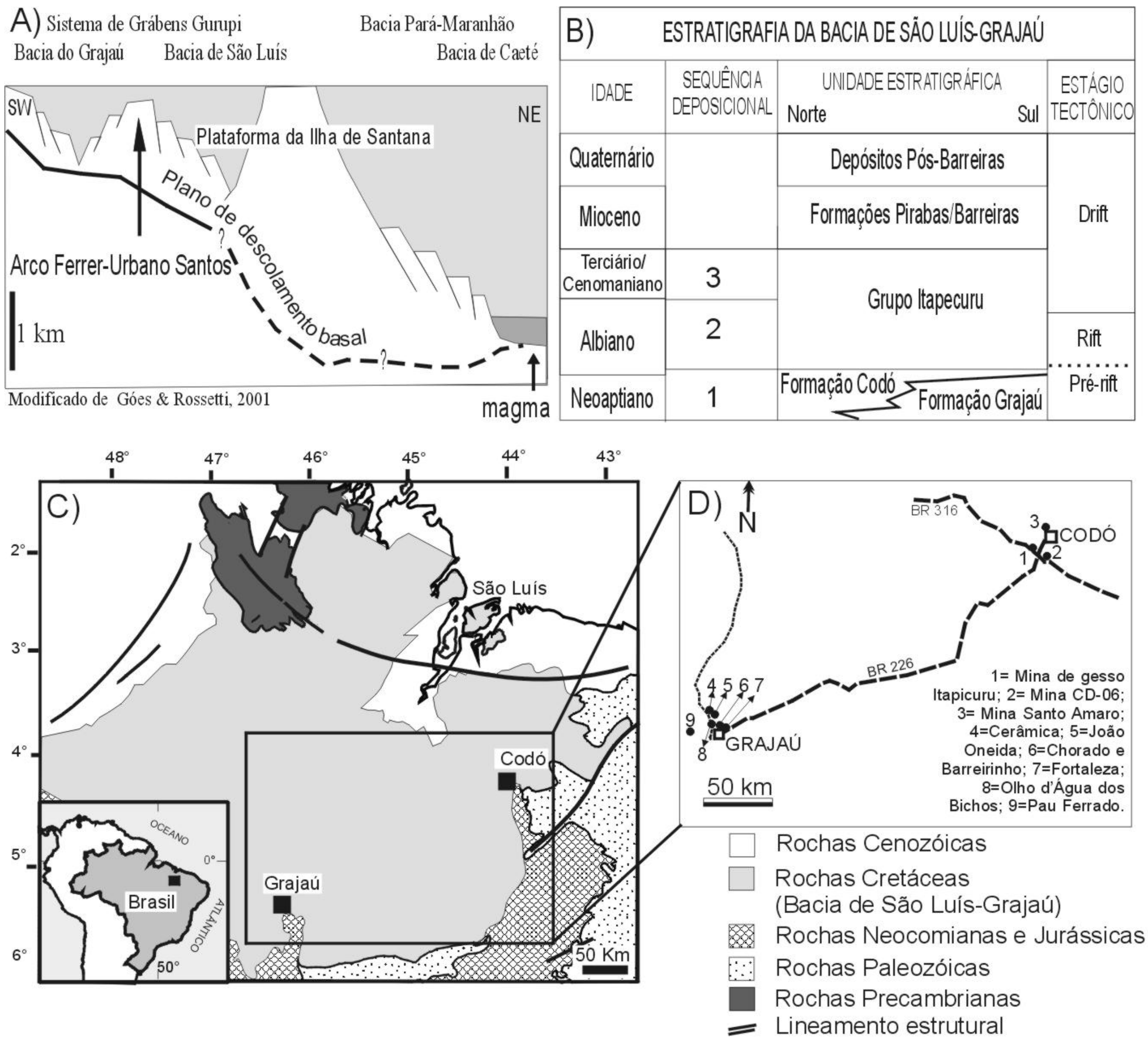

Fig. 1-1: A) Corte esquemático do Sistema de Gráben Gurupi, incluindo as sub-bacias do Grajaú, Sao Luís e Ceaté; B) estratigrafia, preenchimento e tectônica da Bacia de Sao Luís- Grajaú; C) localização da área de estudo nas porções leste e sul da Bacia do Grajaú; D) detalhe da figura anterior, indicando as localidades com minas a céu aberto estudadas neste trabalho (ver texto).

A Formação Codó, objeto deste estudo, representa os depósitos neoaptianos da Bacia de São Luís-Grajaú. Resgata-se a definição original de Lisboa (1914) e Campbell *et al*. (1949)

para o termo Formação Codó que aqui se emprega para referenciar folhelhos betuminosos intercalados a evaporitos e calcários, aflorantes nas regiões em torno das cidades de Codó e Grajaú, no Estado do Maranhão.

A Formação Codó desperta os mais diversos interesses econômicos e científicos. Economicamente, esta unidade pode representar a geradora da bacia, dado o seu alto teor de carbono orgânico associado a folhelhos betuminosos (Fernandes & Della Piazza, 1978). Além disto, calcário, gesso e argilas nobres têm sido exaustivamente explorados, devido à alta qualidade para uso industrial (Rezende, 1997). Cientificamente, o posicionamento estratigráfico da Formação Codó no período Aptiano a coloca como uma chave para o entendimento da paleogeografia, paleoclima e paleohidrologia do Cretáceo e ajuda a compor um quadro mais completo a respeito da implantação dos sistemas lacustres ao longo da margem continental brasileira. O conteúdo fóssil desta unidade, rico em elementos delicados e raros do Aptiano como, por exemplo, insetos, plantas e peixes, bem preservados em ritmitos de calcário e folhelho, ainda são atrativos importantes da Formação Codó (Pinto & Ornellas, 1974; Duarte & Silva-Santos, 1993; Popov & Pinto, 2000).

Dado o interesse despertado sob os mais diversos aspectos, vários estudos teceram considerações sobre os ambientes deposicionais da Formação Codó, com a proposição de modelos mais ou menos concordantes entre si (e.g., Aranha *et al*., 1991; Batista, 1992; Paz, 2000; Paz & Rossetti, 2001). Porém, a caracterização precisa do sistema deposicional (p.e., Batista, 1992; Paz, 2000) e, principalmente, a origem dos evaporitos (p.e., Rodrigues, 1995; Rossetti *et al*., 2000) são temas que permaneceram por ser mais sistematicamente abordados. Além disto, estudos petrográficos detalhados dos evaporitos nunca foram abordados anteriormente, tendo merecido apenas uma caracterização geral em dissertação de mestrado (i.e., Paz, 2000). Da mesma forma, apesar da abundância de calcários e evaporitos em afloramentos, a Formação Codó havia sido investigada em estudos isotópicos somente com base em dados de testemunho (Rodrigues & Takaki, 1993; Rodrigues, 1995). Por fim, a organização estratigráfica desta unidade, e a caracterização e entendimento da origem de sua natureza cíclica, são temas que foram somente superficialmente abordados em trabalhos prévios (p.e., Paz 2000; Gonçalves, 2004).

Assim, a situação existente no início desta tese era de um panorama com informações ainda inadequadas para sustentar solidamente o modelo deposicional dos depósitos aptianos da

Bacia de São Luís-Grajaú. Por outro lado, os estudos preliminares disponíveis sugeriam que estes estratos tinham grande potencial para servir como modelo de integração de dados faciológicos, petrográficos e isotópicos, com o intuito de reconstituição de seu sistema deposicional e entendimento das condições hidrológicas dominantes durante a deposição.

1.2. OBJETIVOS

O objetivo desta tese foi aprimorar (ou redefinir) o modelo paleoambiental da Formação Codó nas regiões de Codó e Grajaú, bordas leste e sul da Bacia de São Luís-Grajaú, respectivamente, integrando-se informações faciológicas, petrográficas e isotópicas (C, O, Sr e S), como ferramenta de análise do sistema deposicional, bem como das condições hidrodinâmicas dominantes durante a sedimentação. O surgimento de novas exposições em minas a céu aberto na região em torno da cidade de Grajaú, ainda não documentada na literatura, mostravam grande potencial de se incrementar as informações de campo. Uma vez superado este obstáculo (Rossetti *et al*., 2004), esta região tornou-se promissora para: 1) testar o modelo deposicional lacustre anteriormente adotado para a região de Codó, confrontando-o diante de novas evidências; 2) reconstituir os processos de formação dos evaporitos da região de Grajaú, comparando-os com a área de Codó; e 3) auxiliar no entendimento do significado das variações do sinal isotópico dos depósitos das áreas de estudo comparando-se ambientes deposicionais em duas áreas distintas da bacia.

1.3. ÁREA DE ESTUDO

As áreas estudadas neste trabalho localizam-se nas proximidades das cidades de Grajaú e Codó, Estado do Maranhão (Fig. 1-1C), onde ocorrem os melhores registros aflorantes da Formação Codó na Bacia de São Luís-Grajaú. Na área de Codó, esta unidade aflora em 3 minas a céu aberto, uma na BR 316, ao lado da Fábrica da Itapicuru Agroindustrial S/A, a 5 Km da entrada para a cidade de Codó, uma na estrada que leva à sede do município de Codó, a 15 Km após o cruzamento com a BR 316, e outra na localidade de Santo Amaro (Fig. 1-1D). A área de Grajaú possui inúmeras minas rudimentares, sendo que para este estudo foram utilizados 7 perfis, correspondentes às localidades de Chorado, Barreirinho, Olho D´Água, Olaria (ou Cerâmica), Faz. São João Oneida, Faz. Pau Ferrado e Faz. Fortaleza, além de um ponto à beira da estrada, no Km 22 da Rodovia Transmaranhense (MA-026). Estas sessões foram escolhidas com base na boa preservação dos estratos. Em geral, os perfis apresentam espessuras em torno de 10 m, com continuidade lateral de até 400 m, como no caso da mina de gesso a 5 Km da entrada para a cidade de Codó da Fábrica Itapicuru Agroindustrial S/A.

O acesso às áreas de estudo é relativamente fácil, sendo feito pelas rodovias BR-316, BR-226 e MA-026. Esta última, entretanto, é intransitável em certos pontos como, por exemplo, entre os municípios de Arame e Entroncamento. Embora a infraestutura seja precária, é possível encontrar boa hospedagem e até ótima uma alimentação tanto em Codó quanto em Grajaú.

1.4. MÉTODOS

A fim de alcançar o objetivo proposto nesta tese foram adotados os seguintes métodos: análise faciológica/estratigráfica, análise petrográfica e análise geoquímica (elementos principais, traços e isótopos).

A análise faciológica e estratigráfica foi feita com base em dados de afloramentos, tendo abrangindo mapeamento vertical e horizontal das fácies deposicionais, observando-se as seguintes feições: litologia, cor, textura e estruturas deposicionais, geometria da fácies e conteúdo paleontológico (cf. Tucker, 2003). Os dados foram registrados pela confecção de perfis litoestratigráficos, mapeamento de superfícies-chaves e documentação fotográfica de seções panorâmicas. Adicionalmente, procedeu-se com a coleta orientada de amostras para estudos de laboratório. Assim, tornou-se possível detalhar a geometria das fácies e reconhecer superfícies de importância estratigráfica. Esta metodologia tem sido adotada com sucesso em diversos trabalhos realizados na Bacia de São Luís-Grajaú (p.e., Anaisse, 1999; Lima & Rossetti, 1999; Paz, 2000; Rossetti & Góes, 2000; Rossetti *et al.*, 2000; Paz & Rossetti, 2001).

A análise petrográfica consistiu no estudo de 220 seções delgadas de carbonatos e evaporitos. A caracterização petrográfica das lâminas foi feita pela: 1) determinação da composição dos carbonatos, através do seu tingimento com alizarina vermelha-S, ferricianeto de potássio e ácido clorídrico diluído em água destilada; 2) identificação e estimativa dos constituintes da seção delgada; e 3) determinação do relacionamento entre as diversas fases mineralógicas. Como ferramenta auxiliar à microscopia óptica convencional (i.e., microscópio petrográfico), aplicação de microscópio eletrônico de varredura (MEV) e espectrometria de energia dispersiva de raios-X (EDS), do Laboratório de Microscopia do Museu Goeldi, ajudaram a solucionar problemas de definição de aspectos morfológicos, composicionais e mineralógicos observados nas amostras e seções delgadas estudadas.

A análise geoquímica elementar consistiu na determinação de Ca, Mg, Fe, Mn, Sr e Na das amostras de rocha total de carbonato, a fim de investigar possíveis modificações diagenéticas. Estes elementos são os mais importantes na estrutura da calcita tanto marinha quanto não marinha e, considerando que os teores destes elementos mantiveram-se mais ou menos constantes através do Fanerozóico (cf. Holland, 1978), uma comparação adicional com valores comumente esperados em águas de formação poderia detectar potenciais influências diagenéticas. O procedimento consistiu na secagem de 1,5 g de 70 amostras a 1000 ^{o}C por duas horas, sendo fundidas com tetraborato de lítio e fluoreto de lítio, fornecendo pastilhas fundidas que foram analisadas pelo espectrômetro de fluorescência de Raios-X do Laboratório de Isótopos Estáveis da Universidade Federal de Pernambuco (LABISE/UFPE), aos cuidados da Profa. Dra. Valderez Ferreira.

A análise geoquímica isotópica consistiu na determinação das razões isotópicas de C e O em carbonatos e de S e Sr em evaporitos da Formação Codó, visando testar variações no regime hidrológico do ambiente deposicional, que ajudassem a entender e compor um quadro mais refinado do sistema deposicional. Esta caracterização tem se mostrado bem sucedida em diversos trabalhos visando-se estabelecer arcabouços hidrológicos e climatológicos, tanto em ambientes modernos, quanto em depósitos de ambientes antigos (p.e., Chivas *et al.*, 1991; Bird *et al.*, 1991; Bellanca *et al.*, 1992; Camoin *et al.*, 1997; Chaves & Sial, 1998; Li & Ku, 1997; Neumann, 1999; Playà *et al.*, 2000; Ortí e Rosell, 2000; Lu *et al.*, 2001; Wignall & Tretchett, 2002; Krull *et al.*, 2004).

Maiores detalhamento sobre os procedimentos utilizados durante as análises geoquímicas encontram-se inseridos nos capítulos respectivos.

1.5. GEOQUÍMICA ISOTÓPICA

1.5.1. Fundamentação teórica

A geoquímica isotópica como ferramenta para auxiliar na interpretação paleoambiental de depósitos lacustres é uma abordagem relativamente nova (Stuiver, 1970). Este tema representa o cerne dos capítulos 4 e 5 desta tese e prima pelo ineditismo deste tipo de abordagem nos depósitos da área de estudo. Merece, portanto, que seus fundamentos teóricos sejam revisados em mais detalhes ao longo deste item.

Isótopos são átomos que possuem o mesmo número atômico, mas que apresentam diferentes números de massa, conseqüentemente de quantidades diferentes de nêutrons em seu núcleo. Na natureza, os elementos químicos são formados por uma mistura de, pelo menos, dois isótopos, onde um deles em quantidade abundante e o outro, subordinada. Os isótopos podem também ser considerados estáveis ou instáveis, sendo que a estabilidade é um fator relativo ao tempo de decaimento radioativo muito longo, da ordem de 10^{18} anos para os isótopos mais leves (massa atômica $\leq$ 34). Como ocupam a mesma posição na tabela periódica, formam um mesmo elemento químico e compartilham das mesmas propriedades químicas, mas por causa do número de massa distinto, apresentam propriedades físico-químicas (p.e., densidade, temperatura de congelamento e de ebulição, viscosidade, pressão de vapor) sutilmente distintas entre si. Esta distinção nas propriedades físico-químicas dos isótopos que constituem um mesmo elemento químico é chamada *efeito isotópico*.

Por causa do efeito isotópico, durante eventos físico-químicos de transformação ou transição dos elementos, estes acabam por se tornar mais enriquecidos ou mais empobrecidos (=depletados) em alguns dos isótopos que os constituem. Este efeito é conhecido por *fracionamento isotópico*, que ocorre fundamentalmente por troca isotópica ou por efeito cinético.

O *fracionamento por troca isotópica* diz respeito aos processos em que não ocorrem mudanças ordinárias no sistema químico, mas na distribuição dos isótopos entre diferentes substâncias químicas, fases, ou ainda, moléculas (cf. Hoefs, 1980). Simplificadamente, a troca isotópica pode ser entendida como um caso especial de equilíbrio químico:

$$aA_1 + bB_2 \leftrightarrow aA_2 + bB_1$$

onde A e B representam os elementos que contêm as moléculas leve ou pesada 1 ou 2. O fracionamento por efeito cinético diz respeito àquelas reações químicas unidirecionais, em que as taxas de reação entre os reagentes e os produtos são sensíveis às diferenças de massas dos átomos. Quando o fracionamento ocorre em equilíbrio isotópico (i.e., sem modificações no sistema físico-químico durante a reação), os isótopos são redistribuídos proporcionalmente de acordo com um fator de fracionamento da reação. O fator de fracionamento α entre duas substâncias A e B é a razão R_A do número de quaisquer dois isótopos na substância A dividida pela razão R_B deste dois isótopos na substância B, de tal maneira que:

$$\alpha_{A\text{-}B} = R_A/R_B$$

O fator de fracionamento em equilíbrio isotópico é dependente da temperatura, experimentalmente determinável e diretamente relacionado à constante de equilíbrio da reação. Em termos absolutos, os valores das razões isotópicas são números muito pequenos e, por convenção, são expressos em notação δ, que expressa o desvio (em partes por mil) da razão isotópica medida em relação a uma amostra padrão, de acordo com a expressão:

$$\delta = ((R_{\text{amostra estudada}} - R_{\text{padrão}}) / R_{\text{padrão}}) * 1000$$

Existem diferentes padrões para cada isótopo estudado. Entre os principais, estão o PDB (PeeDee Belemnite), usado para expressar razões isotópicas de C e/ou O em amostras de carbonatos, o SMOW (*Standard Mean Ocean Water*), usado para expressar razões isotópicas de H e/ou O em amostras de água, silicatos e, ainda, carbonatitos, e o CDT (*Canyon Diablo Troilite* – um composto de FeS oriundo de meteorito), usado para expressar as razões isotópicas do S em amostras dos mais diversos materiais. A principal fornecedora destes padrões ao redor do mundo são a Agência Internacional de Energia Atômica (Áustria) e o *National Bureau Standards* (EUA). Alguns destes padrões já se exauriram ou estão muito perto disso. Por isso, tem sido comum a adoção de padrões alternativos àqueles originais, reconhecidos pelo acréscimo da partícula V- (Viena-) ao nome do padrão (por exemplo, V-PDB, V-SMOW e V-CDT).

1.5.2. Aplicação em depósitos lacustres

O princípio do estudo de isótopos estáveis em depósitos lacustres é que tanto carbonatos quanto evaporitos precipitam-se em equilíbrio isotópico com a água do lago (Stuiver, 1970; Talbor, 1990; Talbot & Kelts, 1990). Os isótopos estáveis leves mais utilizados em estudos de reconstituição paleoambiental de depósitos lacustres são carbono, oxigênio e enxofre.

O carbono possui três isótopos (i.e., ^{12}C, ^{13}C e ^{14}C). O ^{12}C é o mais abundante (~99%), sendo que em depósitos muito antigos (acima de 50.000 anos), todo ^{14}C já sofreu decaimento radioativo para as formas estáveis. O carbono sofre fracionamento por troca isotópica durante a transformação do gás carbônico da atmosfera em bicarbonato dissolvido e precipitação do bicarbonato em carbonato dentro do lago. O fracionamento por efeito cinético ocorre durante a fotossíntese, que favorece o acúmulo de ^{12}C mais “leve” na matéria orgânica do lago e torna a razão isotópica $\delta^{13}C$ residual na água do lago mais “pesada”. Em sistemas lacustres, a variação da composição isotópica de C depende da produtividade do lago, da estratificação da lâmina de água, do tipo de degradação bacteriana, da geologia da área fonte, do tipo de vegetação da área de captação da bacia e da troca de gás carbônico na interface água-ar (Stuiver, 1970; Hoefs, 1980; McKenzie, 1985; Herczeg, 1988; Li & Ku, 1997; Talbot & Lærdal, 2000; Wignall & Twitchett, 2002). Durante períodos em que o nível do lago está mais alto (Fig. 1-2), processos como maior respiração do lago, elevado consumo de matéria orgânica, alto soterramento de carbono orgânico, maior influxo de águas fluviais teoricamente com bicarbonato mais “leve”, baixa troca de gás carbônico com a atmosfera e menor participação do gás carbônico metanogênico na formação do carbono orgânico total dissolvido na água do lago, favorecem que o $\delta^{13}C$ da água do lago seja mais “depletado” do que em períodos em que o nível do lago está mais baixo (cf. Talbot, 1990; Talbot & Kelts, 1990; Guzzo, 1997).

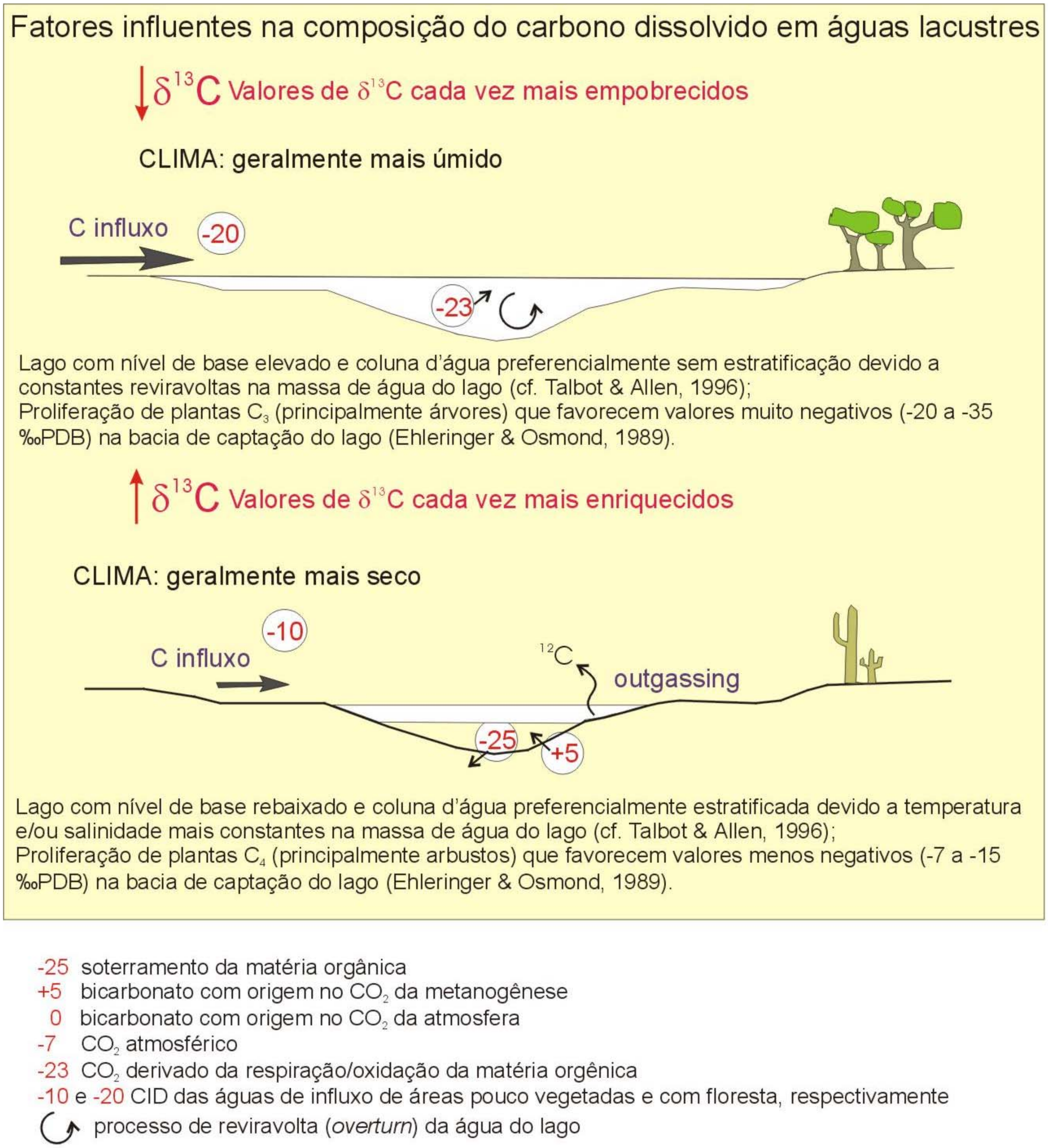

Fig. 1-2: Respiração do lago, consumo de matéria orgânica, soterramento de carbono orgânico, influxo de águas fluviais com bicarbonato mais "leve", baixa troca de gás carbônico com a atmosfera e participação do gás carbônico metanogênico alternam-se em importância durante fases de lago alto e baixo e influenciam indiretamente no valor do $\delta^{13}C$ do carbonato lacustre (Modificado de Guzzo, 1997).

O oxigênio também possui três isótopos (^{16}O, ^{17}O e ^{18}O). O ^{16}O é o mais abundante, respondendo por mais de 99% do oxigênio disponível na natureza. Em geral, a razão mais usada é $^{18}O/^{16}O$ por causa das maiores abundâncias em relação ao ^{17}O e da maior diferença de massa entre eles. O oxigênio sofre fracionamento por troca isotópica, durante as fases do ciclo hidrológico (Fig. 1-3A), quando se torna mais pesado nas fases residuais, e por efeito cinético, durante a fotossíntese, quando provavelmente contribui significaivamente com valores bastante negativos produzidos durante a respiração (cf. Hoefs, 1980, p.122). Embora a temperatura seja o fator mais importante no fracionamento do oxigênio, a variação da composição isotópica do O nas águas do lago refletem preferencialmente variações no balanço hídrico da bacia (cf. Lister *et al.*, 1991; Fig. 1-3B). Durante períodos de nível do lago mais alto, o $\delta^{18}O$ tende a se tornar mais negativo dado o aporte de águas depletadas em ^{18}O. O período de rebaixamento do nível do lago que se segue favorece a evaporação de ^{16}O e torna a água residual do lago mais enriquecida em ^{18}O. Depósitos cretáceos lacustres da região do Recôncavo na Bahia que registram este comportamento isotópico são interpretados neste sentido (p.e., Guzzo, 1997).

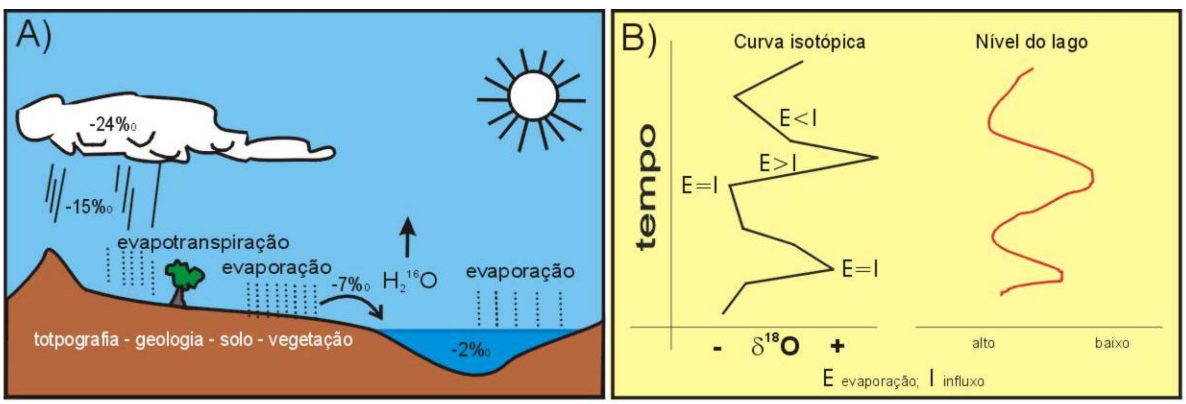

Fig. 1-3: A) processos de enriquecimento em ^{18}O de águas lacustres ligados ao ciclo hidrológico (cf. Lister *et al.*, 1991); B) modelo de sinal paleohidrológico de isótopos de oxigênio em carbonatos lacustres, considerando bacias hidrologicamente fechadas (Lister *et al.*, 1991; Bellanca *et al.*, 1992).

O enxofre possui quatro isótopos (i.e., ^{32}S, ^{33}S, ^{34}S e ^{36}S), dos quais os mais abundantes são o ^{32}S (~ 95%) e o ^{34}S (~ 4%). O fracionamento de enxofre em sedimentos ocorre quase exclusivamente por redução bacteriana de sulfato para H_2S (Fig. 1-4). A troca isotópica durante processos de redox provavelmente desempenha um papel importante ainda não bem definido no registro antigo (Lu *et al.*, 2001). Desta maneira, períodos em que a estratificação da coluna d'água no lago é mantida por um longo período favorecem a proliferação de bactérias sulfato redutoras, que por sua vez promovem o enriquecimento em ^{34}S do sulfato residual na água do lago.

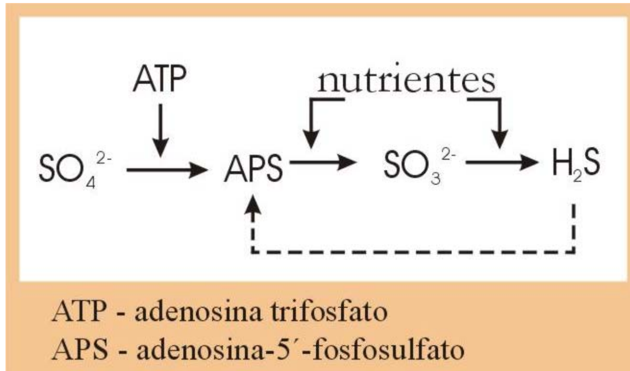

Fig. 1-4: Ciclo resumido do enxofre, enfatizando a passagem do sulfato para sulfeto de hidrogênio por respiração anaeróbica de bactérias sulfato-redutoras (modificado de Hoefs, 1980).

O ^{87}Sr não é um isótopo estável leve, uma vez que surge como produto de decaimento do ^{87}Rb. Entretanto, a análise da razão $^{87}Sr/^{86}Sr$ tem acompanhado diversos trabalhos orientados por isótopos estáveis, uma vez que também apresenta um tempo de meia-vida bastante longo, comparável ao dos isótopos estáveis leves (Holser *et al.*, 1996). Ao contrário dos isótopos leves, o Sr não sofre fracionamento no ambiente sedimentar e é facilmente capturado pela cristalização de evaporitos, que reflete exatamente a composição isotópica da água da qual se precipitou. Outro aspecto curioso, é que as razões dos isótopos de Sr são escritas diretamente de um isótopo em relação ao outro, sem necessidade de padrões de comparação. Os principais meios de alteração da razão $^{87}Sr/^{86}Sr$ numa bacia deposicional são através de maior influxo fluvial, que favorece o aporte de Sr oriundo do intemperismo de rochas continentais, em geral produzindo valores superiores a 0,707, e a "troca" de Sr com basalto de crosta juvenil, cujas razões $^{87}Sr/^{86}Sr$ são iguais ou inferiores a 0,706, mas que só ocorre em ambiente hidrotermal marinho abaixo das cordilheiras meso-oceânicas (Fig. 1-5; Holser *et al.*, 1996). Em sistemas continentais, portanto, a variação na razão $^{87}Sr/^{86}Sr$ está diretamente ligada a variações no aporte fluvial da bacia de captação do sistema (cf. Rhodes *et al*. 2002).

Este quadro mostra que a deposição de carbonatos e evaporitos em lagos reflete fortemente as condições paleohidrológicas atuantes durante a deposição. As variações na composição isotópica destes sedimentos revelam mudanças no balanço físico- e/ou bioquímico na água do lago e/ou na água vadosa da partes emersas do ambiente lacustre. Eventualmente, estas variações isotópicas refletem indiretamente perturbações de ordem climática e, quiçá, tectônica.

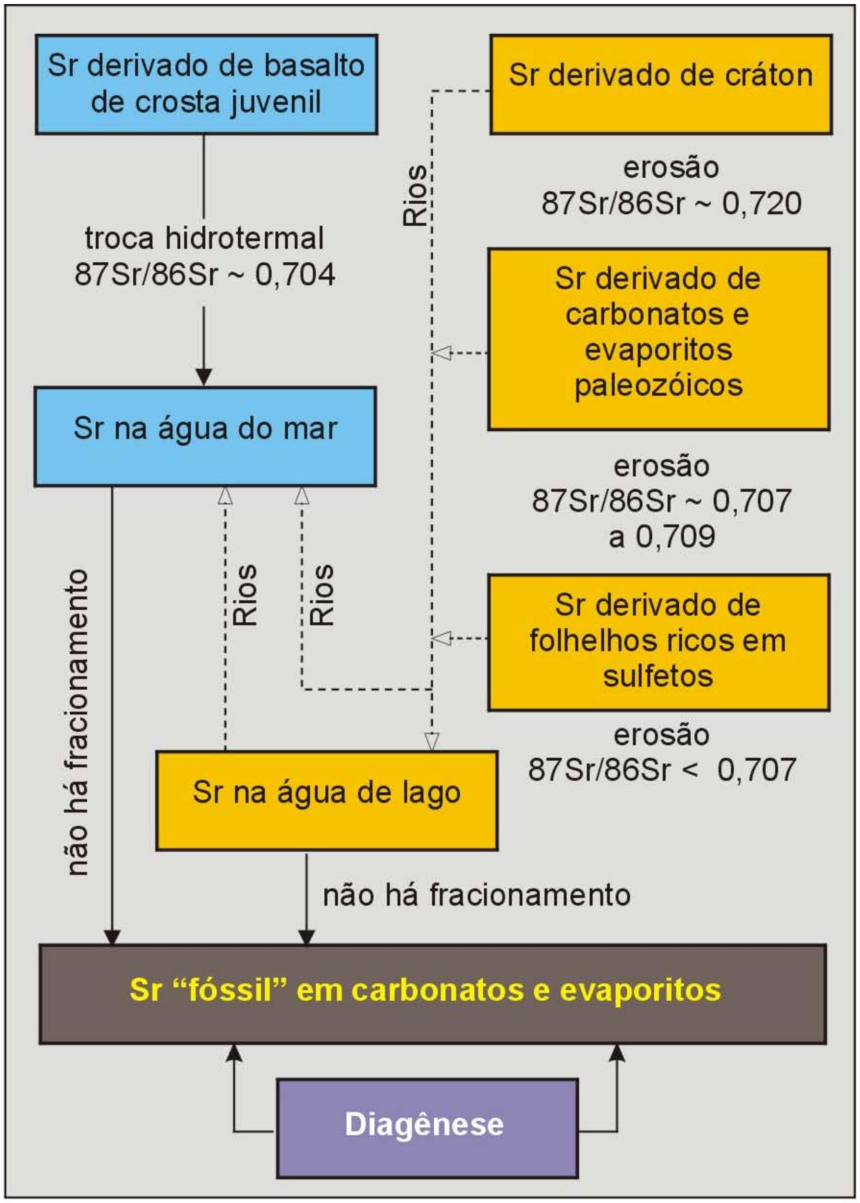

Fig. 1-5: Fatores influentes na composição da razão $^{87}Sr/^{86}Sr$ de depósitos lacustres e de bacias oceânicas (cf. Holser *et al*., 1996). .

REFERÊNCIAS

ANAISSE, J., Jr. 1999. *Fácies costeiras dos Depósitos Itapecuru (Cretáceo), região de Açailância, Bacia do Grajaú*. Belém, Univ. Fed. Pará, 86p. (Dissertação de Mestrado)

ARANHA, L.G.; LIMA, H.P.; MAKINO, R.K.; SOUZA, J.M. 1991. Origem e evolução das bacias de Bragança-Viseu, São Luís e Ilha Nova. In: E.J. MILANI & G.P. RAJA GABAGLIA (eds.) *Origem e evolução das bacias sedimentares*. Rio de Janeiro, PETROBRÁS, p.221-234.

BATISTA, A. M. 1992. *Caracterização paleoambiental dos sedimentos Codó-Grajaú, Bacia de São Luís (MA)*. Belém, Univ. Fed. Pará, 102 p. (Dissertação de Mestrado)

BELLANCA, A., CALVO, J.P., CENSI, P., NERI, R. & POZO, M. 1992. Recongnition of lake-level changes in Miocene lacustrine units, Madrid Basin, Spain. Evidence from facies analysis, isotope geochemistry and clay mineralogy. *Sediment. Geol.*, 76: 135-153.

BIRD, M.I., CHIVAS, A.R., RADNELL, C.J., BURTON, H.R. 1991. Sedimentological and stable isotope evolution of lakes in the Vestfold Hills, Antarctica. *Palaeogeog., Palaeoclim., Palaeoecol.*, 84: 109-130.

CAMOIN, G., CASANOVA, J., ROUCHY, J.M., BLANC-VALLERON, M.M, DECONINCK, J.F. 1997. Environmental controls on perenial and ephemeral carbonate lakes: the central palaeo-Andean Basin od Bolivia during Late Cretaceous to early Tertiary times. *Sedimentary Geology*, 113: 1-26.

CAMPBELL, D.F., ALMEIDA, L.A., SILVA, S.O. 1949. Relatório preliminar sobre a geologia da Bacia do Maranhão. *Boletim do Conselho Nacional do Petróleo*, 1: 1-160.

CHAVES, N.S. & SIAL, A.N. 1998. Mixed oceanic and freshwater depositional conditions for beachrocks of Northeast Brazil: evidence from carbon and oxygen isotopes. *Int. Geol. Rev.*, 40: 748-754

CHIVAS, A.R., ANDREW, A..S., LYONS, W.B., BIRD, M.I., DONELLY, T.H. 1991. Isotopic constraints on the origin of salts in Australian playas. 1. Sulphur. *Palaeogeog., Palaeoclim., Palaeoecol.*, 84: 309-332.

DUARTE, L.S. & SILVA-SANTOS, R. 1993. Plant and megafossils of the Codó Formation, Parnaiba Basin, NE Brazil. *Cretaceous Research*, 14: 735-746.

EHLERINGER, J.R. & OSMOND, C.B. 1989. Stable isotopes. In: R.W. PEARCY, J. EHLERINGER, H.A. MOONEY, P.W. RUNDD (Eds) *Plant Physiological Ecology: Field Methods and Instrumentation*. London, Chapman & Hall, p. 281-300.

FEIJÓ, F.J. 1996. O início da livre circulação das águas do Oceano Atlântico. *Bol. Geoc. Petrobrás*, 10: 157-164

FERNANDES, G. & DELLA PIAZZA, H. 1978. O potencial oleogenítico da Formação Codó. *Bol. Técn. PETROBRAS*, 21: 3-16.

GÓES, A.M. 1995. *A Formação Poti (Carbonífero inferior) da Bacia do Parnaíba*. Universidade de São Paulo, São Paulo, 171 p. (Tese de Doutorado)

GÓES, A.M. & ROSSETTI, D.F. 2001. Gênese da Bacia de São Luís-Grajaú, Meio-Norte do Brasil. In: D.F. ROSSETTI, A.M. GÓES, W. TRUCKENBRODT (Eds) *O Cretáceo na Bacia de São Luís-Grajaú*. Belém, Coleção Friedrich Katzer, Museu Paraense Emílio Goeldi, p. 15-29.

GONÇALVES, D. F. 2004. *Argilominerais da Formação Codó (Aptiano superior) – Bacia do Grajaú: implicações climáticas e ambientais*. Belém, Univ. Fed. Pará, 100 pp. (Dissertação de Mestrado)

GUZZO, J.V.P. 1997. *Estratigrafia integrada e paleolimnologia de uma seção de idade Aratu (Eocretáceo) da Bacia do Recôncavo, NE do Brasil*. Porto Alegre, Univ. Fed. do Rio Grande do Sul, 210 p. (Dissertação de Mestrado)

HERCZEG, A.L. 1988. Early diagenesis of organic matter in lakes sediments: a stable carbon isotope study of pore waters. *Chemical Geology*, 72: 199-209. (Isotope Geoscience Section)

HOEFS, J. 1980. *Stable isotope geochemistry*. 2ª ed. Berlim, Springer-Verlag, 208 p.

HOLLAND, H.D., 1978. *The Chemistry of the Atmosphere and Oceans*. Wiley-Interscience, New York, 351 p.

HOLSER, W.T.; MAGARITZ, M.; RIPPERDAN, R.L. 1996. Global isotopic events. In: H. WALLISER (Ed.) *Global events and event stratigraphy in the Phanerozoic*. Berlim, Springer-Verlag, p. 63-88.

LI, H.-C. & KU, T.-L. 1997. $\delta^{13}C$ and $\delta^{18}O$ covariance as a paleohydrological indicator for closed-basin lakes. *Palaeogeog., Palaeoclim., Palaeoecol.*, 133: 69-80.

LIMA, R.D. & ROSSETTI, D. F. 1999. Depositional facies in Late Cretaceous-?Lower Tertiary deposits from northwestern Maranhão State, Brazil. *Rev. Bras. Geoc*., 29: 237-244.

LISBOA, M.A.R. 1914. The Permian geology of northern Brazil. *Am. J. Sci.*, 177: 425-442.

LISTER, G.S., KELTS, K., CHEN, K.Z., YU, J.-Q., NIESSEN, F., 1991. Lake Qingai, China: closed-lake basin levels and the oxigen isotope record for ostracoda since the latest Pleistocene. *Palaeogeogr., Palaeoclimatol., Palaeoecol.*, 84: 141-162.

LU, F.H.; MEYERS, W.J.; SCHOONEN, M.A. 2001. S and O (SO_4) isotopes, simultaneous modeling, and environmental significance of the Nijar messinian gypsum, Spain. *Geochim. Cosmochim. Acta*, 65: 3081-3092.

KRULL, E.S.; LEHRMANN, D. J.; DRUKE, D.; KESSEL, B.; YU, Y.Y.; LI, R. 2004. Stable carbon isotope stratigraphy across the Permian-Triassic boundary in shallow marine carbonate platforms, Nanpanjiang Basin, south China. *Palaeogeogr., Palaeoclimatol., Palaeoecol.*, 204: 297-315.

MCKENZIE, J. A. 1985. Carbon Isotopes and Productivity in the Lacustrine and Marine Environment. In: STUMM, W. (Ed.) *Chemical Processes in Lakes*. New York, Wiley, 99-118.

NEUMANN, V.H.M.L. 1999. *Estratigrafía, sedimentología, geoquímica y diagénesis de los sistemas lacustres aptienses-albienses de la Cuenca de Araripe (Noreste de Brasil).* Barcelona, Universitat de Barcelona, 234 pp. (Tese de doutorado)

ORTÍ, F. & ROSELL, L. 2000. Evaporative systems and diagenetic patterns in the Calatayud Basin (Miocene, Central Spain). *Sedimentology*, 47: 665-685.

PAZ, J.D.S. 2000. *Análise faciológica da Formação Codó (Aptiano superior), na região de Codó (MA), borda leste da Bacia do Grajaú*. Belém, Univ. Fed. Pará, Belém, 117p. (Disertação de Mestrado)

PAZ, J.D.S & ROSSETTI, D.F. 2001. Reconstrução paleoambiental da Formação Codó (Aptiano), borda leste da Bacia do Grajaú, MA. In: D.F. ROSSETTI, A.M. GÓES, W. TRUCKENBRODT (Eds) *O Cretáceo na Bacia de São Luís-Grajaú*. Belém, Coleção Friedrich Katzer, Museu Paraense Emílio Goeldi, p. 77-100.

PINTO, I.D. & ORNELLAS, L.P. 1974. New cretaceous hemiptera (insects) from Codó Formation – Northern Brazil. In: CONGRESSO BRASILEIRO DE GEOLOGIA, 28. Porto Alegre, *Anais*... SBG, p. 289-304.

PLAYÀ, E.; ORTÍ, F.; ROSELL, L. 2000. Marine to non-marine sedimentation in the upper Miocene evaporites of the Eastern Betics, SE Spain: sedimentological and geochemical evidence. *Sediment. Geol.*, **133:** 135-166.

POPOV, Y.A. & PINTO, I.D. 2000. On some Mesozoic burrower bugs (Heteroptera; Cydnidae). *Paleontological Journal*, 34: 298-302 (Suppl. 3)

REZENDE, N.G.A.M. 1997. *Argilas nobres e zeólitas na Bacia do Parnaíba*. Belém, CPRM, 50 p. (Relatório final de projeto)

RHODES, M.K.; CAROLL, A.R.; PIETRAS, J.T.; BEARD, B.L.; JOHNSON, C.M. 2002. Strontium isotope record of paleohydrology and continental weathering, Eocene Green River Formation, Wyoming. *Geology*, 30: 167-170.

RODRIGUES, R. 1995. *A geoquímica orgânica na Bacia do Parnaíba*. Porto Alegre, Univ. Fed. Rio Grande do Sul, 225 p. (Tese de Doutorado).

RODRIGUES, R. & TAKAKI, T. 1993. Estratigrafia química da Formação Codó, Cretáceo inferior da Bacia do Parnaíba. In: SIMPOSIO SOBRE O CRETACEO DO BRASIL, 3. Rio Claro, *Boletim*... Rio Claro, SBG. v.2 , p. 115-117.

ROSSETTI, D.F. 1998. Facies architecture and sequential evolution of incised valley estuarine fills: the Upper Itapecuru Formation (São Luís Basin), northern Brazil. *J. Sediment. Res.,* 68: 299-310.

ROSSETTI, D.F. 2001. Arquitetura deposicional da Bacia de São Luís-Grajaú. In: D.F. ROSSETTI, A.M. GÓES, W. TRUCKENBRODT (Eds) *O Cretáceo na Bacia de São Luís-Grajaú*. Belém, Museu Paraense Emílio Goeldi, Belém, Museu Paraense Emílio Goeldi, pp. 31-46. (Coleção Friedrich Katzer)

ROSSETTI, D.F. & GÓES, A.M. 2000. Deciphering the sedimentological imprint of paleoseismic events: an example from the Aptian Codó Formation, northern Brazil. *Sediment. Geol.*, 135: 137-156.

ROSSETTI, D.F. & TRUCKENBRODT, W. 1997. Classificação estratigráfica para o Albiano-Terciário Inferior (?) na Bacia de São Luís, MA. *Boletim do Museu Paraense Emílio Goeldi* - Série Ciências da Terra, 9: 31-43.

ROSSETTI, D.F.; PAZ, J.D.S.; GÓES, A.M. 2004. Facies analysis of the Codó Formation (Late Aptian) in the Grajaú Area, Southern São Luís-Grajaú Basin. *An. Acad. Bras. Ciênc.*, 76: 791-806.

ROSSETTI, D.F.; PAZ, J.D.; GÓES, A.M.; MACAMBIRA, M. 2000. A marine versus non-marine origin for the Aptian-Albian evaporites of the São Luís and Grajaú basins, Maranhão state (Brazil) based on sequential analysis. *Rev. Bras. Geoc.*, 30: 642-645.

STUIVER, M. 1970. Oxygen and carbon isotope ratios of freshwater carbonates as climatic indicators. *Journal of Geophysical Research*, 75: 5247-5257.

SZATMARI, P., FRANÇOLIN, J.B.L., ZANNOTTO, O.; WOLFF, S. 1987. Evolução tectônica da margem equatorial brasileira. *Rev. Bras. Geoc.*, 17: 180-188.

TALBOT, M.R., 1990. A review of the paleohydrological interpreatation of carbon and oxygen isotopic ratios in primary lacustrine carbonates. *Chem. Geol.*, 80: 261-279.

TALBOT, M.R. & ALLEN, P.A. 1996. Lakes. In: H.G. READING (Ed.) *Sedimentary Environments: Process, Facies and Stratigraphy*. Oxford, Blackwell, pp. 83-124.

TALBOT, M.R. & KELTS, K., 1990. Paleolimnological signatures from carbon and oxygen isotopic ratios in carbonates from organic carbon-rich lacustrine sediments. In: B.J. KATZ (Ed.) *Lacustrine Basin Exploration: Case Studies and Modern Analogs*. Tulsa, AAPG, pp. 99-112. (Memoir, 50)

TALBOT, M.R. & LÆRDAL, T. 2000. The late Pleistocene-Holocene palaeolimnology of Lake Victoria, East Africa, based upon elemental and isotopic analyses of sedimentary organic matter. *Journal of Paleolimnology*, 23: 141-164.

TUCKER, M.E. 2003. *Sedimentary rocks in the field* (3rd Ed.). John Wiley & Sons, 244 p.

WIGNALL, P.B. & TWITCHETT, R.J. 2002. Extent, duration, and nature of the Permian-Triassic superanoxia event. *Geol. Soc. Am. Spec. Publ.*, 104: 171-176.

ZANNOTTO, O. & SZATMARI, P. 1987. Mecanismo de rifteamento da porção ocidental da margem norte brasileira, Bacia do Pará-Maranhão. *Rev. Bras. Geoc.*, 17: 189-197.

2. LINKING LACUSTRINE CYCLES WITH SYN-SEDIMENTARY TECTONIC EPISODES: AN EXAMPLE FROM THE CODÓ FORMATION (LATE APTIAN), NORTHEASTERN BRAZIL[*]

2.1. ABSTRACT

The Codó Formation exposed in the eastern Grajaú Basin consists mostly of black shales, limestones and evaporites arranged into several shallowing-upward cycles formed by progadation of lake deposits. Three ranks of cycles are distinguished. The lower rank cycles correspond to milimetric interbeddings of: bituminous black shales with evaporites, calcimudstones or peloidal wackestone-packstone; grey/green shale with calcimudstone, peloidal wackestone-packstone or ostracodal wackestone/grainstone; and ostracodal wackestone/grainstone and/or calcimudstones with cryptomicrobial mats and ooidal/pisoidal packstones. The intermediate rank cycles average 1.7 m thick and are formed by complete and incomplete cycles. Complete cycles show a transition from central to intermediate and then to marginal facies associations and include two types: C1 cycle with central lake deposits consisting of evaporites and black shales; and C2 cycle with central lake deposits formed by grey/green shale. Complete cycles are attributed to the upward gradation from central to marginal environments of the lake or saline pan-sabkha system. Incomplete cycles are either successions with central and intermediate facies associations (I1) or successions with

[*] Authors: J.D.S. Paz & D.F. Rossetti. *Geological Magazine*, in press.

intermediate and marginal facies associations (I2), which represent shallowing-upward successions where at least one facies association is lacking. The higher rank cycles average 5.2 m thick and consist of four depositional units that display shallowing-upward successions formed by complete and incomplete intermediate rank cycles that vary their distribution upward in the section, and are bounded by sharp surfaces.

While the lower rank cycles display characteristics that reveal their seasonal signature, detailed sedimentological characterization and understanding of stratal stacking patterns related to the intermediate and higher rank cycles supports a genesis linked to syn-sedimentary tectonic activity. This is particularly suggested by the high facies variability, limited lateral extension, and frequent and random thickness changes of the intermediate-rank cycles. Additionally, the four higher rank cycles recognized in the Codó Formation match with stratigraphic zones having different styles of soft-sediment deformation structures attributed to seismic activities. Therefore, the several episodes of lake shallowing recorded in the Codó Formation are linked to seismic pulses that alternated with sediment deposition. This process would have created significant changes in the lake water level, and resulted in sharply bounded successions internally displaying deeper to relatively shallower facies associations in the upward direction.

Key-words: lake system, cyclic sedimentation, evaporites, syn-sedimentary tectonics, Late Aptian, Brazil.

2.1. INTRODUCTION

Shallowing-upward cycles are one of the most common characteristics of lacustrine successions, and many authors have related them to orbital forcing (e.g., Olsen, 1986; Glenn & Kelts, 1991; Olsen & Kent, 1996, 1999; Juhász *et al.*, 1997; Vugt *et al.*, 1998; Steenbrick *et al.*, 2000; Hofmann *et al.*, 2000; Aziz *et al.*, 2000). Developments in the understanding of facies relationship and thickness consistency have also allowed lacustrine cycles to be related to tectonic pulses. However, only a few studies have clearly demonstrated the linkage between shallowing-upward cycles and tectonics (e.g., Martel & Gibling, 1991; Anadon *et al.,* 1991).

The Codó Formation (Upper Aptian) exposed in several quarries along the eastern Grajaú Basin, northeastern Brazil (Fig. 2-1), is a saline lacustrine to sabkha complex characterized by different ranks of shallowing-upward cycles. This unit, particularly well exposed in the Codó and Grajaú areas, consists chiefly of bituminous shales, evaporites and limestones, forming a succession up to 25 m thick. Internally, the Codó Formation displays several depositional cycles formed by episodes of upward shallowing. Although smaller scale cycles are probably attributed to seasonal fluctuations, intermediate and higher rank cycles show features that do not match with climate influence. In this work we present a detailed sedimentological and stratigraphic analysis of the shallowing upward cycles recognized in the Codó Formation, in order to demonstrate that their genesis are, at least in part, related to syn-sedimentary tectonic pulses.

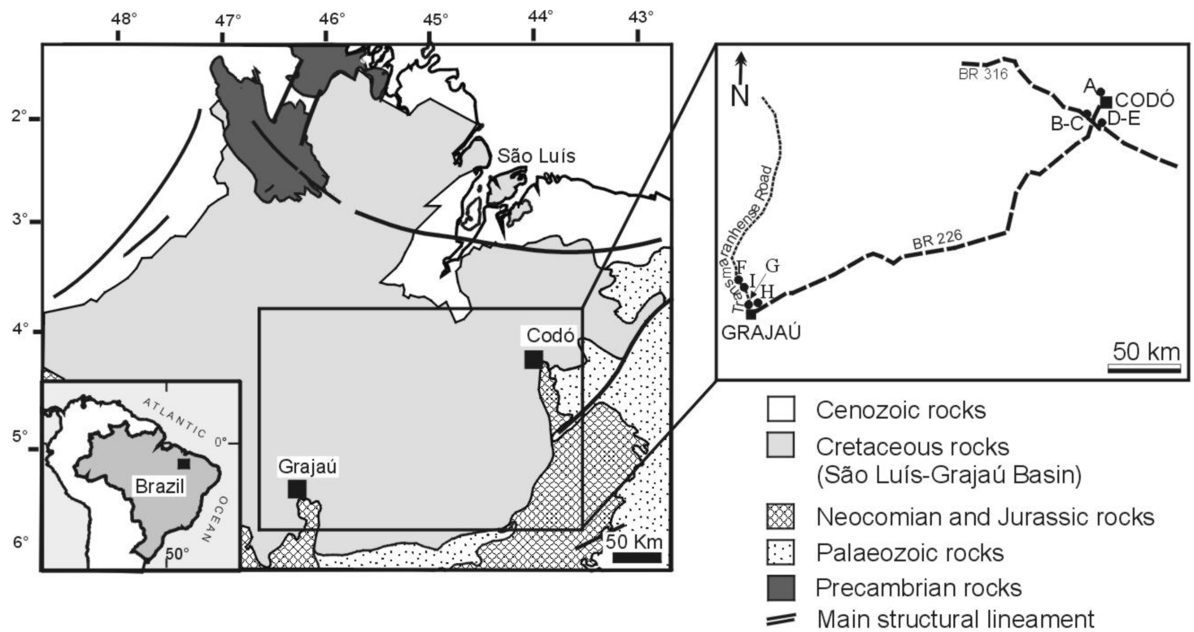

Fig .2-1: Location map of the study area in the eastern and southern of São Luís-Grajaú Basin, northern Brazil, with indication. The map to the right indicates the studied localities where the Codó Formation is well exposed in limestone and evaporite quarries. (A=Santo Amaro; B-C=Itapicuru Evaporite Quarry; D-E=Itapicuru D-6 Limestone Quarry; F= Transmarenhense Road-Km 22; G=Olho D´água Quarry; H=Chorado Quarry; I=Transmaranhense Road-Km 16.

2.3. GEOLOGICAL SETTING

The split up of Africa and South America continents led to the establishment of several rift basins along the equatorial Brazilian margin. The São Luís and Grajaú basins are expressive examples of this tectonic phase, occupying together more than 150,000 km^2. These basins are interpreted to represent a unique structural feature formed by combination of pure shear stress and strike-slip deformation associated with an intracontinental rift (Góes & Rossetti, 2001). Fault displacement (Fig. 2-2a,b) initiated during the Aptian, resulting in a shallow basin where the Codó Formation was deposited. During the main rifting in the Albian, fault offsets reached up to 400 m, culminating with the amplification of the rift system. Vertical to sub-vertical, normal and reverse faults cut through the entire sedimentary package, with some continuing downward into the crystalline and Palaeozoic basement. Three main fault trends can be distinguished (Fig. 2-2a): NE/SW, NW/SE, and less commonly E-W (Rezende & Pamplona, 1970; Azevedo, 1991). The latter is closely associated with the E-W-oriented Sobradinho Fault, which represents the continuity of the Romanche Transcurrent Zone (Pindell, 1985). E-W oriented thrust faults with offsets of a few meters are present in outcrops located in the southern and eastern margins of the basin (Góes & Rossetti, 2001).

The Codó Formation records the Upper Aptian deposition of the São Luís-Grajaú Basin. Gamma-ray log correlation in this basin shows that the sedimentary record consists, from bottom to top, of three major, probably second-order, depositional sequences bounded by regional discontinuity surfaces, interpreted as sequence boundaries (Rossetti, 2001; Fig. 2-3). The two lowermost sequences (S1 and S2) are Aptian to Middle Albian in age, and show an internal tripartite organization into lowstand, transgressive and highstand systems tracts (Rossetti, 2001), as expected in a complete depositional sequence. The lowstand systems tracts of sequences S1 and S2 comprise continental (i.e., fluvial, deltaic, eolian and lacustrine) deposits in the southern margin of the Grajaú Basin, which interfinger with shallow marine/estuarine deposits to the north in the São Luís Basin. In both sequences, the transgressive systems tracts are characterized by muddy lithologies with marine fossils that sharply cover the underlying sandier deposits, resulting in wedges that pinch out southward. Discontinuity surfaces marked by sharp lithological contrast define the base and top of these successions and are interpreted as transgressive and maximum marine flooding surfaces, respectively (Rossetti, 2001). The highstand systems tracts are characterized by deposits displaying aggradational stratal patterns that grade upward into intervals with an overall prograding character, formed when the relative sea level started to decline at the end of the highstand stage. In contrast to sequences S1 and S2, sequence S3 does not show a tripartite internal organization, but consists of several sharply bounded, fining- and then coarsening-

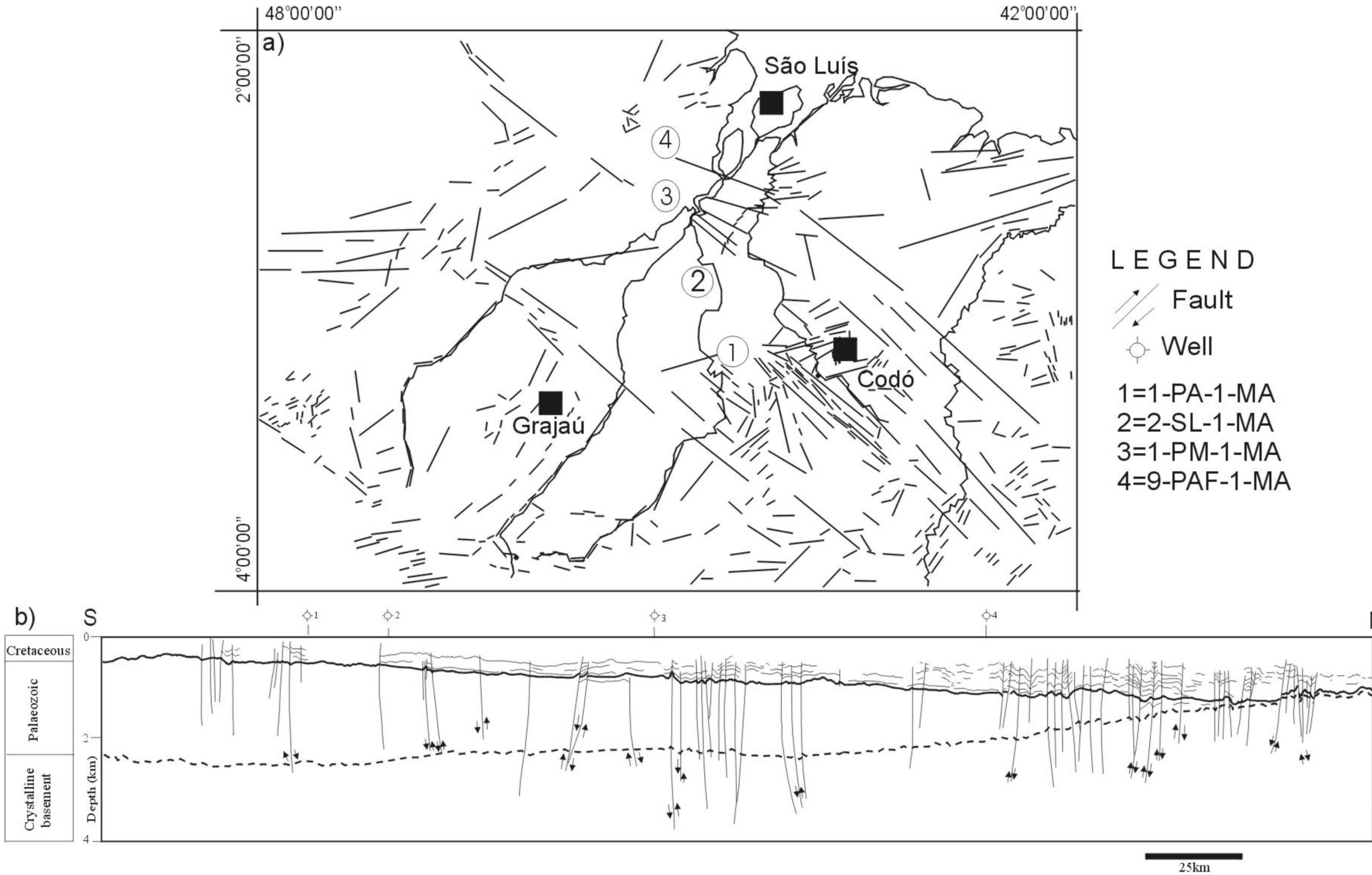

Fig .2-2: a) Map displaying the structural lineaments of the São Luís-Grajaú Basin. Note the main NW-SE, and NE-SW oriented fault traces, and the subordinate E-W lineaments, the later representing the record of the strike-slip phase of the basin. b) A geological section interpreted from a seismic line and the well logs indicated in figure a, with the plot of the main fault traces. Note that these are vertical to nearly vertical and represent reactivations of faults derived from the crystalline and Palaeozoic basement. The faults cut throughtout the entire basin, particularly disrupting the Cretaceous successions, attesting the rift development (Modified after Góes & Rossetti, 2001)

TECTONIC STAGE	AGE	DEPOSITIONAL SEQUENCE	STRATIGRAPHIC UNIT	
Drift	Plio-Pleistocene		Post-Barreiras Sediments	
	Miocene		Barreiras Formation (II)	
	Early Tertiary?		Barreiras Formation (I)	Pirabas Formation
	Late Cretaceous	Sequence S3	Itapecuru Group	Cujupe Formation
	Late Albian/ Cenomanian			Alcântara Formation
Rift	Upper and Middle Albian	Sequence S2		Undifferentiated Unit
Pre-rift	Lower Albian/ Upper Aptian	Sequence S1	Codó Formation	Grajaú Formation

Fig .2-3: Stratigraphy of the São Luís-Grajaú Basin.

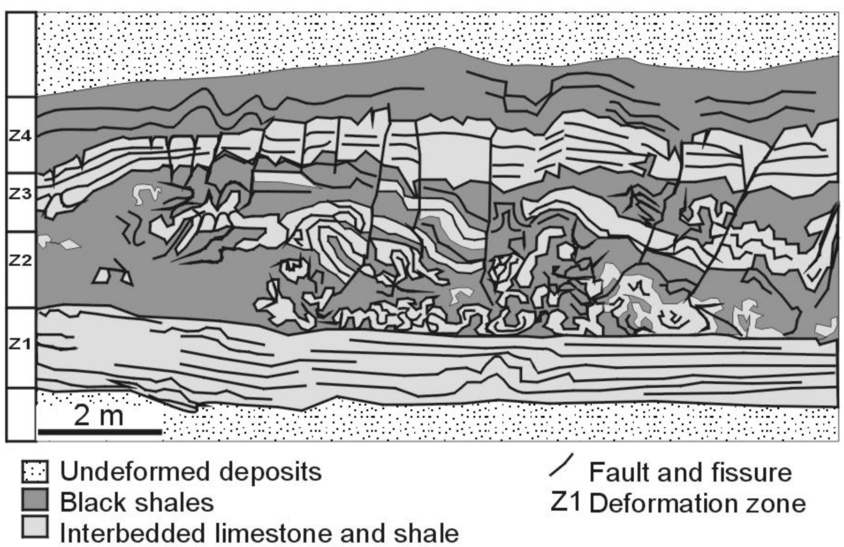

Fig .2-4: Exposure of the Codó Formation in a limestone quarry, near the town of Codó, eastern São Luís-Grajaú Basin, with indication of the syn-sedimentary soft sediment deformation zones formed by seismic activity as described in the text.

upward successions. At least the two uppermost ones are partly exposed and record estuarine systems formed during the Late Cretaceous (Rossetti, 2001).

The Codó Formation correlates with the lowstand deposits of sequence S1 described above (Fig. 2-3). It is interesting to note that, in the southern margin of the basin, the Codó Formation contains a horizon marked by soft-sediment deformation sandwiched within entirely undisturbed deposits, which are attributed to syn-sedimentary seismic activity. Four zones of deformation were recognized (Rossetti & Góes, 2000), which are briefly summarized here (Fig. 2-4) due to their close relationship with the shallowing-upward cycles discussed in this paper. They include: (1) zone Z1, with cracks filled by fine-grained calcite crystals, small-scale faults, fissures and stylolites inclined at a high angle to bedding; (2) zone Z2, represented by complex convolute folds associated with thrust faults, pseudonodules, and mound-and-sag structures, the later requiring alternating periods of deposition and sediment deformation; (3) zone Z3, which is associated with intraformational boulders up to 2.5 m long, consists of normal faults and fissures that are vertical to near vertical, present ragged morphologies, with small, delicate edges, and taper both downward and upward after a few centimeters; and (4) zone Z4, characterized by shales with irregular convolute folds. This vertical succession of deformation events were attributed to syn-sedimentary shear stresses associated with the early rifting that gave rise to the São Luís-Grajaú Basin. These syn-sedimentary seismic pulses seem to have had a strong influence on the evolution of the Codó lake and saline pan/sabkha complex and on the origin of its shallowing-upward cycles, as proposed in this paper.

2.4. DEPOSITIONAL ENVIRONMENT

A detailed facies analysis of the Codó Formation was presented elsewhere (Paz & Rossetti, 2001; Rossetti *ert al.*, 2004). However, given its importance to provide a general overview on the depositional setting and define the shallowing-upward cycles discussed here, the main descriptions and interpretations will be summarized in this section, together with some new information that helps to support the proposed paleoenvironmental model. The Codó Formation can be described in terms of four facies associations in the study areas (Fig. 2-5), which are attributed to central lake, intermediate lake, marginal lake, and saline pan/sabkha depositional environments. Ostracods, including two genera, *Harbinia* and

Candona, are abundant throughout these deposits, occurring either dispersed or as thin (up to 10 cm thick) beds of shell mittens. Disarticulated and articulated shells, including both young and adult individuals, are present, as are freshwater *Charophytes* algae.

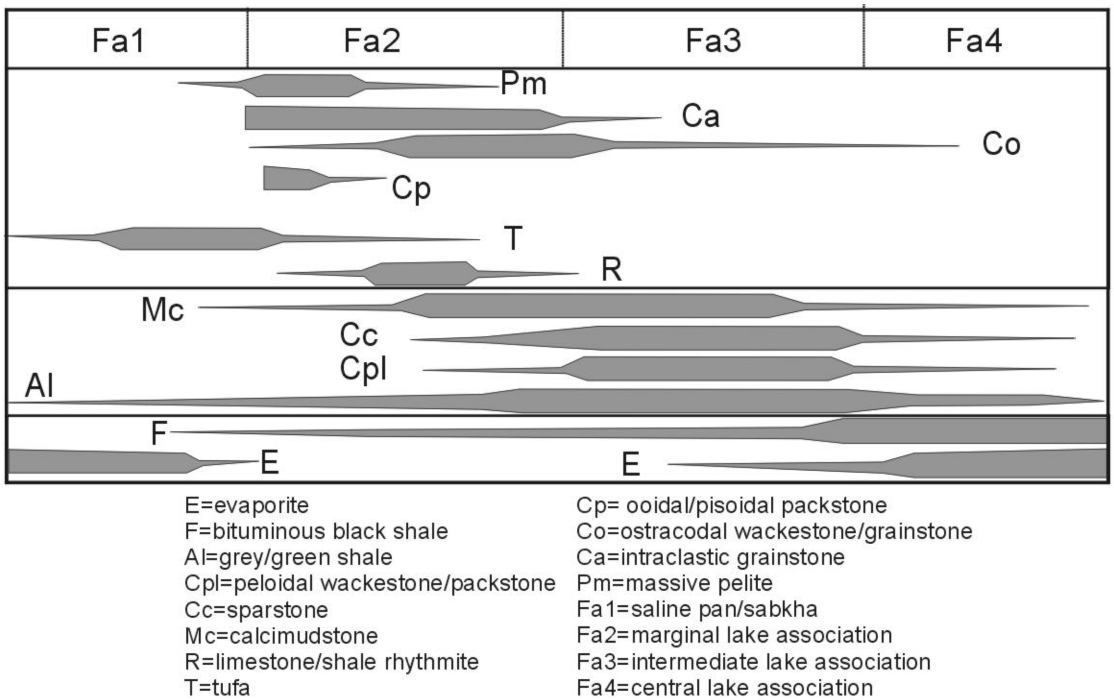

Fig .2-5: A summary of sedimentary facies described in the Codó Formation, with their distribution arranged according to facies associations Fa1 to Fa4, attributed to marginal, intermediate and central lake environments, as well as saline pan/sabkha complex, respectively.

2.4.1. Central lake facies association:

The central lake deposits (Fig. 2-6a,b) occur at the base of the shallowing-upward cycles, and consist mostly of bituminous black shale and evaporite (mostly gypsum). The bituminous black shale is the most frequent facies in this association, occurring as packages up to 3 m thick. It consists of bituminous shales (Fig. 2-6b), with total organic content up to 30%, which contain plant remains, pyrite crystals that are as large as 0.5 cm, and lenses of native sulphur. Silt grain sizes include quartz and feldspar grains, while clays are composed mostly of detrital (irregular, laminated flakes) smectite and, secondarily, kaolinite and illite. Bioturbation does not occur in this facies association.

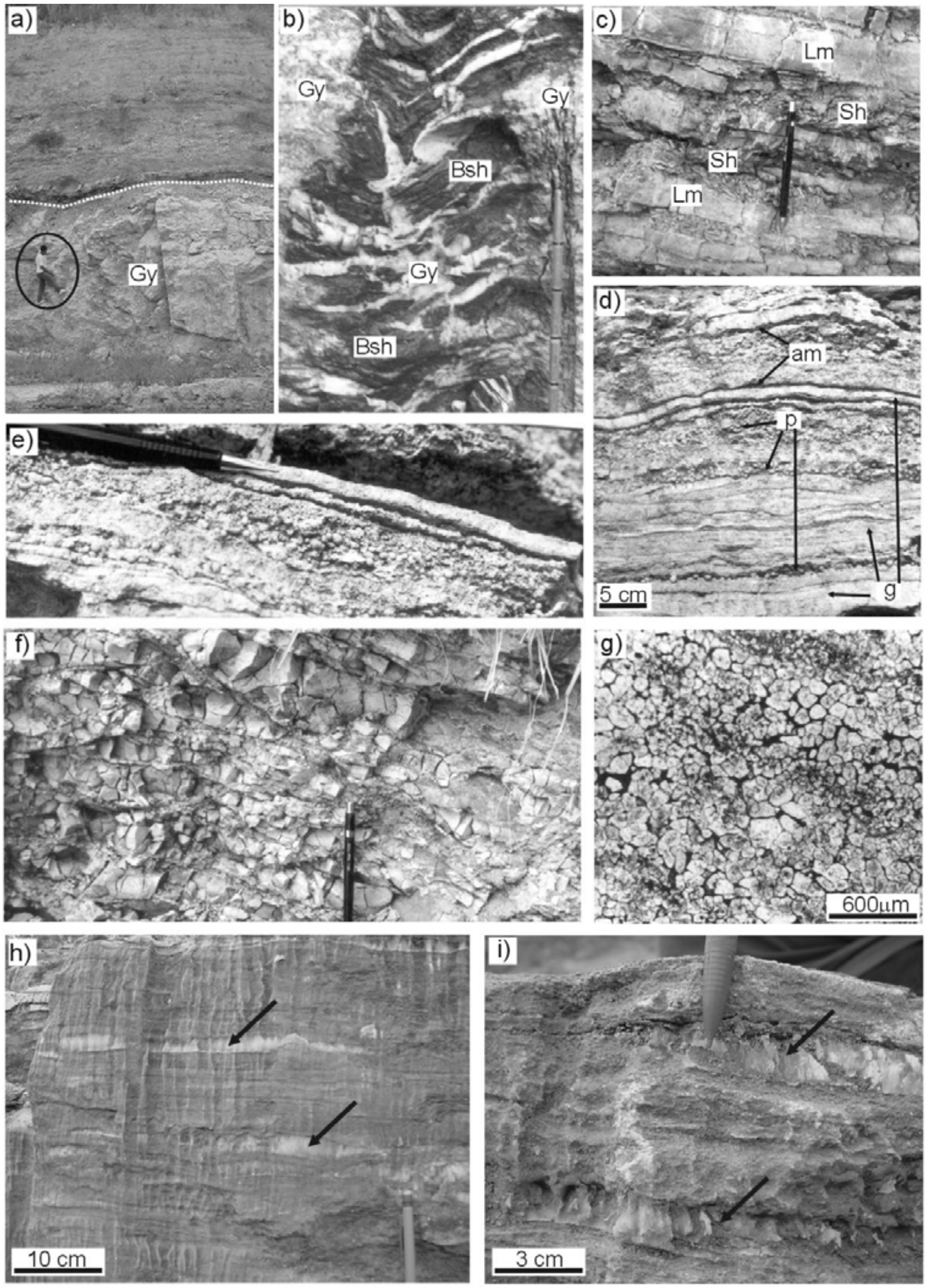

Fig .2-6: Sedimentary facies representative of the Codó Formation in the study area. a, b) Central lake deposits, with massive macronodular evaporites (Gy) and bituminous black shales (Bsh) within evaporites. The hatched line in a, indicates the top of the evaporite beds. The deposits overlying this surface consists of limestone and grey/green shale interbeddings, attributed to transitional lake settings. (person in a for scale=1.6 m tall; rod subdivision in b=10 cm). c) Transitional lake deposits, consisting of limestone (Lm) and grey/green shale (Sh) interbeddings. (pen for scale=15 cm long) d-g) Marginal lake deposits, illustrating: rhythmites of ooidal/peloidal packstone (p) and ostracodal wackestone-grainstone (g) with cryptomicrobial mats (am) in d; a detail of the ooidal/peloidal packstone in e; fractured massive pelite in f; and photomicrography of intraclastic grainstone in g. (pen for scale in e and f=15 cm long). h-i) Saline pan/sabkha deposits, illustrating the layered gypsum. (arrows indicate laminae of gypsum formed by vertical aligned chevron crystals). Note in h the cycles formed by darker/lighter couplets, which consist of microgranular gypsum/vertical aligned gypsum, respectively, attributed to seasonal fluctuations.

The evaporite facies reaches up to 5 m in thickness and includes massive/macronodular (Fig. 2-6a) and, subordinately, layered gypsum. Packages of gypsum up to 1 m thick showing well-developed horizontal lamination are locally present. The massive gypsum forms unstructured bodies intergraded with macronodular gypsum, the latter consisting of centimeter-sized nodules with or without a shale matrix. The gypsum nodules display an almond-like form, defined by a web of undulating, horizontal to oblique fractures filled by bladed crystals up to 0.5 cm thick and with compromise contacts that grow perpendicularly to the fracture walls. Rosettes of dark gypsum up to 5 cm in diameter are common in this facies. The massive/macrogranular gypsum is in sharp contact with the layered gypsum, locally forming diapirs several meters long. The latter comprises laterally continuous, horizontal alternating dark/light beds that vary from few mm up to 10 cm thick. The dark beds are formed by either crystals or micronodules of gypsum less than 0.5 cm long distributed within a matrix of black shale, while the light beds consist of upward-oriented chevron gypsum crystals.

2.4.2. Transitional lake facies association:

The transitional facies association (Fig. 2-6c) consists of interbedded grey/green shale and limestones. Bioturbation is locally present, as are symmetrical ripple marks at the top of some limestone beds. The grey/green shale is the dominant facies in this association, occurring particularly well developed in the Grajaú area, where it reaches up to 4 m thick. The total organic content of this facies is much lower than in the black shale, reaching only up to 1 %. Films of gypsum or calcite as acicular or fibrous, vertically aligned crystals, are locally present on bed planes.

The limestones can be described in terms of three facies: calcimudstone, peloidal wackestone-packstone, and sparstone. The calcimudstone is the dominant limestone facies in this association. It consists of microcrystalline calcite, locally silicified to chalcedony, which occurs as laterally continuous, either laminated or massive beds up to 15 cm thick. Grains of quartz and mica (mostly muscovite) occur disperse or parallel to bed planes. The peloidal wackestone-packstone facies forms beds up to 20 cm thick, characterized by well sorted, rounded to sub-rounded, spherical to oblate peloids within a micrite matrix. Disarticulated ostracod shells and microspherules are frequently present, reaching up to 15 % of the allochemical grains. This facies is commonly parallel laminated and, less commonly, massive. Films of microbial mats might be present paralleling bed planes. The sparstone facies (cf. Wright, 1992) consists exclusively of calcite crystals ranging in size from 250-500 μm and displaying sutured contacts, arranged as a blocky mosaic.

2.4.3. Marginal lake facies association:

The marginal lake facies association (Fig. 2-6d-g) occurs at the top of the shallowing-upward cycles and comprises a variety of intergrading lithofacies, including: pelite, intraclastic grainstone, ostracodal wackestone to grainstone, ooidal/pisoidal packstone, rhythmite (Fig. 2-6D,E), tufa, and sandstone. Wave-ripple marks are commonly observed within this facies association, and gypsum occurs locally as discontinuous laminae. Bioturbation is, in general, absent, though a few undetermined tiny traces were locally observed.

The pelite facies is endurated, massive, and display a blocky texture (Fig. 2-6f). Its colour varies upward from olive-green to brownish-red. The intraclastic grainstone (Fig. 2-6g) consists of well sorted and well rounded, fine- to coarse-grained calcite grains. This facies forms structureless and, less commonly, tabular and sigmoidal cross-stratified beds that are up to 20 cm thick. Mm-cm long lensoid cavities (i.e., fenestrae), locally filled by mosaics of sparite, are typical of this facies, as are microkarstic structures, and vadose meniscate calcite cement. Ostracodal wackestone to grainstone occurs as beds or concretions up to 15 cm thick, the latter typically displaying articulated shells with a mixture of young and adult individuals. Ooidal/pisoidal packstone consists of coalescing, well-rounded or elongated ooids and pisoids (diameter<5 mm) displaying internal botryoidal or fibrous radial fabric. This facies forms layers up to 5 cm thick, but which are laterally continuous for the entire extension of the exposures (at least hundreds of meters). Rounded to slightly elongated fenestrae are abundant in this facies. The tufa facies is a highly porous limestone with sparry calcite filaments arranged into a dendritic web. Rounded calcite grains less than 200 μm of diameter occur encrusting the branches. Rhythmite occurs as packages 10-20 cm thick of thinly (millimeter-scale) laminated, ostracodal wackestone-grainstone, shale, and less commonly, siltstone beds. Fish are abundant in this facies. Cryptomicrobial mats are abundant in association with ooidal/pisoidal packstone and rhythmites, being recognized in the field as black, corrugated films parallel to bed planes.

The sandstone facies is structureless and occurs only locally as lenses up to 0.5 m thick, being represented by moderately sorted, well rounded, fine-grained, quartz grains.

2.4.4. Saline pan/sabkha facies association

This facies association is up to 6 m thick, being mostly present in the Grajaú area, where it occurs between lacustrine deposits. This is an evaporite-dominated association constituted by layered gypsum, gypsarenite, and secondarily tufa, grey/green shale, and calcimudstone. The three latter facies will not be described here, as they have the same characteristics described in previous facies associations. Tufa is much more expressive in this facies association than in the marginal lake deposits, occurring as beds up to 5 cm thick that disappear laterally within few meters. A typical feature of this facies association is the preservation of primary horizontal layering.

The layered gypsum (Fig. 2-6h,i) consists of horizontal beds typically formed by alternating darker and lighter couplets that become progressively thicker upward, varying from few mm to 30 cm. The darker beds consist of either crystals or micronodules of gypsum, in general less than 5 mm long, which occur within a matrix of dark mudstone. The lighter gypsum consist of upward-oriented crystals displaying aligned twin-planes and superimposed growth faces with acute angles arranged in zig-zag, perpendicularly to the crystal long axe (i.e., chevron gypsum); the chevron gypsum intergrades with acicular gypsum.

The gypsarenite is interbedded with the layered gypsum, and forms layers few cm thick of moderate to poorly sorted, rounded to sub-rounded gypsum grains with sizes varying from very coarse to pebbly. Calcite cement is common. This facies increases in frequency upward in this association. Shallow (i.e., <2 mm deep) potholes averaging 3 cm in diameter and with ragged concave up shapes completely filled up by layers of growth-aligned gypsum crystals, are present at the top of some gypsarenite beds. A film of yellow to light brownish calciferous clay is settled out on the bottom of these structures.

2.4.5. Interpretation:

Although displaying similar lithologies, a comparison of the sedimentary features and facies architecture between the Grajaú and Codó areas revealed some basic differences in their depositional systems. Hence, the Codó area displays deposits formed in comparatively more stable, well-stratified lakes with significant periods of anoxia and closure, when evaporites where formed almost exclusively in deeper, central areas. Facies analysis, added to the abundance of continental ostracods and *Charophyte* algae, as well as the absence of any marine fauna, led us to attribute these deposits to a dominantly lacustrine system. The abundance of shales in the central lake deposits shows a low energy depositional setting. Pyrite, bitumen, well-preserved fossils (i.e., ostracods and fishes) and the almost complete lack of bioturbation support anoxic conditions. Under such circumstance, the preservation of large amounts of organic matter is favoured, being derived from organisms living in upper, more oxygenated water layers (Trewin, 1986; Martill, 1988).

The transitional lake facies association is characterized by its position between central and marginal lake facies associations. The abundance of fine-grained deposits, recorded by calcimudstones and grey/green shales consistent with a low energy environment with abundant mud deposition below wave base (e.g., Specht & Brenner, 1979; Shinn *et al.*, 1989). In this sense, this association resembles central lake deposits, but the lighter colour, suggesting less preservation of organic matter and absence of bitumen, as well as the local bioturbated horizons, symmetrical ripple marks, and disarticulated ostracod shells, support a shallower environment relative to the central lake association, with more oxygenated waters and wave action.

The marginal lake facies association was recognized by its position at the top of the shallowing-upward cycles and by the abundance of sedimentary features attributed to subaerial and/or meteoric exposure, such as palaeosoil (recorded by the massive pelite), microkarstic surface, fenestrae and meteoric cement. The presence of coalescing pisoids with variable sizes, elongated shapes that are associated with microbial mats suggests stagnant, shallow water condition and/or even subaerially exposed environments (e.g., Risacher & Eugster, 1979; Chafetz & Butler, 1980; Schreiber *et al.*, 1981; Tucker & Wright, 1990). Under such conditions, microbes lead to *in situ* formation of pisoids (cf. Ferguson *et al.*, 1978), an interpretation favoured in the study area due to the close association of pisoids and microbial mats. Fenestrae support formation close to the vadose zone. The concretions of ostracodal wackestone-packstone associated with these deposits might have resulted from a microbial influence (Raiswell, 1976) combined with anisotropic permeability, since the concretions occur within more permeable limestone/shale rhythmite that overlies less permeable shales. The local occurrence of sandstone facies in this association is probably related to episodic influx of sands during raining episodes through small deltas.

As opposed to the Codó area, much more ephemeral conditions prevailed in the Grajaú area, which presented better-oxygenated water pans having evaporite precipitation only in their margins and along the surrounding mudflats, configuring a saline pan/sabkha complex. This depositional setting displays widespread pans and evaporitic flats, the first being restricted to more depressed local areas of the system. The distinguished depositional setting recorded in the Grajaú area might have been crucial to control the distribution of the evaporite deposits. A saline pan/sabkha facies association is indicated by evaporite precipitation in a very shallow subaqueous environment that was interrupted by periodic exposure. The thin beds of grey/green shales and calcimudstones are attributed as the record of deeper waters, probably representing central saline pans. Shallower areas of the pans and surrounding flats were dominated by evaporite deposition. The dominance of gypsum with well-preserved horizontal lamination reflects original bedding on flatter-lying environments surrounding the saline pans. The chevron growth-aligned crystals of the lighter beds attest to primary gypsum deposition on the floor of brine pools. Precipitation of similar features in many modern and ancient environments occurs when water depths is less than only 2 m (e.g., Logan, 1987; Hovorka, 1987; Handford, 1991; Smoot & Lowenstein, 1991). Shallow waters favour a high degree of supersaturation, as well as a less dense and unstable brines, which are conditions required to promote the upward growth of crystals. The darker beds in the couplets record displacive intrasediment growth of crystals beneath the brine from supersaturated pore fluids in the capillary and/or upper phreatic zone, thus requesting periods of descending ground waters and eventual exposure (e.g., Kerr & Thomson, 1963, Warren, 1999). These deposits formed slightly post-depositionally, but still under a strong influence of the depositional setting as precipitation took place within only a few mm of the depositional surface. The alternating dark and light gypsum couplets are attributed to pulsating episodes of water table.

The growth-aligned crystals grew up in the interface sediment-brine during times when saturated brines were flushed into the basin. The formation of such evaporite layers requires a subaqueous environment with stable phases to allow the aggradation of the upper euhedral surface of the crystals (Warren, 1999). As the water level falls, precipitation of this type of crystals is precluded. During these episodes, evaporite precipitation in the study area occurred only below the sediment interface.

The gypsarenite records moments when evaporite crystals were reworked. Because these deposits are mostly associated with the layered gypsum, it is possible that its formation is due to reworking of growth-aligned crystals as the water level slightly decreased, but with the process occurring still subaqueously. The increased occurrence of this facies upward in the evaporite section attests to progressive shallowing, an interpretation that is supported by the presence of numerous potholes attributed to partial evaporite dissolution due to subaerial exposure. As the evaporite basin was dissected, the deposits were at least momentously kept above the water level and dissolution took place forming these small depressions. Water accumulated in these depressions, bringing suspended sediments, that were settle down forming the clay films. A later submergence of the dissolved planes led to the infill of the potholes by thin layers of growth-aligned crystals.

2.5. SHALLOWING-UPWARD CYCLES AND DEPOSITIONAL UNITS

2.5.1. Description

Three ranks of shallowing-upward cycles are distinguished in the Codó Formation. The lower rank cycles display regular thickness ranging from 5 to 10 cm, and consist of facies that vary according to the position in the lake setting. Hence, the central lake deposits show interbeddings either of bituminous black shales and evaporites, or bituminous black shales with streaks of calcimudstone and bituminous black shales with native sulphur. The intermediate lake deposits display bituminous black shale interbedded with peloidal wackestone-packstone or grey/green shale interbedded either with calcimudstone or peloidal wackestone-packstone. The marginal lake deposits show either grey/green shale and ostracodal wackestone/grainstone, as well as alternations of ostracodal wackestone/grainstone and/or calcimudstones with cryptomicrobial mats and ooidal/pisoidal packstones. The lower rank cycles in the saline pan/sabkha deposits consist of alternating dark and lighter gypsum, consisting of microgranular gypsum grown within shales and vertical aligned gypsum crystals, respectively. These are locally arranged into packages containing 3 to 7 couplets (Fig. 2-6H); a succession of 4/7/5/6/6/7/6 couplets was counted at one place.

The intermediate rank cycles vary from a few 0.3 m up to 5.6 m thick (averaging 1.7 m thick), and contain the lower rank cycles. They can be either complete or incomplete according to the relative proportion of facies associations representing the several lacustrine and saline pan/sabkha sub-environments (Fig. 2-7). Hence, complete cycles display facies associations that record the upward gradation from central to marginal environments of the lake or saline pan-sabkha system, attesting to the complete preservation of one shallowing episode. Three different types of complete cycles were recognized (Fig. 2-8): complete cycles type 1 (C1), where central lacustrine deposits are entirely formed by evaporites and bituminous black shales; and complete cycle type 2 (C2), where central lake deposits consist of black and/or grey/green shales and limestones; and complete cycle type 3 (C3), where grey/green shale and calcimudstone record central saline pan environments, and evaporites (layered gypsum, gipsarenite) and tufa record shallower saline pan and surrounding evaporitic flats. Incomplete cycles are defined by shallowing-upward successions where at least one facies association is lacking. There are also three types of incomplete cycles (Fig. 2-8): incomplete cycle type 1 (I1), where central and intermediate lake associations dominate; incomplete cycle type 2 (I2), composed mostly of intermediate and marginal lake facies associations; incomplete cycle type 3 (I3), consisting of only shallower saline pan and evaporitic flat deposits.

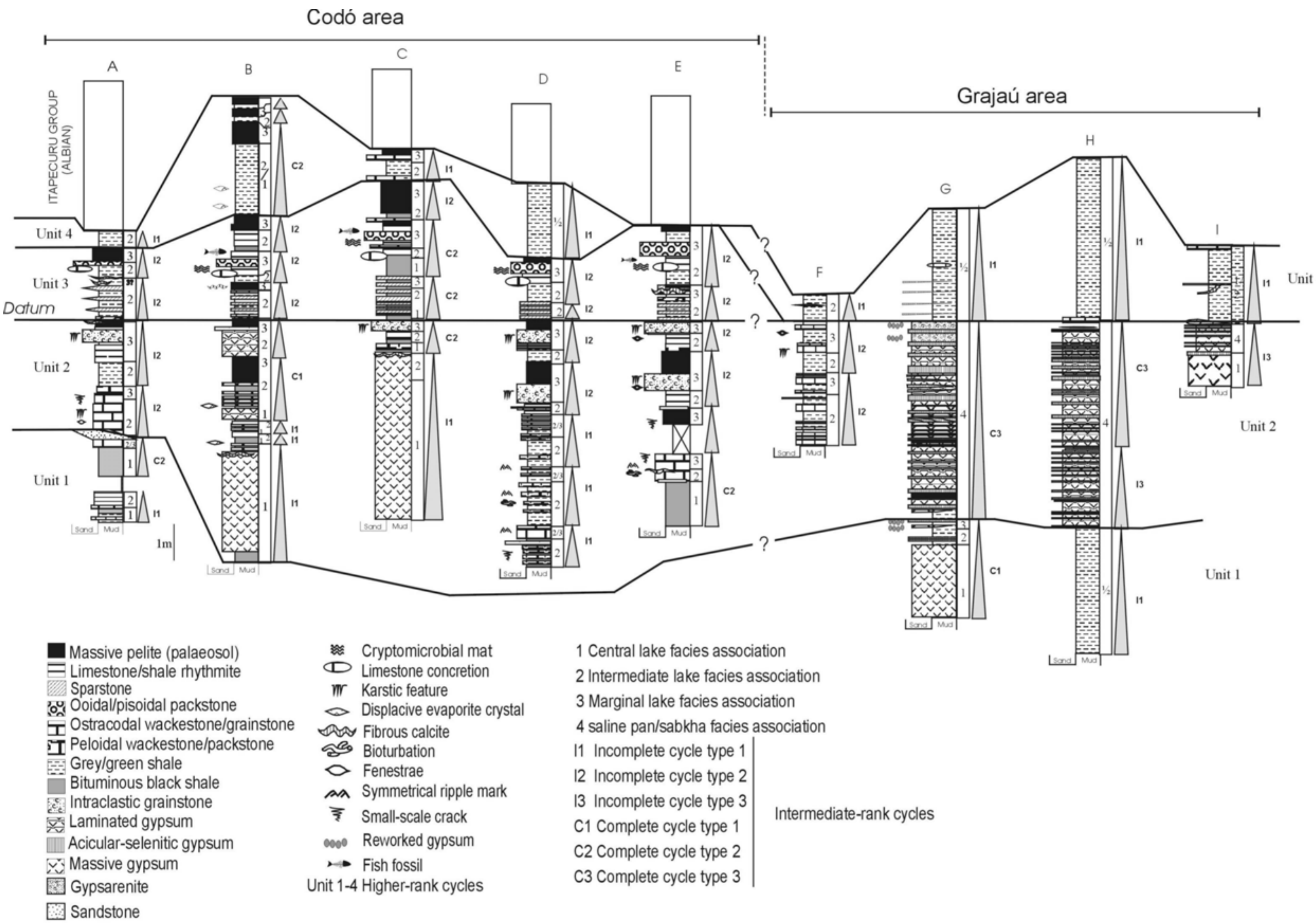

Fig .2-7: Lithostratigraphic profiles representative of the Codó Formation exposed in the study area, with the main facies characteristics and the two ranks of shallowing-upward cycles described in the text. (See figure 1 for location of the profiles A-I). *Datum*=discontinuous surface with evidences for maximum subaereal exposure within the Codó Formation.

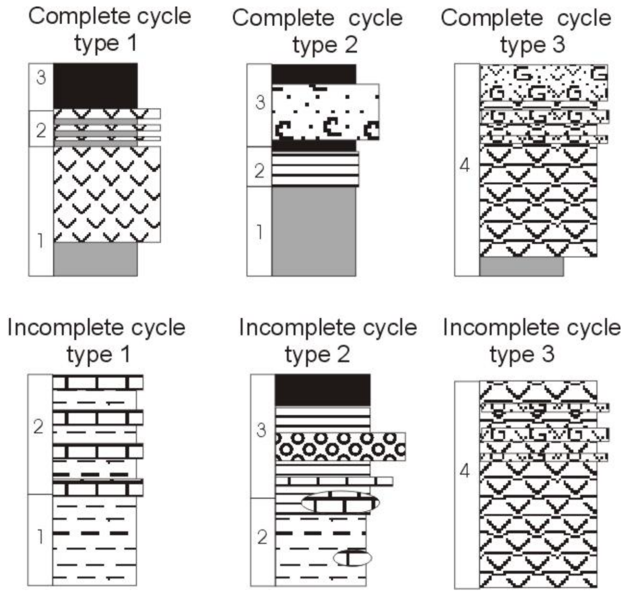

Fig .2-8: Diagrams illustrating the four types of lower-rank, shallowing-upward cycles of the Codó Formation. Thickness of individual cycles range from 0.3-5.6 m. See figure 2-7 for legend.

The higher rank cycles define four laterally continuous depositional units, referred as 1 to 4 from bottom to top (Figs. 2-7, 9a,b). Unit 1 is only partly exposed at the base of the sections and form an interval that reaches up to 3.6 m thick (averaging 2.7 m thick) composed of thin I1 cycles. Its top is either marked by a horizon of breccia containing clasts of grey/green shale up to 5 cm long, or by lenses of medium- to coarse-grained sandstones, which occur along a sharp surface with erosional relief up to 4 m. Unit 2 (Fig. 2-7) reaches up to 8 m thick (averaging 5.2 m) and contains all types of cycles. Although in number there is a prevalence of incomplete cycles, this unit displays the highest volume of complete cycles of the whole Codó Formation exposed in the study area. Up to five successive shallowing-upward cycles were observed in this unit, with C1 cycles being the thickest and dominant ones. These occur mainly in profiles 2 and 3 of the Codó area and profiles 7 and 8 of the Grajaú area (Fig. 2-7). It is noteworthy that the marginal facies of the shallowing-upward cycles located closer to the top of unit 2 are characterized by the abundance of gypsarenite, intraclastic grainstone with fenestrae, karstic features and nodular chert (silcrete). The top of unit 2 is marked by a sharp bounding surface that is either planar or displays an erosional relief up to 1 m at the outcrop scale.

Unit 3 (Figs. 9b and c), confined to the eastern portion of the study area, is up to 3.8 m thick (averaging 2.6 m thick) and is comprised mostly (i.e., nearly 80%) of I2 cycles, with the remaining 20% being represented by C2 cycles. A remarkable and exclusive feature of this unit is the presence of ooids/pisoids and concretions of ostracodal wackestone-grainstone, which constitute important stratigraphic markers throughout the study area. The latter occur invariably at the transition from intermediate to marginal lacustrine deposits, while the ooids/pisoids are present in marginal lake deposits located close to the top of unit 3. The concretions bearing articulated ostracod shells include a mixture of juvenile and adult individuals. These lithologies are interbedded with rhythmites bearing abundant articulated and disarticulated fish bones, and which also contain a high volume of former microbial mats. Unit 3 is also bounded at the top by a sharp surface with erosional relief up to 2,5 m.

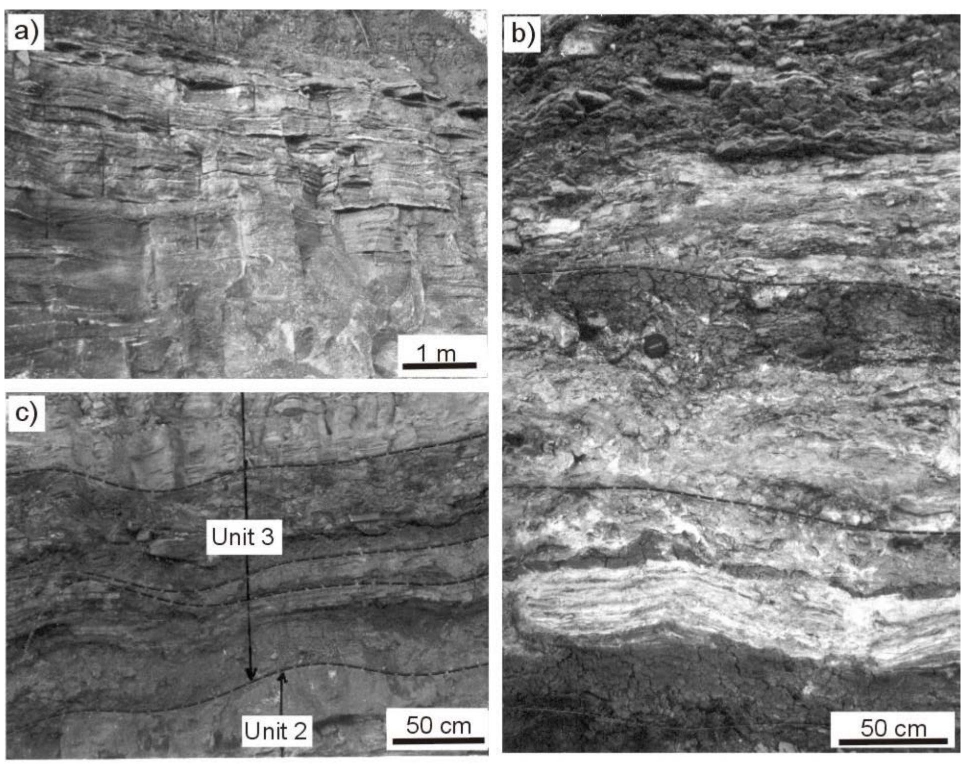

Fig .2-9: Types of shallowing-upward units present in the Codó Formation, illustrating: a) Unit 2, represented by one complete cycle type 1 with evaporites and shales. b) Unit 3, presented from base to top by two incomplete cycles type 1 and one complete cycle type 2. c) The uppermost portion of unit 2 and the base of unit 3, with the latter showing three incomplete cycles type 1 and an upper incomplete cycle type 2.

The uppermost unit 4 (Fig. 2-9b) is up to 4.6 m thick (averaging 2.2 m thick) and typically starts at the base with grey/green shales containing only thin (< 1 mm thick) laminae of gypsite and/or fibrous calcite, both formed by vertically aligned crystals. Upward, the shales are interbedded with few and thin (mm to few cm) layers of calcimudstones. I1 cycles are dominant in this interval, but no black shales are present. Secondarily, this unit also shows I2 cycles. Unit 4 is truncated by a discontinuity surface showing erosional relief up to 5 m, marked by a red-coloured palaeosol horizon overlain by Albian sandstones and argillites of the Itapecuru Group (Fig. 2-7).

2.5.2. Interpretation:

The lower rank cycles recognized in the Codó Formation record minor changes in depositional conditions, attesting to alternations between mud settling and chemical precipitation of evaporites or limestones. This characteristic, added to the regular thickness variation, is consistent with seasonal fluctuations, with mud deposition and chemical precipitation taking place during less and more arid phases, respectively.

The intermediate rank, shallowing-upward cycles reflect periods of progradation of the lake shoreline resulting from superposition of marginal lake deposits upon intermediate and/or central lake deposits. The higher rank cycles record several episodes of upward-shallowing due to lake desiccation, bounded by subsequent floodings. In this sense, they are good continental analogs for parasequences described in marginal marine settings (Vandervoort, 1997). The maximum shallowing was reached at the top of each unit, and it is marked by better-developed marginal lacustrine facies associations, evidenced by the features recording wave reworking and subaerial exposure such as palaeosol, karstic features, fenestrae, and chert (silcrete) nodules.

Units 1 and 2 reflect the prevalence of anoxic conditions and a water column with sufficient depth to favour stratification. The abundance of C1 cycles in unit 2, rich in bitumen and evaporites, is the most representative record of this phase, and is attributed to a phase when the lake had the maximum relative depth, which is consistent with the fact that in this unit cycles are thicker than in the other units.

Unit 3 records a time with the greatest development of marginal lake deposits, suggesting prevalence of shallower water conditions due to lake desiccation. The abundance of ostracodal wackestone-grainstone displaying a mixture of juvenile and adult, articulated ostracod shells, as well as both articulated and disarticulated fish bones, attests to episodes of mass mortality. This event was probably associated to the reduction in the lake area due to shallowing, which is suggested by the fact that only marginal lake deposits display evidence for ostracod and fish mortality. Fish mass mortality recorded in lacustrine settings of the Achanarras Middle Old Red Sandstone of Middle Devonian age from the Orcadian Basin in Scotlant has also been interpreted in a similar way (Trewin, 1986). The reasons that led to this rapid drought in the study area will be discussed below.

Unit 4 records a return to dominantly deeper water conditions, but without significant evaporite precipitation and no black shale formation, as indicated by the prevalence of I1 cycles, characterized by deepest-water deposits with only grey/green shales. This unit is interpreted as deposited during a time when the lake was oxygenated throughout the water column and no water stratification was present. The thickness of the shallowing-upward cycles suggests that the lake depth was again as deep as in unit 2. However, a better understanding of the conditions leading to the formation of unit 2 is precluded due to the strong erosion associated with the development of the late Aptian/Albian unconformity (Fig. 2-2).

2.6. ORIGIN OF THE SHALLOWING-UPWARD CYCLES

Analysis of the vertical stratal stacking patterns represented by the shallowing-upward cycles recognized in the Codó Formation is the key to understand their nature. These cycles were formed as the lake or saline pan/sabkha base level episodically decreased through time. In this depositional system, drop in base level, with resulting facies progradation, is caused chiefly from one or the interaction of the following factors: increase in sediment supply either from a fluvial drainage or a marine inflow, progressively increased aridity, or increase in subsidence due to syn-sedimentary tectonics.

In the particular case of the Codó Formation, the influence of sediment supply might be considered negligible, since siliciclastic sands supplied into the lake system was reduced, as indicated by their scarcity even in marginal deposits. Deciphering whether climate or subsidence linked with syn-sedimentary seismic activity, was the main cause for progradation is not so straightforward, particularly because both factors might be combined in order to produce shallowing-upward units (e.g., Anadon *et al*., 1991).

Climate has been claimed to explain many shallowing-upward lacustrine deposits recorded in ancient and modern environments (e.g., Smoot & Olsen, 1994; Olsen & Kent, 1996; Hofmann *et al.*, 2000; Aziz *et al*., 2000; Steenbrink *et al*., 2000). The small, lower rank cycles, particularly recognized in the saline pan/sabkha deposits of the Codó Formation, record minor changes in depositional conditions, attesting to alternations between mud settling and chemical precipitation of either evaporites or limestones. This characteristic, added to the rhythmic and regular thickness variation, is consistent with seasonal fluctuations, with alternating mud deposition and chemical precipitation taking place during less and more arid phases, respectively. This is specially suggested by the succession of evaporite couplets, which are attributed to pulsating episodes of water table. Although locally observed, packages displaying regularly distributed bundles varying from 4 to 6 are probably resulting from seasonal base level changes.

While seasonal fluctuations may be applied to explain the lower rank cycles recognized in the Codó Formation, the origin of the intermediate and higher rank cycles are probably related to syn-sedimentary tectonics. A climatic cause seems to be unlikely in these instances because, if so, then one would expect an increased precipitation of evaporite minerals during phases of maximum shallowing, when the lake and saline pan level was at the minimum (Carroll & Bohacs, 1999). This did not happen in the Codó Formation, neither in the intermediate cycles, nor in the overall higher rank cycles that form the depositional prograding units described herein.

The intermediate and higher rank cycles recognized in the Codó Formation show characteristics that are better explained by a tectonic signature. A line of evidence might be claimed to suggest tectonics as the main cause for the intermeditate rank cycles: 1. the high variability of facies within individual cycles; 2. the limited lateral distribution, usually on the order of less than a few tens of meters; and 3. the frequent and random change in cycle thickness in the upward direction, ranging from few centimetres up to several meters. These characteristics match better with those typically recorded from tectonically-influenced, shallowing-upward cycles (Martel & Gibling, 1991; Benvenuti, 2003), as climatically related cycles are expected to have more regular thicknesses and more monotonous facies distribution throughout large distances (Hofmann *et al.*, 2000; Harvey, 2003).

The higher rank cycles of the Codó Formation exposed in the Codó area are particularly suggestive of formation under the influence of syn-sedimentary tectonics. These units have been correlatable to Grajaú area based on distinctive features of the surfaces overlying each unit, as formerly discussed in the item 2.5.1. The four higher rank cycles reflect lower frequency episodes of lake shallowing. The two lowermost units record progressive episodes of lake shallowing in deep-water, anoxic conditions, when lake stratification prevailed. Following this phase, progradation of lake shoreline proceeded under shallower water conditions, as recorded by unit 3. The fossil assemblage preserved in this unit indicates mass mortality, suggesting that the reduction in the lake area might have been subtle. Stagnant waters favoured a widespread distribution of microbial mats. A renewed episode of significant lake deepening took place during deposition of unit 4, which at this time occurred under dominantly oxidizing conditions.

A tectonic influence is also proposed for the origin of the higher-rank cycles recorded by deformational structures in the depositional units 1 to 4. This is suggested because these units have good correspondence with stratigraphic intervals representing different styles of deformation zones that characterize the Codó Formation in the Codó area. As summarized in a previous section (see geological setting), these deformation zones (Fig. 2-4) were attributed to alternating periods of sediment accumulation and shear stress associated with syn-sedimentary seismic activity linked to the rifting of the São Luís-Grajaú Basin during the Late Aptian (Rossetti & Góes, 2000). Hence, depositional units 1 and 2 are stratigraphically correlatable with deformational zones Z1 and Z2 (Fig. 2-10), respectively. In other words, during the two first episodes of shallowing recorded in the study area, sedimentation in the lake system was strongly affected first by extensional and, then by compressional forces, as shown by the upward gradation from small scale cracks and normal faults to complex convolute folds associated with thrust faults and vertical to sub-vertical stylolites. Deformation would have initially increased the accommodation space, promoting the development of a thicker higher-rank shallowing-upward cycle (i.e., unit 1) with increased deeper water facies, as recorded by a higher volume of C1 and I1 cycles. As the sedimentary succession evolved, the area might have experienced some compression, with consequent local uplift giving rise to the development of shallower-water facies at the top of depositional unit 2.

Uplift or more stable tectonic conditions would have produced even shallower-water environments in the Grajaú area, represented by the saline pan/sabkha deposits that are represented by complete and incomplete cycles of types C3 and I3, respectively. After this time, a relative stability seems to have prevailed, with the lake basin becoming progressively shallower due to low accommodation rate and resulting in deposition of unit 3, which is characterized by the abundance of I2 cycles. A period of extension led to development of several normal faults and slumpings at the top of unit 3, which corresponds to deformation zone Z3. As a result of this extension, new accommodation space was created and the lake system became relatively deeper, favouring deposition of unit 4, characterized by thicker C2 and I1 cycles. However, anoxic conditions no longer existed during this time, as revealed by the scarcity of organic matter in the shales of this unit. Tectonic activity seems to have continued, resulting in convolution of these deposits and producing deformation zone Z4.

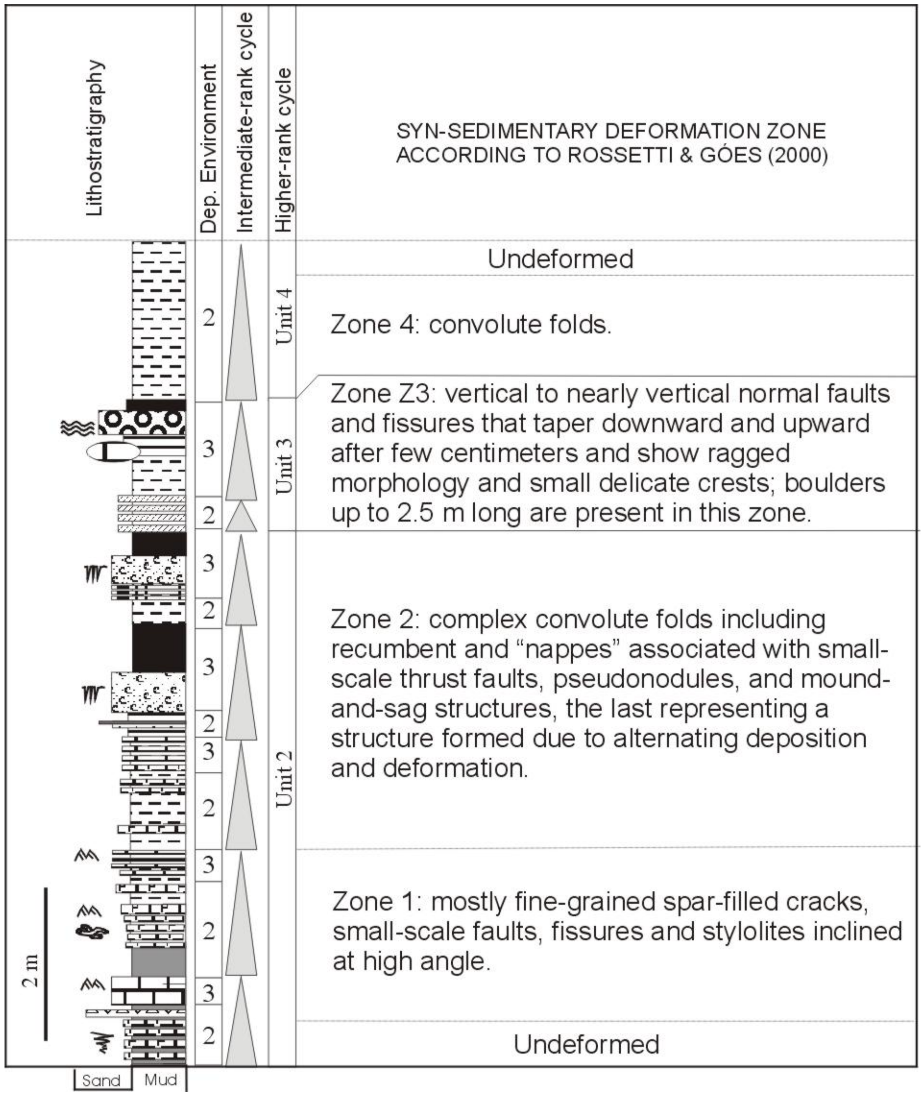

Fig .2-10: A representative lithostratigraphic profile of the Codó Formation showing the good match between higher-rank shallowing-upward cycles, represented by depositional units 2 to 4, and the syn-sedimentary deformational zones described by Rossetti and Góes (2000). (See Fig. 2-7 for legend).

The seismic interpretation of the shallowing-upward cycles provided here is in agreement with the structural framework of the São Luís-Grajaú Basin. As previously presented, the main rift stage of this basin took place during the Albian, but reactivation of ancient fault systems started earlier in the Aptian, with the establishment of a shallow, but widespread basin where the Codó Formation was deposited. The presence of deposits with evidence for soft sediment deformation in this unit is taken as an indication for syn-sedimentary tectonics (Rossetti & Góes, 2000). At the basin margins, where the study areas are located, the displacement of faults with small offsets would have favoured the development of subsiding areas, promoting the establishment of lake systems. The prevalence of fine- grained and chemical deposits in the depositional setting is not inconsistent with this model. Tectonically-influenced settings are usually considered to be recorded by a dominance of coarse-grained siliciclastic deposits. However, modern examples have shown that coarse-grained deposits will not occur immediately following tectonics. Instead, it has been suggested that the first response to tectonics in several settings from marine to lacustrine is represented by fine-grained deposition, as a depositional setting usually takes a time to re-equilibrate and respond to tectonics (Blair & Bilodeau, 1988). In areas dominated by mild tectonics with fine-grained and chemical sedimentation, as occur in the Codó Formation, higher rates of accommodation will give rise to deposition of evaporites and preservation of shales with high organic content in central lake areas (Carroll & Bohacs, 1999). On the other hand, periods of quiescence will favour deposition of shallower-water limestones and evaporites as the accommodation space is reduced. It is possible that the increased sediment reworking, recorded by the occurrence of gypsarenites and intraclastic grainstones in marginal deposits of depositional unit 2, might also be related to this tectonic phase. The presence of breccia and coarse-grained sandstones only at the top of the lowermost higher-rank cycle, represented by depositional unit 1, is probably an indication for a progressive decrease in the intensity of the tectonic process through time.

2.7. CONCLUSION

Although more often attributed to climate fluctuations, many shallowing-upward lacustrine cycles might be resulting from pulsating tectonism taking place contemporaneously with sediment deposition. The Codó Formation, exposed in the eastern Grajaú Basin, seems to be an unequivocal example of an ancient lacustrine system displaying two ranks of shallowing-upward cycles reflecting prograding episodes driven by syn-sedimentary seismic activity. Despite the seasonal signature recognized in the lower rank cycles, a tectonic cause is proposed for the intermediate and higher rank cycles described in this unit. In the particular case of the intermediate rank cycles, a tectonic origin is revealed on the basis of: (1) high facies variability; (2) limited lateral extension; and (3) frequent and random thickness change. The higher-rank cycles were also formed as a result of tectonic episodes that alternated with sediment deposition, a conclusion supported by their matching with stratigraphic zones characterized by different styles of soft sediment deformation that are attributed to contemporaneous seismic activity. Based on the observations made in the study area, one can state that extension affecting lake deposits, with subsequent creation of accommodation space, promotes the development of prograding successions internally formed by thicker (deeper) water cycles. Bed shortening by compression and/or stability reduces the water depth and lead to the development of thinner and shallower-water cycles. Therefore, different styles or/and intensities of seismic pulses alternating with sediment deposition might cause substantial changes in lake level, promoting alternating deeper and shallower water phases, and ultimately resulting in cyclic deposition. Deciphering the genesis of such prograding episodes in ancient lacustrine successions is a task that requires detailed facies analysis and precise mapping of the stratal stacking patterns, as well as their association with tectonically-driven structures.

Acknowlegement. The Itapicuru Agroindustrial S/A is acknowledged for the permission to access the quarries with the exposures of the Codó Formation. This work was supported by the Conselho Nacional de Desenvolvimento Científico e Tecnológico-CNPq (Grant #460252/01). The authors want to gratefully thank Paulo Milhomem (Petrobras) for the ostracod identification.

REFERENCES

ANADON, P., CABRERA, Ll., JULIA, R. & MARZO, M. 1991. Sequential arrangement and asymmetrical filling the Miocene Rubielos de Mora Basin (northeast Spain). In Lacustrine Facies Analysis (eds P. Anadón, Ll. Cabrera and K. Kelts), pp. 257-275, International Association of Sedimentologists Special Publication no. 13. Oxford: Blackwell.

AZEVEDO R.P., 1991. Tectonic evolution of Brazilian Equatorial Continental Margin Basins. Doctoral Thesis, University of London, London, 455 p.

AZIZ, H.A., HILGEN, F., KRIJGSMAN, W., SANZ, E. & CALVO, J.P. 2000. Astronomical forcing of sedimentary cycles in the middle to late Miocene continental Catalayud Basin (NE Spain). Earth and Planetary Science Letters 177, 9-22.

BENVENUTI, M. 2003. Facies analysis and tectonic significance of lacustrine fan-deltaic successions in the Pliocene-Pleistocene Mugello Basin, Central Italy. Sedimentary Geology 157, 197-203.

BLAIR, T.C. & BILODEAU, W.L. 1988. Development of tectonic cyclothems in rift, pull-apart, and foreland basins: sedimentary response to episodic tectonism. Geology 16, 517-520.

CARROLL, A.R. & BOHACS, K. M. 1999. Stratigraphic classification of ancient lakes: balancing tectonic and climatic controls. Geology 27, 99-102.

CHAFETZ, H.S. & BUTLER, J.C. 1980. Petrology of recent caliche pisoliths, spherulites (after *Microcodium*) and speleothem deposits. Sedimentology 27, 497-518.

FERGUSON, J., BUBELA, B. & DAVIES, P.J. 1978. Synthesis and possible mechanism of formation of radial carbonate ooids. Chemical Geology 22, 285-308.

GLENN, C.R. & KELTS, K. 1991. Sedimentary rhythms inlake deposits. In Cycles and events in stratigraphy (eds G. Einsele, W. Ricken, A. Seilacher), pp. 188-221. Berlin: Spring-Verlag.

GÓES, A.M. & ROSSETTI, D.F. 2001. Gênese da Bacia de São Luís-Grajaú, Meio-Norte do Brasil. In O Cretáceo na Bacia de São Luís-Grajaú (eds D.F. Rossetti, A.M. Góes, W. Truckenbrodt), pp. 15-29, Coleção Friedrich Katzer. Belém: Museu Paraense Emílio Goeldi.

HANDFORD, C.R. 1991. Marginal marine halite: sabhkas and salinas. In Evaporites, petroleum and mineral resources (ed J.D. Melvin), pp. 1-66, Developments in Sedimentology 50, Amsterdam: Elsevier.

HARVEY, A.M. 2003. The role of base-level change in the dissection of alluvial fans: case studies from southeast Spain and Nevada. Geomorphology 45, 67-87.

HOFMANN, A., TOURANI, A. & GAUPP, R. 2000. Cyclicity of Triassic to lower Jurassic continental red beds of the Argana Valley, Morocco: implications for paleoclimate and basin evolution. Palaeogeogeography, Palaeoclimatology, Palaeoecology 161, 229-266.

HOVORKA, S.D. 1987. Depositional environments of marine-dominated bedded halite, Permian SanAndres Formation, Texas. Sedimentology 34: 1029-1054.

JUHÁSZ, E., KOVÁCS, L.Ó., MÜLLER, P., TOTH-MAKK, Á., PHILLIPS, L. & LANTOS, M. 1997. Climatically driven sedimentary cycles in the Late Miocene sediments of the Pannonian Basin, Hungary. Tectonophysics 282, 257-276.

KERR, S.D. & THOMSON, A.1963. Origin of nodular and bedded anhydrite in Permian shelf sediments, Texas and New Mexico. AAPG Bulletin 47, 1726-1732.

LOGAN, B.W. 1987. The MacLeod Evaporite Basin, Western Australia: Tulsa: American Association of Petroleum Geologists Memoir 44, 140 pp.

MARTEL, A.T. & GIBLING, M.R. 1991. Wave-dominated lacustrine facies and tectonically controlled cyclicity in the Lower Carboniferous Horton Bluff Formation, Nova Scotia Canada. In Lacustrine Facies Analysis (eds P. Anadón, Ll. Cabrera and K. Kelts), pp. 223-244, International Association of Sedimentologists Special Publication no. 13. Oxford: Blackwell.

MARTILL, D. 1988. Preservation of fish in the Cretaceous Santana Formation. Paleontology 31, 1-18.

OLSEN, P.E. 1986. A 40-million-year lake record of Early Mesozoic orbital climatic forcing. Science 234, 842-848.

OLSEN, P.E. & KENT, D.V. 1996. Milankovitch climate forcing in the tropics of Pangea during the Late Triassic. Palaeogeogeography, Palaeoclimatology, Palaeoecology 122, 1-26.

OLSEN, P. E. & D.V. KENT. 1999. Long-period Milankovitch cycles from the Late Triassic and Early Jurassic of eastern North America and their implications for the calibration of the early Mesozoic time scale and the long-term behavior of the planets. Trans. Roy. Soc. Lond. A, 357, 1761-1786.

PAZ, J.D.S & ROSSETTI, D.F. 2001. Reconstrução paleoambiental da Formação Codó (Aptiano), borda leste da Bacia do Grajaú, MA. In O Cretáceo na Bacia de São Luís-Grajaú (eds D.F. Rossetti, A.M. Góes, W. Truckenbrodt), pp. 77-100, Coleção Friedrich Katzer. Belém: Museu Paraense Emílio Goeldi.

PINDELL, J.L. 1985. Alleghenian reconstruction and the subsequent evolution of the Gulf of Mexico, Bahamas and proto-Caribbean. Tectonics 4, 1-39.

RAISWELL, R. 1976. The microbiaological formation of carbonate concretions in the Upper Lias of NE England. Chemical Geology 18, 227-244.

REZENDE, W.M. & PAMPLONA, A.H.R.P., 1970. Estudo do desenvolvimento do Arco Ferrer-Urbano Santos. PETROBRAS, Boletim Técnico 13, 5-14.

RISACHER, F. & EUGSTER, H.P. 1979. Holocene pisoliths and encrustations associated with spring-fed surface pools, Pastos Grandes, Bolivia. Sedimentology 26, 253-270.

ROSSETTI, D.F. 2001. Arquitetura deposicional da Bacia de São Luís-Grajaú. In O Cretáceo na Bacia de São Luís-Grajaú (eds D.F. Rossetti, A.M. Góes, W. Truckenbrodt), pp. 31-46, Coleção Friedrich Katzer. Belém: Museu Paraense Emílio Goeldi.

ROSSETTI, D.F. & GÓES, A.M. 2000. Deciphering the sedimentological imprint of paleoseismic events: an example from the Aptian Codó Formation, northern Brazil. Sedimentary Geology 135, 137-156.

ROSSETTI, D.F., PAZ, J.D.S. & GÓES, A.M. 2004. Facies analysis of the Codó Formation (Late Aptian) in the Grajaú area, southern Sao Luís-Grajaú Basin. Anais da Academia Brasileira Ciências, in press.

SCHREIBER, B.C., SMITH, D. & SCHREIBER, E. 1981. Spring peas from New York State: nucleation and growth of fresh water hollow ooliths and pisoliths. Journal of Sedimentary Petrology 51, 1341-1346.

SHINN, E.A., STEINEN, R.P., LIDZ, B.H. & SWART, R.K. 1989. Whitings, a sedimentologic dilemma. Journal of Sedimentary Petrology 59, 147-161.

SMOOT, J.P. & LOWENSTEIN, T.K. 1991. Depositional environments of non-marine evaporites. In Evaporites, petroleum and mineral resources (ed J.D. Melvin), pp. 189-347, Developments in Sedimentology 50, Amsterdam: Elsevier.

SMOOT, J.P. & OLSEN, P.E. 1994. Climatic cycles as sedimentary controls of rift-basin lacustrine deposits in the Early Mesozoic Newark Basin based on continuous core. In Lacustrine Reservoirs and Depositional Systems (eds A.J. Lomando, B. Charlotte Schreibber & P.M. Harris), pp. 239-295, SEPM Core Workshop no. 19, Tulsa: Society for Sedimentary Geology.

SPECHT, R.W. & BRENNER, R.L. 1979. Storm-wave genesis of bioclastic carbonates in Upper Jurassic epicontinental mudstones, East-Central Wyoming. Journal of Sedimentary Petrology 49, 1307-1322.

STEENBRINK, J., VAN VUGT, N, KLOOSTERBOER-VAN HOEVE, M.L., HILGEN, F.J. 2000. Refinement of the Messinian APTS from sedimentary cycle patterns in the lacustrine Lava section (Servia Basin, NW Greece). Earth and Planetary Science Letters 181, 161-173.

TREWIN, N. H. 1986. Palaeoecology and sedimentology of the Achanarras fish beds of the Middle Old Red Sandstone, Scotland. Transactions of the Royal Society of Edinburgh: Earth Sciences 77, 21-46.

TUCKER, M.E. & WRIGHT, V.P. 1990. Carbonate sedimentology. Oxford: Blackwell, 482 pp.

VANDERVOORT, D.S. 1997. Stratigraphic response to saline lake-level fluctuation and the origin of cyclic non-marine evaporite deposits: the Pleistocene Blanca Lila Formation, northwest Argentina. Geological Society of America Bulletin 109, 210-224.

VUGT, N. VAN, STEENBRICK, J., LANGEREIS, C.G., HILGEN, F.J. & MEULENKAMP, J.E. 1998. Magnetostratigraphy-based astronomical tuning of the early Pliocene lacustrine sediments of Ptolomais (NW Greece) and bed-to-bed correlation with the marine record. Earth and Planetary Science Letters, Amsterdam 164, 535-551.

WARREN, J. 1999. Evaporites: Their Evolution and Economics. Oxford, Blackwell Science, 438 pp.

WRIGHT, V.P. 1992. A revised classification of limestones. Sedimentary Geology 76, 177-185.

3. PETROGRAPHY OF GYPSUM-BEARING FACIES OF THE LATE APTIAN CODÓ FORMATION*

3.1. ABSTRACT

An original and detailed study focusing the petrographic aspects of evaporites from the Neoaptian Codó Formation exposed in the eastern and southern margins of the São Luís-Grajaú is presented herein, with the aim to discriminate between evaporites with primary and secondary origin and reconstruct their post-depositional evolution. Seven phases of evaporite formation were recognized: 1. chevron (selenite) gypsum; 2. nodular/lensoidal gypsum/anhydrite; 3. acicular gypsum; 4. mosaic gypsum; 5. brecciated gypsum/gypsarenite; 6. pseudo-nodular anhydrite/gypsum; and 7. rosettes of gypsum. The chevron gypsum, the nodular/lensoidal gypsum/anhydrite and the brecciated gypsum/gypsarenite display petrographic characteristics that conform to a primary nature. Their occurrence forming well-layered, horizontal beds displaying a cyclic arrangement are consistent with this interpretation. The acicular and mosaic gypsums were formed by replacement of these primary gypsums, but their formation took place very early in the diagenetic history, being still influenced by the depositional environment. Noteworthy is that these gypsum morphologies are closely related to the layered evaporites, serving to demonstrate that their formation were related to replacements that were mild, not enough to cause any significant change in the primary

---

* Authors: J.D.S. Paz & D.F. Rossetti. Submitted to *Anais da Academia Brasileira de Ciências*

sedimentary structures. The pseudo-nodular anhydrite/gypsum seems to have originated due to intrastratal fluids during burial, probably been related to halokinesis. The rosettes of gypsum, which intercept all the other variety of gypsum, represent the latest phase of evaporite formation in the study area, resulting from either intrastral waters or surficial waters during weathering.

Key-words: evaporite, petrography, paleolake, sabkha, late Aptian, São Luís-Grajaú Basin

3.2. INTRODUCTION.

Ancient evaporites are economically important as sources for salts (e.g., halite and potash) and metals (e.g., Cu, Zn, Au), and as indicators for structural traps of oil and gas (Warren, 1999). These deposits are abundant in sedimentary basins located along the Brazilian continental passive margin, being particularly developed in the Aptian-Albian transition (Hashimoto et al., 1987; Uesugui, 1987; Silva-Telles, 1996). The evaporites of the Codó Formation in the São Luís-Grajaú Basin (Fig. 3-1) are the only ones available for surface studies in the north equatorial Brazilian margin. Detailed facies analysis of fresh exposures in several open quarries located in the southern and eastern margins of this basin has provided elements to support a depositional system representing a lacustrine/sabkha complex (Paz & Rossetti, 2001; Rossetti *et al*., 2004). In addition, the deposits exposed in these localities represent an excellent opportunity to better understand the post-depositional processes that took place after primary evaporite formation. Such approach concerning to the Aptian Brazilian evaporites from the north equatorial Brazilian margin has not been conducted yet.

A preliminary field investigation showed that the evaporites from the Codó Formation include several morphologies, suggesting they might not be all primary in origin. Petrographic studies of evaporites are useful to help deciphering their origin (e.g., Ogniben, 1955; Kerr & Thomson, 1963; Holliday, 1970; Arakel, 1980; El-Tabakh et al., 1997; Aref, 1998), thus this type of study applied to the Codó Formation might contribute to better define and/or reconsider the proposed lacustrine/sabkha system. Furthermore, petrographic studies can serve as the basis to determine the sequence of events that took place following deposition (e.g., Arakel, 1980; Morad et al., 2000; Pérez et al., 2002). Determining the post-depositional history of these evaporites might help to decide on their potential for future strontium and sulphur isotopic studies attempting to test the hypothesis of a possible marine influence during sedimentation, as previously proposed elsewhere (e.g., Batista, 1992; Rodrigues, 1995; Rossetti *et al*., 2000).

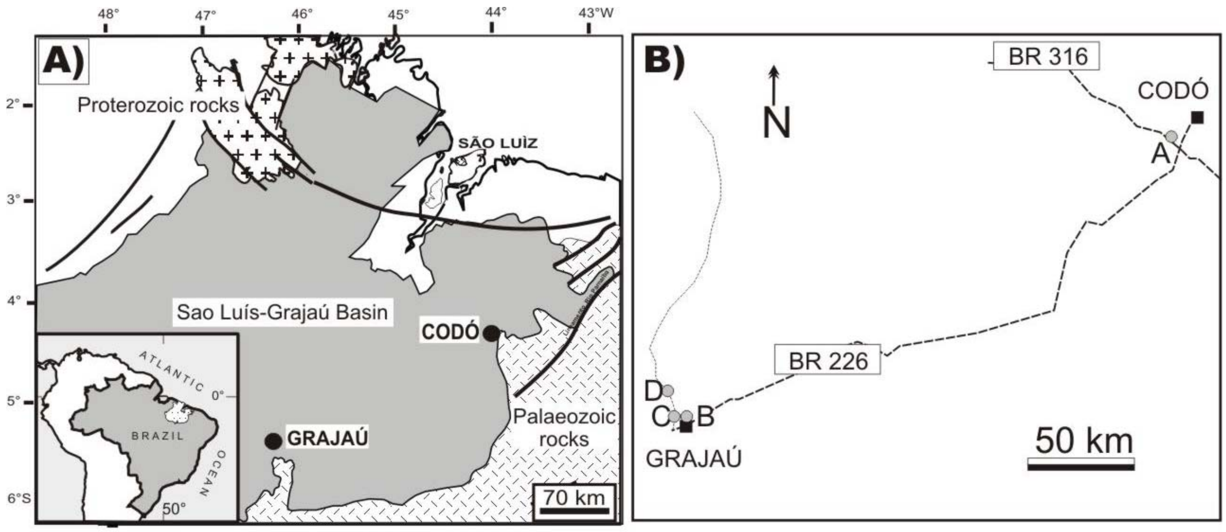

Fig. 3-1: A) Location map of the study areas in the São Luís-Grajaú Basin, northeastern Brazil. B) A close up map, indicating the location of the studied sections in the Codó and Grajaú areas.

3.3. GEOLOGICAL SETTING

The Gondwana split up took place through several steps, culminating in the Aptian with the break up of African and South American continents (Feijó, 1996; Góes & Rossetti, 2001). This process led to final establishment of several rift basins along the equatorial Brazilian margin, where the São Luís-Grajaú Basin is one of the largest, occupying 150,000 km^2. This basin has been interpreted as a unique structural feature formed by combination of pure shear stress and strike-slip deformation (Góes & Rossetti, 2001). The main rifting developed in the Albian, when fault offsets reached up to 400 m and (Fig. 3-2A,B), but fault displacement initiated in the Aptian, giving rise to a shallow and widespread basin where the Codó Formation was deposited in the late Aptian. This unit is defined at the top by a regionally correlatable unconformity marked by erosion and paleosols (Rossetti *et al*., 2001).

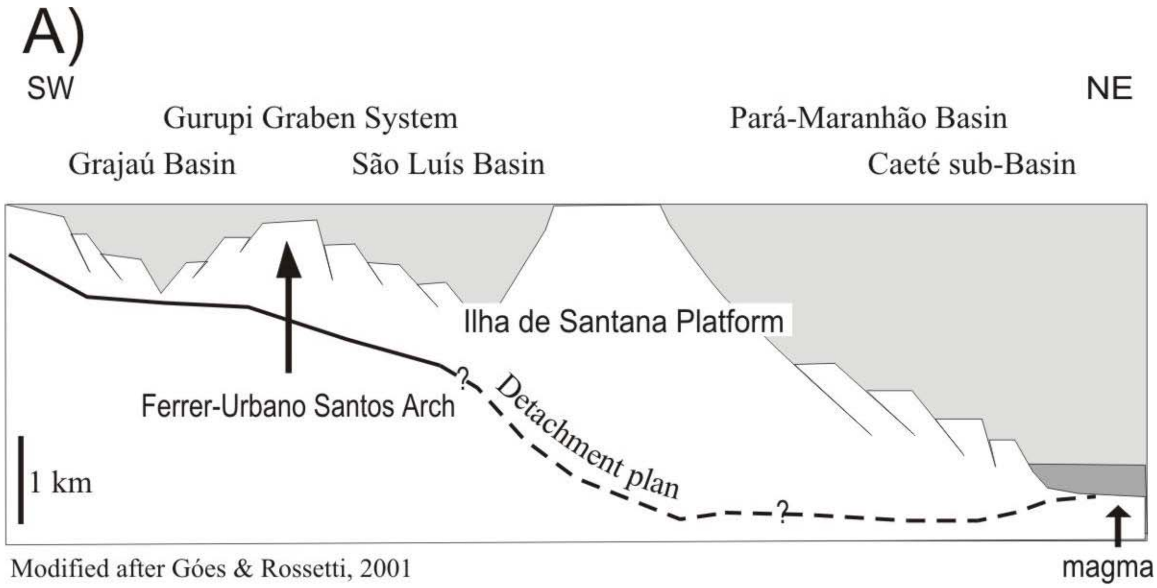

B) STRATIGRAPHY OF THE SÃO LUÍS- GRAJAÚ BASIN

AGE	Sequence architecture	STRATIGRAPHICAL UNIT (North)	STRATIGRAPHICAL UNIT (South)	Tectonic stage
Quaternary		Pós-Barreiras Deposits		Passive Margin
Upper Miocene?		Barreiras Formation (II)		Passive Margin
Lower Miocene?		Pirabas Formation	Barreiras Formation (I)	Passive Margin
Lower Tertiary?	Sequence 3	Cujupe Formation	Itapecuru Group	Drift
Cenomanian	Sequence 3	Alcântara Formation	Itapecuru Group	Drift
Upper and Middle Albian	Sequence 2	Undifferentiated Unit	Itapecuru Group	Rift
Lower Albian	Sequence 2	Undifferentiated Unit	Itapecuru Group	Rift
Upper Aptian	Sequence 1	Codó Formation	Grajaú Formation	Pre-rift

Fig. 3-2: A) Diagram with the sketched representation of the proposed structural pattern of the São Luís-Grajaú Basin in the Gurupi Graben System, and its relation with the Pará-Maranhão Basin. In this model, the Ferrer-Urbano Santos Arch is considered as an intrabasin horst within an abandoned intracontinental rift system formed by combination of pure shear stress and strike-slip deformation. The northeastward rifting migration through time gave rise to the development of a deeper basin, represented by the Caeté Sub-basin (cf. Góes & Rossetti, 2001). B) Stratigraphic framework of the São Luís-Grajaú Basin (cf. Rossetti, 2001).

Exposures of the Codó Formation include shallowing-upward deposits attributed to lacustrine or saline pan/sabkha depositional environments (Paz & Rossetti, 2001; Rossetti *et al*., 2004; Fig. 3-3). In the Codó area, where a lacustrine system dominates, the shallowing-upward cycles consist of bituminous black shales, evaporites and, subordinately, calcimudstones attributed to central lake depositional environments. These deposits grade upward into gray/green shale and limestones (i.e., calcimudstone, laminated to massive peloidal wackestone to grainstone, and sparstone), attributed to intermediate lake environments. The top of the shallowing-upward cycles comprises massive pelite, shale, limestone (e.g., intraclastic grainstone, ostracodal wackestone/grainstone, ooidal/pisoidal packstone, tufa) and rhythmite of limestone and shale. These lithologies display with a variety of sedimentary features consistent with marginal lake deposition, such as paleosol, karstic surface, fenestrae, meteoric calcite cement, vadose pisoid. In the Grajáu area, a saline pan/sabkha depositional environment was proposed (Rossetti *et al*., 2004), being represented by evaporite and locally tufa, gray-green shale, and calcimudstone.

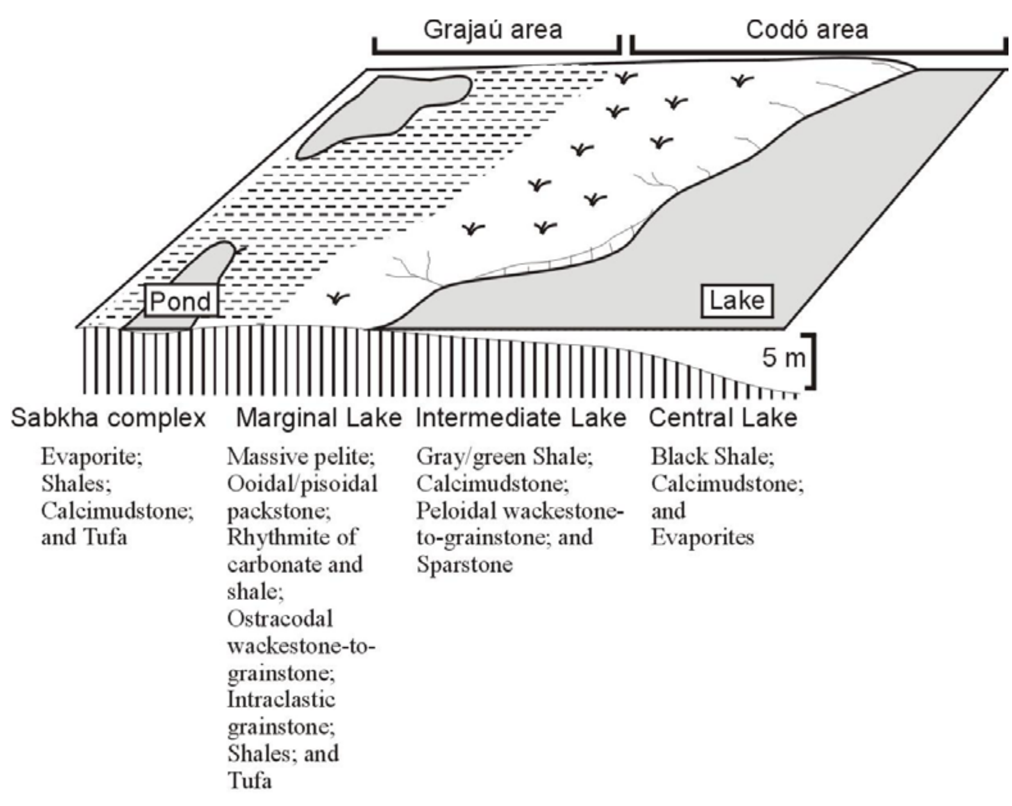

Fig. 3-3: Depositional model proposed for the Codó Formation in the Codó and Grajaú areas (cf. Paz & Rossetti, 2001).

The evaporite facies consists of layered gypsum (formed by alternating darker and lighter couplets that are up to 15 cm thick), gypsarenite, and massive-macronodular gypsum, which record deposition in flat lying areas, intraformational reworking of previously deposited evaporites, and remobilization of salts during burial, respectively. Layered gypsum occurs in both of the study areas, being dominant in the Grajaú area, while gypsarenite was observed only in the latter. Massive/macronodular gypsum is widespread in the Codó area, occurring mostly in the nucleus of evaporite lenses that are up to 5 m thick, which enclose chunks of black bituminous shales. In the Grajaú area, these deposits form diapiric features that are up to 6-8 m high at the outcrop scale. The contact between the massive-macrogranular gypsum and the layered gypsum is gradational, except locally where the diapirs are well defined by sharp boundaries.

3.4. PETROGRAPHY OF THE EVAPORITES

The evaporite facies from the Codó Formation were characterized petrographycally through the analysis of 86 thin sections distributed along four vertical sections (Fig. 3-4). Based on morphology and crystal relationships, eight phases of evaporite formation were recognized, which include (Fig. 3-5): 1. chevron (selenite) gypsum; 2. nodular/lensoidal gypsum/anhydrite; 3..acicular gypsum; 4. mosaic gypsum; 5. brecciated gypsum/gypsarenite; 6. pseudo-nodular anhydrite/gypsum; and 7 rosettes of gypsum. In addition to these evaporite phases, an episode of carbonate (calcite/dolomite) cementation/replacement took place in these deposits.

3.4.1. Chevron gypsum (selenite)

This type of gypsum was recorded in both areas, however it is much more widespread in sections located in the Grajaú area. The chevron gypsum, which represents the lighter component of the layered gypsum facies, was described in a previous work (e.g., Rossetti *et al.*, 2004), and it forms horizontal beds that are up to 10 cm thick of vertically aligned crystals. Under the microscope, the selenite crystals form twin planes and superimpose growth faces with acute angles arranged as a zig-zag, perpendicularly to the crystal long axis (Fig. 3-6A). The selenite crystals usually grew up or are mantled by thin discontinuous layers of shales (mostly smectites). Some thicker layers of chevron gypsum might display packages of crystals that slumped down into the muds, resulting in a series of segments with superimposed lower concave-up shapes.

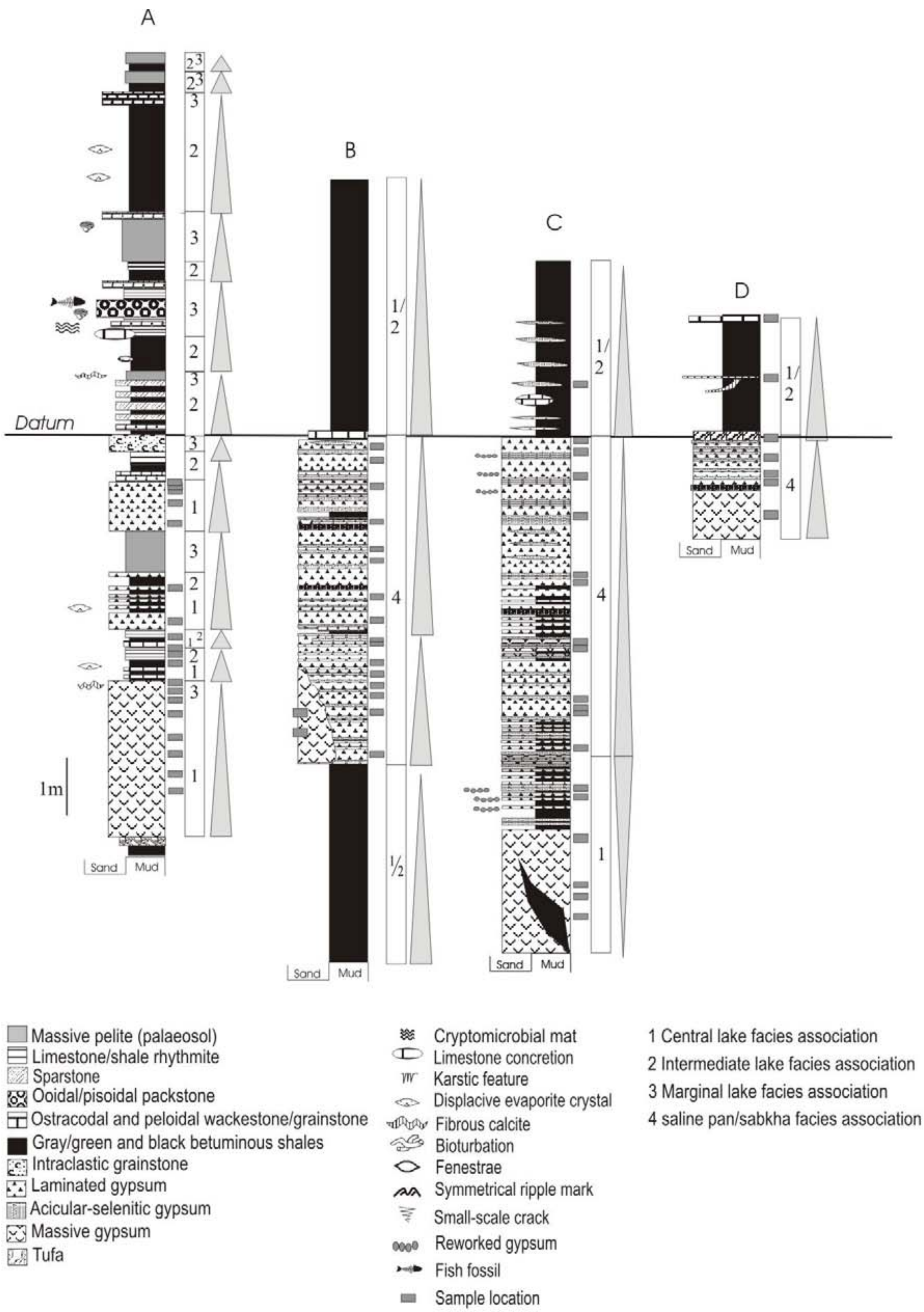

Fig. 3-4: Measured vertical sections representative of the evaporites studied in the Codó Formation (see Fig. 3-1 for section location).

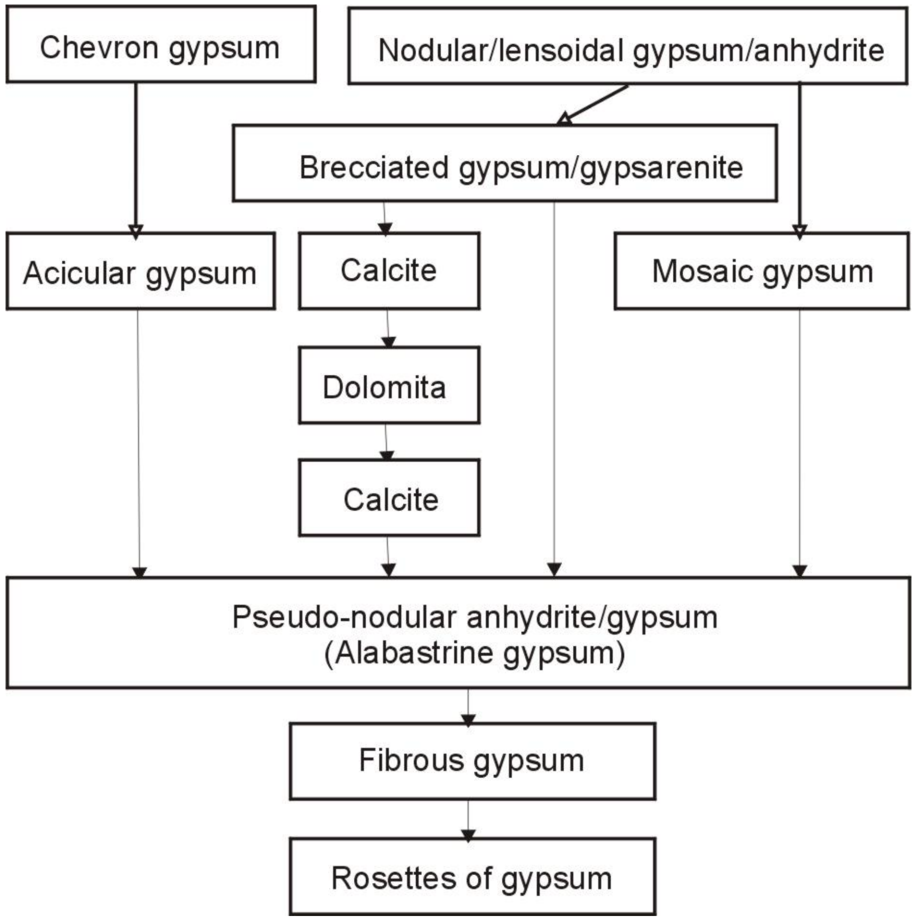

Fig. 3-5: The several phases of evaporites recognized in the Codó Formation, with paragenesis indicated by lateral position of the boxes.

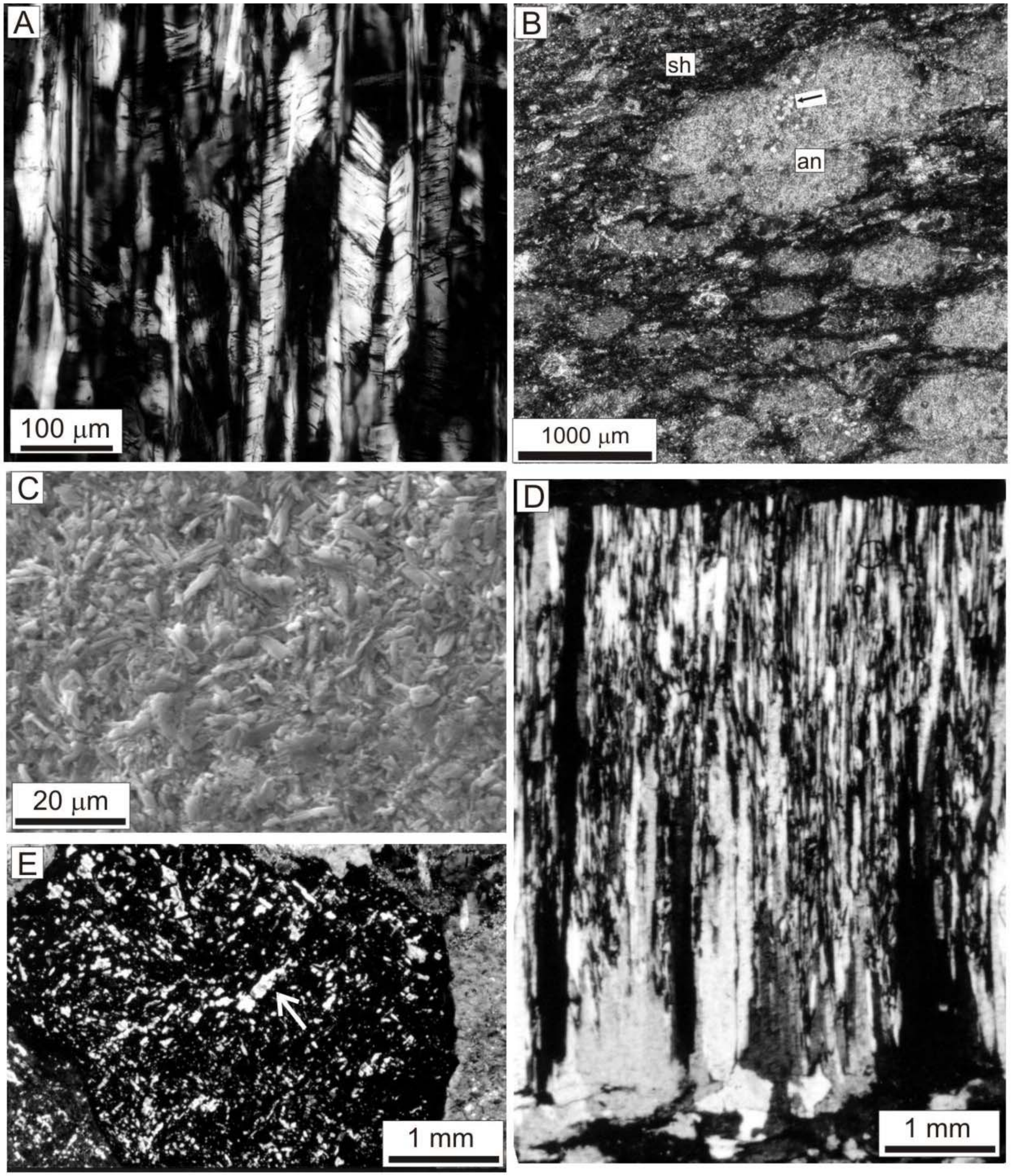

Fig. 3-6: Textures of the evaporites from the Codó Formation exposed in the study areas. A) Photomicrography of chevron gypsum. B) Photomicrography of the nodular gypsum (ng) within bituminous black shales (sh). Note calcite relicts (arrow) within nodules (crossed nicols). C) A close up in SEM view from the gypsum nodules shown in figure B, illustrating their composition by micrometric, equant, lath-like crystals, typical of anhydrite. D) Photomicrography of the acicular gypsum and, at the base, mosaic gypsum. E) Photomicrography of relics of anhydrite (arrow) within a large mosaic gypsum crystal.

3.4.2. Nodular/lensoidal gypsum/anhydrite

This evaporite was recorded only in sub-surface, occurring in association with shales. It consists of either nodules of gypsum or isolated lensoidal gypsum crystals that are parallel to bedding planes (Fig. 3-6B,C). The nodules are up to 5 mm long, and internally composed of a dark mixture of anhydrite and gypsum that form a massive cryptocrystalline framework.

3.4.3. Acicular gypsum

The acicular gypsum occurs invariably in association with the chevron gypsum, likewise forming vertically oriented crystals similar to needles (Fig. 3-6D). Although areas with dominance of acicular gypsum were observed, in general these types of gypsum are intergraded, resulting in a closely interlaced framework. Noteworthy it is the frequent presence of relics and/or ghosts of the chevron gypsum within the acicular crystals.

3.4.4. Mosaic gypsum

This type of evaporite occurs particularly within the dark bundles of the layered gypsum. It consists of inequidimensional crystals of gypsum averaging 300 μm in length that are arranged into a mosaic framework. The contact between crystals is usually ragged and sutured. The mosaic gypsum typically displays an abundance of relics of floating anhydrite, forming a poikilitic texture (Fig. 3-6E).

3.4.5. Brecciated gypsum/gypsarenite

This type of evaporite occurs most frequently intergrading with the mosaic gypsum within the darker bundles of the layered gypsum facies. It consists of gypsum that occur as clasts ranging from μm to 1 cm in diameter (Fig. 3-7A,B). The clasts might be either angular to subangular, when a fitted texture is recognized, or rounded, forming locally a texture that is similar to gypsarenite (Fig. 3-7C). The clasts are surrounded by either a continuous or discontinuous dark cutan formed by a mixture of clay, organic matter and iron oxides. Under crossed nichols, several clasts might display optical continuity, forming large crystals that can reach up to 3 mm of diameter (Fig. 3-7D). These contain abundant relics of anhydrite.

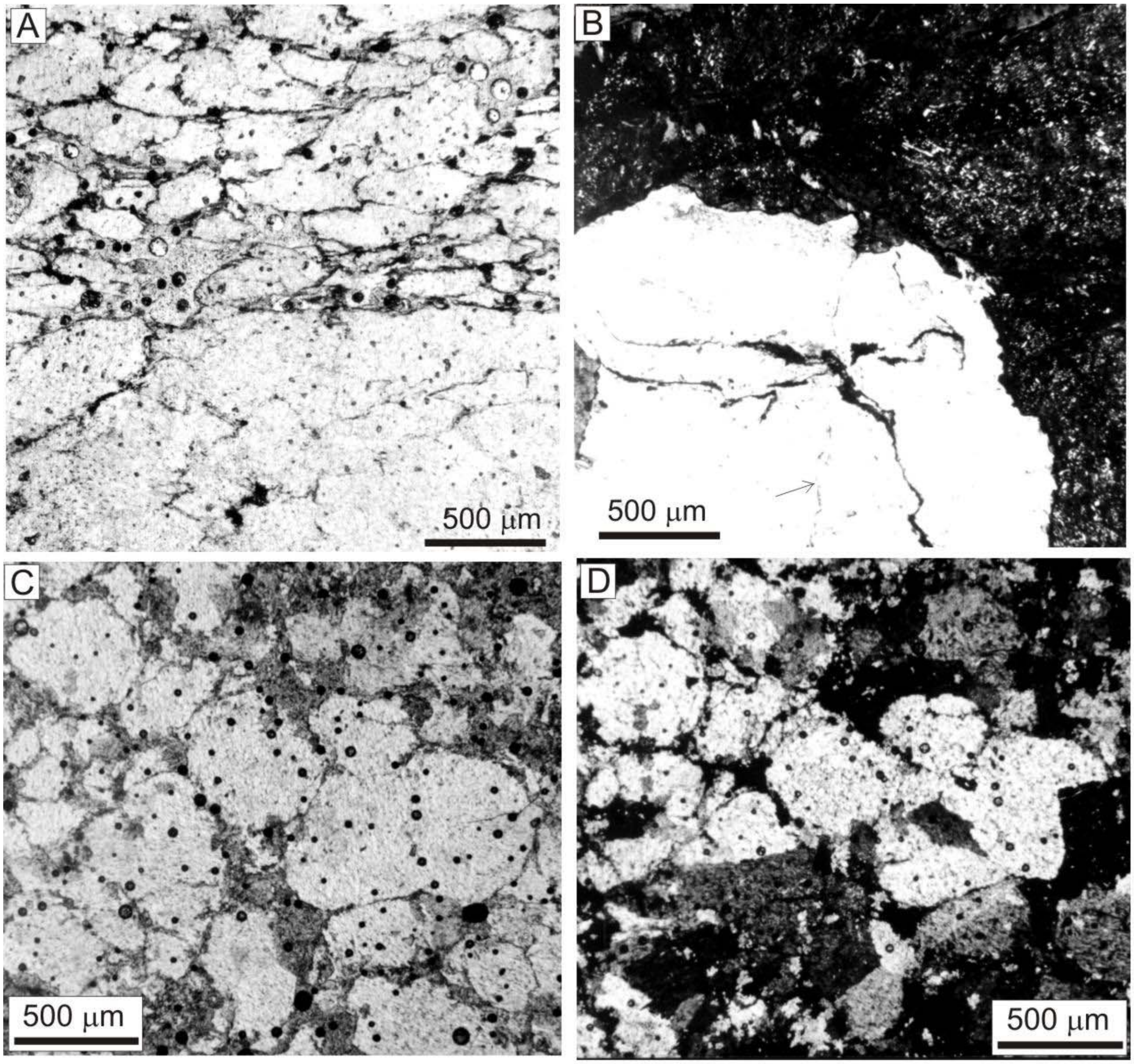

Fig. 3-7: Textures of the evaporites from the Codó Formation exposed in the study areas. A) Brecciated gypsum (upper part) evolved from mosaic gypsum (lower part). The dark lines around the clasts in the upper part of the photograph were formed by muds resulting from mechanical infiltration (parallel nicols). B) A detailed of the brecciated gypsum illustrating a crystal with several fractures (arrow). Note that the optical continuity beyond fractures, attesting fracturing occurred within a single large crystal (crossed nicols). C and D) Brecciated gypsum locally displaying well rounde clasts resembling gypsarenite (C=parallel nicols; D=crossed nicols). Note in D that several clasts are in optical continuity, revealing they were most likely formed by fracturing of a same large crystal.

3.4.6. Pseudo-nodular anhydrite/gypsum

At the outcrop scale, this evaporite phase consists of either slightly elongated or spherical fragments up to 5 cm long of evaporites displaying a fitted texture (Fig. 3-8A-C). Petrographically, the clasts are composed of alabastrine gypsum, fibrous gypsum, and anhydrite. In general, alabastrine gypsum is the most widespread, occurring as a mosaic of crystals less than 200 μm in diameter (Fig. 3-8D). The crystals are very limpid, i.e., typically with no inclusions. The fibrous gypsum occurs secondarily as a series of parallel columns that can reach up to 1 cm long, which grew within the fractures that define the clasts, being perpendicular to fracture walls (Fig. 3-8A-C). Unlike to the alabastrine, the fibrous gypsum might display relics of anhydrite. In addition, ghosts of fibrous crystals may occur within the alabastrine gypsum (Fig. 3-8D). In places, some elongated clasts are composed of microcrystalline lath-like anhydrite (Fig. 3-8E). Where these clasts are in contact with mosaics of large gypsum crystals similar to the ones described above, the latter form concave embayments toward the anhydrites, leaving a “dust” of anhydrite relics behind (Fig. 3-8E). Inasmuch, both the anhydrite clasts and the mosaic gypsum might display etched margins as they grade into fibrous and alabastrine gypsum. Electronic scanning microscopic analysis of the anhydrite clasts reveal a mixture of anhydrite and limpid gypsum crystals that are similar to those observed in the nodular/lensoidal gypsum/anhydrite (Fig. 3-9A, compare with Fig. 3-6C). Noteworthy is that the anhydrite clasts occur as spots that intergrade with alabastrine and fibrous gypsum.

3.4.7. Rosettes of gypsum

Rosettes of amber-colored gypsum occur disperse within the evaporites of the Codó area, being restricted to the massive/macronodular gypsum (Fig. 3-8C). The rosettes reach up to 5 cm of diameter, and consist of fibrous crystals arranged into a radial pattern. The rosettes unconformably cut into all the other gypsum phases described above.

The carbonates associated with the gypsum/anhydrite consist of calcite cement filling fractures in the brecciated gypsum/gypsarenite (Fig. 3-9B), even where this facies is obliterated by pseudo-nodular anhydrite/gypsum. The calcite also occurs as enlarged crystals that grew upon the gypsum from both sides of the fractures (Fig. 3-9C), in which case it forms caries in the mosaic gypsum. On the other hand, the alabastrine gypsum enters into relics of calcite, forming caries toward them (Fig. 3-9D). Rhombs of calcite after dolomite are locally present (Fig. 3-9E). Celestite might be also present in association with the carbonates, occurring as pyramidal crystals with etched edges.

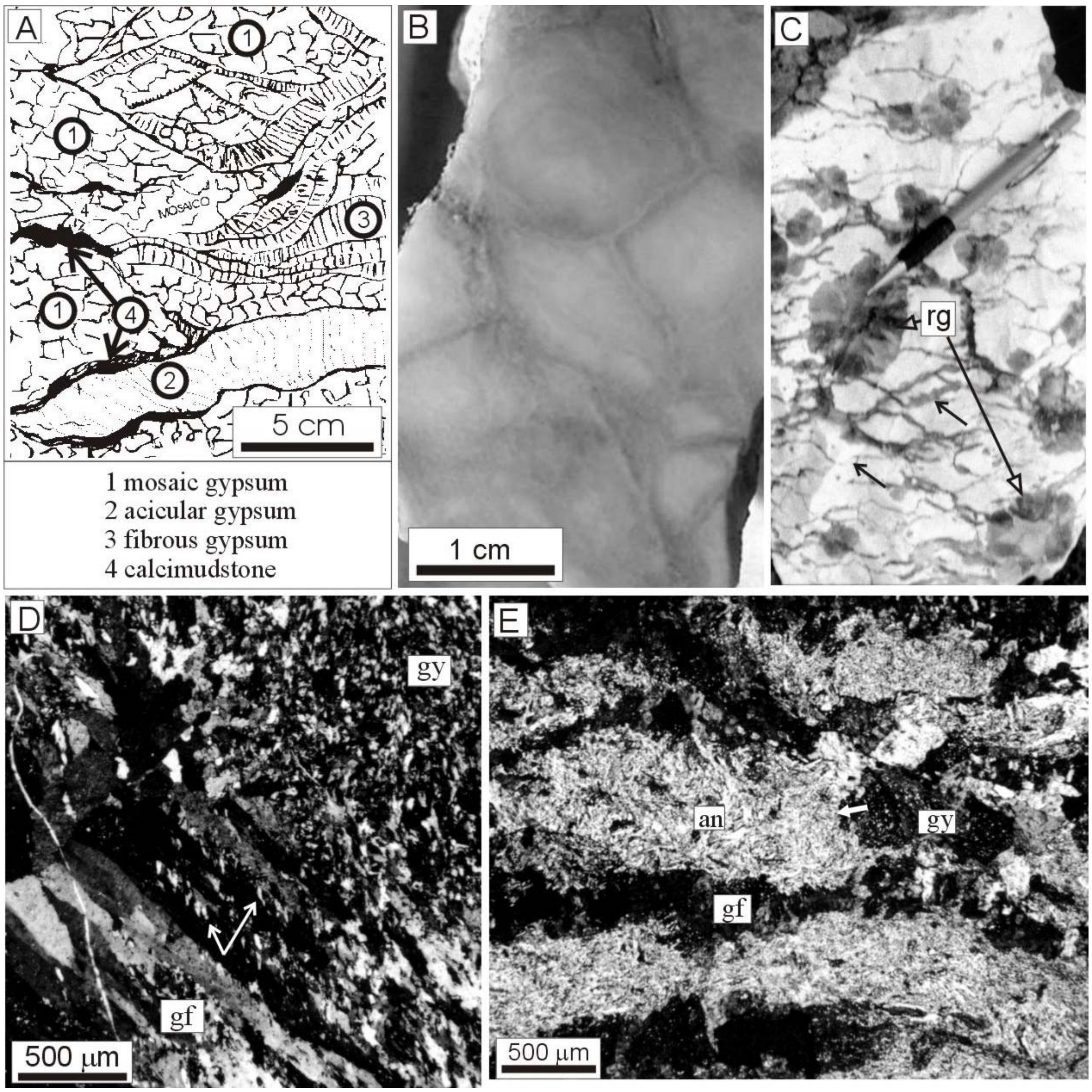

Fig. 3-8: Textures of the evaporites from the Codó Formation exposed in the study areas. A) Overlay field drawing illustrating a spot within the pseudo-nodular anhydrite/gypsum with relics of a complex arrangement formed by mosaic, acicular and fibrous gypsum, bounded by films of calcimudstone. B) Pseudo-nodular gypsum, formed by fracturing. C) A spot within the pseudo-nodular anhydrite/gypsum, with nodules of anhydrite bound by films of fibrous gypsum (arrows). Note the superimposed rosettes of gypsum of variable sizes (rg). D) Alabastrine (gy) and fibrous (gf) gypsum in gradational contacts. The arrows indicate places where the fibrous gypsum is partly replaced by the alabastrine gypsum, recorded by numerous crystals of the later over the fibrous gypsum, which in turn remains as diffuse relics. E) Photomicrography of the nodules shown in C, illustrating their composition of tiny, equant, lath-like crystals (an). Note that the edges of the nodules were replaced by fibrous (gf) or mosaic (gy) gypsum.

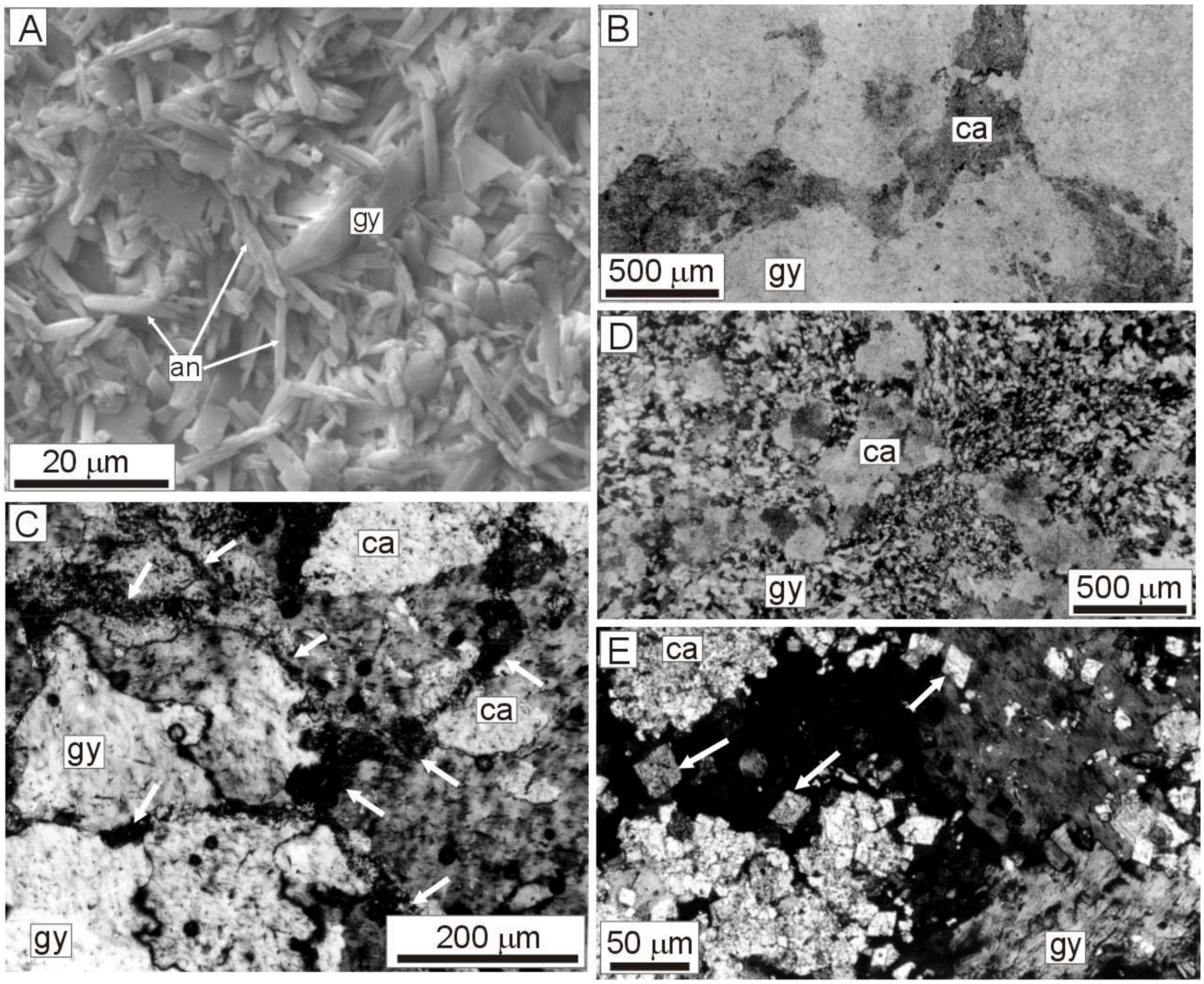

Fig. 3-9: Textures of the evaporites from the Codó Formation exposed in the study areas. A) SEM view of the pseudo-nodular anhydrite/gypsum, with lath-like anhydrite (an) interlaced with gypsum (gy). This material comes from a nodule of anhydrite depicted in figure 8C. B) Calcite (ca) cementing fractures in the pseudo-nodular anhydrite/gypsum (gy). C) A detail of the pseudo-nodular anhydrite/gypsum showing several fractures (arrows) filled by a mixture of calcite and muds. Note larger calcite crystals (ca) that grew sidewards from the fractures trough replacement of gypsum (gy). D) Relics of calcite (ca) within alabastrine gypsum (gy) from the pseudo-nodular anhydrite/gypsum. E) Rhombs of calcite after dolomite (arrows). (Except for the SEM micrography shown in A, all the other figures were obtained under petrographic microscope with crossed nicols).

3.5.PARAGENESIS

The combination of facies and petrographic characteristics revealed that the foregoing described evaporites show features supporting both primary and secondary formations (Fig. 3-10). In addition, the petrographic study also showed that at least great part of the secondary gypsum might have been formed under influence of the depositional surface, thus reflecting the original brine characteristics. Evidences for primary evaporite precipitation is particularly recorded in the layered gypsum. First, this is suggested by the preservation of sedimentary structures forming laterally continuous, horizontal beds. Second, the primary nature is confirmed by the presence of chevron gypsum in the lighter bundles of this facies. Such feature is attributed to the progressive upward precipitation of salts on the floor of shallow (usually less than 2 m deep), supersatured brine pools (e.g., Logan, 1987; Hovorka, 1987; Handford, 1991; Smoot & Lowenstein, 1991), as suggested in a previous work (i.e, Rossetti *et al*., 2004).

The cyclic alternation of selenite beds with dark gypsum containing nodular/lensoidal gypsum/anhydrite is also a reflex of changes in the depositional conditions. The formation of these morphologies is consistent with accumulation taking place a few mm beneath the depositional surface by displacive intrasediment growth of crystals from supersaturated pore fluids in the capillary and/or upper phreatic zone (e.g., Kerr and Thomson 1963, Warren 1999). As the brine level decreased, nodular/lensoidal gypsum grew displacively within the underlying sediments, here represented by shales. This is the most common habit of gypsum precipitated within sediment, either in mudflats or other environments subjected to palustrine conditions (Magee, 1991).

The presence of nodules composed of a dark mixture of anhydrite and gypsum forming a massive cryptocrystalline framework is consistent with this interpretation, being related to increased evaporation, probably due to climatic changes (Rossetti *et al*., 2004). Similar masses of mixing gypsum have been considered as the record of sulphate replacements during seasonal variations next to the depositional surface (p.e., Arakel, 1980; Mees, 1998; Mees & Stoops, 2003).

The mosaic gypsum was formed by replacement of anhydrite, as indicated by the fact the abundant remains of this mineral within it. Mosaics of gypsum crystals with sutured contacts have been interpreted as a non-equilibrium texture of grain interpenetration at low temperature (cf. Voll, 1960), probably reflecting formation under early diagenesis (e.g., Spencer & Lowenstein, 1990). The occurrence of mosaic gypsum in association with the dark bundles alternated with selenite/acicular gypsum within the layered gypsum might be taken as an evidence for replacement soon after deposition.

Extreme low brine level with subaereal exposure resulted in gypsum fracturing due to desiccation, a process that gave rise to *in situ* brecciated gypsum and ultimately gypsarenite, the latter recording local reworking at the surface as recorded in other evaporite deposits (e.g., Sanz-Rubio *et al*., 1999; Schreiber & El Tabakh, 2000). The frequent upward gradation from the brecciated to the gysarenite is consistent with this interpretation. The presence of mud cutans surrounding the clasts is attributed either to mechanical infiltration from downward flows or to the adhesion of residues on clast surfaces during reworking.

Following brecciation, there was a phase of widespread replacement, which gave rise to mosaics of large gypsum crystals affecting the dark beds of the layered gypsum facies. This sequence of event is proposed based on the observation that large gypsum crystals encompass several clasts, attesting to pervasive cementation and/or replacement. The presence of abundant relics of microcrystalline lath-like anhydrite within the mosaics attests to their formation following a period of anhydritization. Noteworthy is the fact that the mosaics were developed only in the darker bundles of the layered gypsum, not affecting the lighter components. Instead, the chevron gypsum was replaced by acicular gypsum, as indicated by the presence of ghosts of selenite within the latter. This morphology reflects crystal growth from very pure, supersaturated fluids, which favors extreme elongation parallel to the *c*-axis (Magee, 1991). The close association of the acicular gypsum with the selenites leads to suggest that formation fluids were driven from remobilization of sulphates from the selenites, whose formation naturally required high brine saturation. It is important to mention that neither of these authigenic processes were enough to destroy the primary lamination. This is taken as evidence to suggest that the formation of mosaic and acicular gypsum took place cyclically close to the depositional surface just shortly after formation of the individual bundles.

Fracturing at the surface created a porosity that was cemented by calcite. Calcite also replaced gypsum near the fracture sides. Under subaerial conditions (i.e., vadose to freshwater phreatic), sulphate-undersaturated pore fluids dissolves gypsum and/or anhydrite and release Ca^{2+} for precipitation of calcite as the CO_3^{2-} has more affinity with calcium than with SO_4^{2-} (cf. Back et al., 1983). Rare dolomite rhombs might have been formed either by replacement of calcite or simultaneous dolomite precipitation. The dolomite was in turn replaced by calcite. Dedolomitization is a process that might be closely linked to karstification (Cañaveras et al., 1996). This process might have contributed to release Sr^{2+}, which combined with SO_4^{2-}, promoted precipitation of celestite (cf. Olaussen, 1981; Taberner et al., 2002). The celestite formation in turn also releases Ca^{2+} that increases the Ca/Mg ratio, and could dissolve dolomite and renew precipitation of calcite (p.e., Back et al., 1983; Kushnir, 1985). The close association of calcite, dolomite and celestite in the study evaporites of the Codó Formation suggest these processes as the most likely.

The pseudonodular anhydrite/gypsum is interpreted to represent a later phase of gypsum formation. First, this is suggested by its occurrence restricted to the massive/macronodular gypsum, where primary sedimentary structures were almost entirely lost. The presence of massive gypsum grading into the layered gypsum, and the diapiric geometry enclosing chunks of black bituminous shales is related to salt remobilization during halokinesis. Second, the pseudonodular anhydrite/gypsum contains limpid alabastrine and fibrous crystals, not observed in association with the layered gypsum, which is consistent with the proposed late formation. Fine crystalline gypsum have been considered as secondary in origin (Holliday, 1970), forming in consequence of hydration, especially of anhydrite, induced by diapirism or other mechanism that allow percolation of water through evaporite rocks (Holliday, 1970; Price & Cosgrove, 1990; Warren, 1999). Fracturing seems to have been the cause of the pseudonodular aspect of this gypsum. Under stress, probably related to salt remobilization, part of the gypsum might have had a ruptile behavior, ultimately braking apart to form individual fragments (e.g., Price & Cosgrove, 1990; Marco *et al*., 2002). Saturated fluids percolating along the secondary porosity created by this process would have promoted precipitation of the fibrous gypsum. In the following, there might have had the enlargement of the fractures due to forcing caused by crystal growth. While this process took place, most of the primary sedimentary features, as well as the previous phases of evaporites, became obliterated. As the salt became mobile, there was a pervasive development of alabastrine gypsum. The later nature of this phase of gypsum is revealed by its limpid aspect free of anhydrite inclusions and by the fact that it contains ghosts of fibrous gypsum.

The spots with microcrystalline lath-like anhydrite that occur within the macronodular gypsum is probably a relic of one of the earliest phase of evaporite precipitation in the study area The paragenesis reconstituted with basis on petrographic relationships shows that these anhydrites form nodules that were in part replaced by the mosaic gypsum, as revealed by the fact that the later form concave embayments that enter into the anhrydrite. The margins of this gypsum is in turn ragged due to reaction with fibrous and alabastrine gypsum. These relationships support that the anhydrite nodules had an early development relative to all other gypsum phases present in the pseudonodular gypsum. If so, then it is possible that the anhydrite is temporally related to the anhydrite formed in the dark bundles of the layered gypsum, which represents one of the earliest evaporite phases developed in the Codó Formation.

The final phase of evaporite formation is recorded by the rosettes of gypsum, as confirmed by the fact that these truncate all the other evaporite morphologies. Aggregates of large fibrous gypsum crystals forming rosettes similar to the ones of the study area have been attributed to the action of either intrastratal waters during burial or surficial waters during weathering (e.g., Shearman, 1966; Holliday, 1970; Warren, 1999).

3.6.CONCLUSIONS

Despite the many varieties of evaporites recorded in the Codó Formation exposed in the eastern and southern margin of the Grajaú Basin, these deposits display many petrographic and faciological attributes that are consistent with an early formation either by primary precipitation or early replacements when the sediments were still under the influence of the depositional surface. These types of evaporites prevail particularly in the Grajaú area, where layered gypsum is the dominant facies. In both areas, burial phases of gypsum seem to have developed only where gypsum was remobilized during halokinesis.

The lack of significant deep diagenetic modification of the Codó Formation is recorded also by studies focusing the limestones and shales interbedded with the evaporites. The limestones are dominated by lithologies consisting of calcimudstones and peloidal wackestones/packstones with only local evidences of cementation or replacement. These lithologies usually display primary features, as normal grading and horizontal crenulated lamination. Inasmuch, the shales associated with the evaporites consist almost entirely by smectite, with only subordinate kaolinite and illite. Among these clay minerals, smectite is far the dominant one, being represented by detrital flakes, while the kaolinite and illite are mostly authigenic but related to pedogenetic horizons (Gonçalves, 2004). These data are consistent with the proposition that burial did not cause significant textural or mineralogical modification of the Codó Formation.

The petrographic studies presented here strongly motivate to undertake isotopic studies in the evaporites of the Codó Formation. The analysis should be carried out using samples from the layered facies only, which preserves evaporites formed both primarily and shortly after deposition. For these reasons, these deposits should provide information of the original brine characteristics. On the other hand, the pseudo-nodular anhydrite/gypsum and the rosettes of gypsum should not be considered in this type of studies, as they represent later stages of gypsum formation due to deeper salt remobilization. Inasmuch, the spots of anhydrite within the pseudo-nodular anhydrite/gypsum should be also discarded in these analyses. Despite the interpretation that these evaporites might have formed contemporaneously to the early-formed nodular/lensoidal anhydrite, the microscopic studies revealed they were strongly replaced by limpid, alabastrine gypsum, being inappropriate for isotopic analysis that can be used for paleoenvironmental purposes.

Acknowledgements. The Itapicuru Agroindustrial S/A is acknowledged for the permission to access the quarries with the exposures of the Codó Formation. This work was financed by the Brazilian Council for Research–CNPq (Project #460252/01).

REFERENCES

Arakel, A.V.1980. Genesis and diagenesis of Holocene evaporitic sediments in Hutt and Leeman lagoons, western Australia. J. Sedim. Petrol. 50: 1305-1326.

Aref, M.A.M. 1998. Holocene stromatolites and microbial laminites associated with lenticular gypsum in a marine-dominated environment, Ras El Shetan Ara, Gulf of Aqaba, Egypt. Sedimentology 45: 245-262.

Back, W., Hanshaw, B. B., Plummer, L. N., Rahn, P. H., Rightmire, C. T. and Rubin, M., 1983, Process and rate of dedolomitization: mass transfer and ^{14}C dating in a regional carbonate aquifer: G.S.A. Bull. 94: 1414-1429.

Batista, A.M.N. 1992. Caracterização Paleoambiental dos sedimentos Codó-Grajau, Bacia de São Luís (MA). Belém, 102 p. (Tese de Mestrado, UFPA)

Cañaveras, J.C., Sánchez Moral, S., Calvo, J.P., Hoyos, M. & Ordoñez, S. (1996): Dedolomites associated with karstification: An example of early dedolomitization in lacustrine sequences from the Tertiary Madrid Basin, Central Spain. Carbonates and Evaporites 11: 85-103.

El-Tabakh, M., Riccioni, R., Schreiber, B.C., 1997. Evolution of Late Triassic rift basin evaporites (Passaic Formation); Newark Basin, eastern North America. Sedimentology 44: 767-790.

Feijó, F.J. 1996. O início da livre circulação das águas do Oceano Atlântico. Bol. Geoc. PETROBRAS 10: 157-164.

Góes, A.M. & Rossetti, D.F. 2001. Gênese da Bacia de São Luís-Grajaú, Meio-Norte do Brasil. In D.F. Rossetti, A.M. Góes, W. Truckenbrodt (Eds) O Cretáceo na Bacia de São Luís-Grajaú. Belém: Coleção Friedrich Katzer. Belém: Museu Paraense Emílio Goeldi. p. 15-29.

Gonçalves, D. F. 2004. Argilominerais da Formação Codó (Aptiano superior) – Bacia do Grajaú: implicações climáticas e ambientais. Belém, 100 pp. (Tese de Mestrado, UFPA)

Handford, C.R. 1991. Marginal marine halite: sabkhas and Salinas. In: J.L. Melvin (Ed.) Evaporites, petroleum and mineral resources. Amsterdan: Elsevier, Developments in Sedimentology 50: 1-66.

Hashimoto, A.T., Appi, C.J., Soldan, A.L. & Cerqueira, J.R. 1987. O Neo-Alagoas nas bacias do Ceará, Araripe e Potiguar (Brasil): caracterização estratigráfica e paleoambinetal. Revista Brasileira de Geociências 17: 118-122.

Holliday, D.W. 1970. The petrology of secondary gypsum rocks: a review. J. Sedim. Petrol. 40: 734-744.

Hovorka, S.D. 1987. Depositional environments of marine-dominated bedded halite, Permian SanAndres Formation, Texas. Sedimentology 34: 1029-1054.

Kasprzyk, A. & Ortí, F. 1998. Paleogeographic and burial controls on anhydrite genesis: tha Badenian Basin in the Carpathian Foredeep (southern Poland, western Ukraine). Sedimentology 45: 889-907.

Kerr, S.D. & Thomson, A. 1963. Origin of nodular and bedded anhydrite in Permian shelf sediments, Texas and New Mexico. AAPG Bull 47: 1726-1732.

Kushnir, S.V. 1985. The epigenetic celestite formation mechanism for rocks containing $CaSO_4$. Geokhimiya 10: 1455-1463. (Translation from Scripta Technica, Inc., 1986 ©)

Logan, B.W. 1987. The MacLeod evaporite basin, western Australia. A.A.P.G. Memoir 44, 140p.

Magee, J.W. 1991. Late Quaternary lacustrine, groundwater, Aeolian and pedogenic gypsum in the Prungle Lakes, southeastern Australia. Palaeogeography, Palaeoclimatology, Palaeoecology 84: 3-42.

Marco, S.,Weinberger, R, & Agnon, A. (2002). Radial fractures formed by a salt stock in the Dead Sea Rift, Israel. Terra Nova 14:288-294.

Mees, F. 1998. The alteration of glauberite in lacustrine deposits of the Taoudenni-Agorgott basin, northern Mali. Sedimentary Geology 117: 193-205.

Mees, F. & Stoops, G. 2003. Circumgranular bassanite in a gypsum crust from eastern Algeria – a potential palaeosurface indicator. Sedimentology 50: 1139-1145.

Morad, S., Ketzer, J.M. & De Ros, L.F. 2000. Spatial and temporal distribution of diagenetic alterations in siliclastic rocks: implications for mass transfer in sedimentary basins. Sedimentology, Supple.1, 47: 95-120.

Ogniben, L. 1955. Inverse graded bedding in primary gypsum of chemical deposition. J. Sed. Petrol. 25: 273-281.

Olaussen, S. 1981. Formation of celestite in the Wenlock, Oslo region Norway – evidence for evaporitic depositional environments. J. Sed. Petrol. 51: 37-46.

Paz, J.D.S & Rossetti, D.F. 2001. Reconstrução paleoambiental da Formação Codó (Aptiano), borda leste da Bacia do Grajaú, MA. In: D.F. Rossetti, A.M. Góes, W. Truckenbrodt (Eds) O Cretáceo na Bacia de São Luís-Grajaú. Belém: Coleção Friedrich Katzer, Museu Paraense Emílio Goeldi, p. 77-100.

Price, N. J. & Cosgrove, J. W. 1990. Analysis of Geological Structures. Cambridge, 502 p. (pp. 89-122)

Pérez, A., Luzón, A., Roc, A.C., Soria, A.R., Mayayo, M.J., Sánchez, J.A. 2002. Sedimentary facies distribution and gênesis of recent carbonate-rich saline lake: Gallocanta Lake, Iberian Chain, NE Spain. Sedimentary Geology 148: 185-202.

Rodrigues, R. 1995. A geoquímica Orgânica na Bacia do Parnaíba. Porto Alegre, 225 pp. (Tese de Doutorado, UFRGS).

Rossetti, D.F. 2001. Arquitetura deposicional da Bacia de São Luís-Grajaú. In: D.F. Rossetti, A.M. Góes, W. Truckenbrodt (Eds) O Cretáceo na Bacia de São Luís-Grajaú. Belém: Coleção Friedrich Katzer, Museu Paraense Emílio Goeldi, p. 31-46.

Rossetti, D.F., Paz, J.D.S., Góes, A.M. 2004. Facies analysis of the Codó Formation (Late Aptian) in the Grajaú Area, Southern São Luís-Grajaú Basin. An. Acad. Brás. Ciên. 76: 791-806.

Rossetti, D.F., Paz, J.D.S., Góes, A. M. & Macambira, M. 2000. A marine versus non-marine origin for the Aptian-Albian evaporites of the São Luís and Grajaú basins, Maranhão State (Brazil) based on sequential analysis. Rev. Bras. Geocienc. 30: 642-645.

Sanz-Rubio, E., Hoyos, M., Calvo, J.P. & Rouchy, J.M. 1999. Nodular anhydrite growth controlled by pedogenic structures in evaporite lake formations. Sedimentary Geology 125: 195-203.

Schreiber, B.C. & El Tabakh, M. 2000. Deposition and early alteration of evaporites. Sedimentology, Suppl. 1, 47: 215-238.

Shearman, D.J. 1966. Origin of marine evaporites by diagenesis. Inst. Min. Metal. Trans., Section B, 75: 208-215.Smoot, J.P. & Lowenstein, T.K. 1991, Depositional environments of non-marine evaporites. In: JL. Melvin (Ed.) Evaporites, petroleum and mineral resources, Amsterdam: Elsevier, Developments in Sedimentology 50: 189-347.

Silva-Telles Jr., A.G. 1996. Estratigrafia de Seqüências de Alta Resolução do Membro Coqueiros da Formação Lagoa Feia (Barremiano?/Aptiano da Bacia de Campos-Brasil) Porto Alegre, 2v., 268 pp. (Dissertação de Mestrado, UFRGS).

Smoot, J.P. & Lowenstein, T.K. 1991. Depositional environments of non-marine evaporites. In: JL. Melvin (Ed.) Evaporites, petroleum and mineral resources, Amsterdam: Elsevier, Developments in Sedimentology 50: 189-347.

Spencer, R.J. & Lowenstein, T.K. 1990. Evaporites. In I.A. Macilreath & D.W. Morrow (eds.) *Diagenesis*. St. Johns, New Foundlands, Geological Association of Canada, Geosciences Canada Reprint Series, 4, p.141-163.

Taberner; C., Marshall, J.D., Hendry, J.P., Pierre, C.; Thirlwall, M.F. 2002. Celestite formation, bacterial sulphate reduction and carbonate cementation of Eocene reefs and basinal sediments (Igualada, NE Spain). Sedimentology 49: 171-190.

Uesugui, N. 1987. Posição estratigráfica dos evaporitos da Bacia de Sergipe-Alagoas. Rev. Bras. Geociênc. 17**:** 131-134.

Voll, G. 1960. New work on petrofabrics. Liverpool and Manchester Geological Journal 2: 503-567.

Warren, J. 1999. Evaporites: Their Evolution and Economics. Oxford: Blackwell Science, 438p.

4. GENESIS AND PALEOHYDROLOGY OF A SALINE PAN/LAKE SYSTEM (LATE APTIAN) FROM THE BRAZILIAN EQUATORIAL MARGIN: INTEGRATION OF FACIES, SR AND S ISOTOPES*

4.1. ABSTRACT

Facies analysis was combined with Sr and S isotope data to unravel the brine source of Late Aptian evaporites from the Codó Formation exposed in the southern and eastern margins of the São Luís-Grajaú Basin, northern Brazil. Comparisons of facies distribution between the two investigated areas show: 1. stable, well-stratified and hypersaline lakes with periods of anoxia and closure prevailing in the eastern margin of the basin, with salt precipitation only in more saturated, central basin environments; and 2. prevalence of relatively more ephemeral conditions to the south, where a saline pan complex developed and evaporite precipitation took place mainly in marginal salinas and surrounding mudflats. In both areas, expansion/contraction cycles were formed as sedimentation took place, which was followed by decrease, and then increase, in isotope values. This, combined with the wide dispersion of Sr and S isotope data within individual depositional cycles, as well as petrographic and scanning electronic microscopic data, led to the conclusion that diagenesis in some of the examined facies (i.e., laminated argillite and gypsarenite) was not enough to modify the primary texture or the geochemical signature. This is because the diagnetic processes took

---

* Authors: J.D.S. Paz, D.F. Rossetti & M. Macambira. Submitted to *Sedimentology*

place shortly after deposition or even penecontemporaneously, thus the newly formed minerals still keep the primary signature, thus serving for paleoenvironmental purposes. A non-marine brine source is suggested by $^{87}Sr/^{86}Sr$ ratios ranging from 0.707824 to 0.709280, which are higher than those from Late Aptian seawaters (i.e., between 0.70720 and 0.70735). The $\delta^{34}S$ varies from 16.12 to 17.89 ‰$_{(V\text{-}CDT)}$ in the eastern margin of the basin, which is in disagreement with Late Aptian marine values (13 to 16 ‰$_{(V\text{-}CDT)}$) Both geochemical tracers were influenced by facies characteristics, and thus a model is provided, where expansion of saline pan/lake systems led to decreasing $^{87}Sr/^{86}Sr$ values due to the release of ^{87}Sr from clay minerals by internal draining of mud flats. During expansion peaks, the $^{87}Sr/^{86}Sr$ values were lower because this process is cut off due to submergence of mud flats, added to the introduction of external ^{87}Sr-depleted waters resulting from weathering of Permian to Neocomian marine limestones and evaporites, as well as Triassic to Neocomian basaltic rocks. Furthermore, the sulphur isotope values decrease in the southern margin of the basin to a range that varies from 14.79 to 15.60 ‰$_{(V\text{-}CDT)}$ probably due to increased evaporation in shallower water settings.

Keywords: Sr and S isotopes; facies; mineralogy; Late Aptian; evaporites; continental paleoenvironment; Northern Brazil.

4.2. INTRODUCTION

Distinguishing between marine and nonmarine evaporites has been always challenging (Hardie, 1984; Brookins, 1988; Hovorka *et al*., 1993; Plàya *et al*., 2000), especially in places where the associated deposits lack diagnostic features to help reconstructing the depositional environments. This problem increases when evaporites evolve from hybrid brines, which is probably the most likely in many cases (Denison *et al.,* 1998). Lack of sedimentological parameters has motivated the use of Sr and S isotopes to help investigating the genesis of many evaporite deposits throughout the world (e.g., Denison *et al.*, 1998; Hovorka *et al.*, 1993; Playà *et al.*, 2000; Schreiber & El Tabakh, 2000). Both elements are abundant and uniformly distributed in seawater, displaying isotope ratios that vary through time in a known manner (e.g., Burke *et al.*, 1982; Bralower *et al.*, 1997). Once age is well established, these isotope tracers might provide reliable information on brine sources. Excursions from the established seawater curve are taken as indicators of continental or hybrid brines (Claypool *et al.*, 1980; Burke *et al.*, 1982), as long as other influences such as diagenesis can be discarded.

Late Aptian Codó deposits from northern Brazil (Fig. 4-1A) contains evaporites formed throughout the last stages of the Gondwana break-up, which ultimately led to opening of the South Atlantic Ocean. Determining whether the evaporitic brine evolved in a marine or non-marine setting has important implications for the paleogeographic modeling of the initial Brazilian Equatorial Margin. Hence, facies analysis and isotope geochemistry based on $^{87}Sr/^{86}Sr$ and $^{34}S/^{32}S$ were applied to help ascertain the genesis of evaporites in the Codó Formation exposed in the eastern and southern margins of the Grajaú Basin, near the towns of Codó and Grajaú. Based on sequence stratigraphic modelling (Rossetti, 2001), the first basinward marine transgression in this basin took place during the Albian when rifting fully developed. However, the occurrence of evaporites up to the basin margins has led to argue a widespread marine incursion as early as the Late Aptian (Batista, 1992; Rodrigues, 1995). Sr and S isotope analysis might help to better define the origin of the evaporitic brine source, and hence determine when the inland areas of the basin experienced the first marine incursion, narrowing the estimate of the time when the Brazilian Equatorial Margin established an ocean connection. In addition, previous facies analysis has attributed the deposits studied herein to a cyclic record formed by episodes of expansion and contraction of saline pan/lake systems (Paz & Rossetti, 2001). This study might also contribute to analyse the behavior of Sr and S isotopes relative to facies changes, an approach not extensively focused in the literature yet, but which is of great significance for reconstructing past hydrologic patterns.

4.3. MATERIAL AND METHODS

Sedimentary facies information available from previous field studies was combined with isotopic analysis of 36 samples from the Codó Formation collected along fresh quarry exposures. Isotopic analyses were carried out on whole-rock gypsum (eventually anhydrite) from selected facies. The samples were subdivided into three aliquots. The first one was disaggregated and the sulphate minerals picked from dried material. About 10 mg of powered sample was dissolved in 2.5 ml HCl (2.5 N) and heated at 70^{o} C during 12 hours to allow complete evaporation. Then, 1 ml HNO_3 (3.5 N) was added in order to separate the Sr cation.

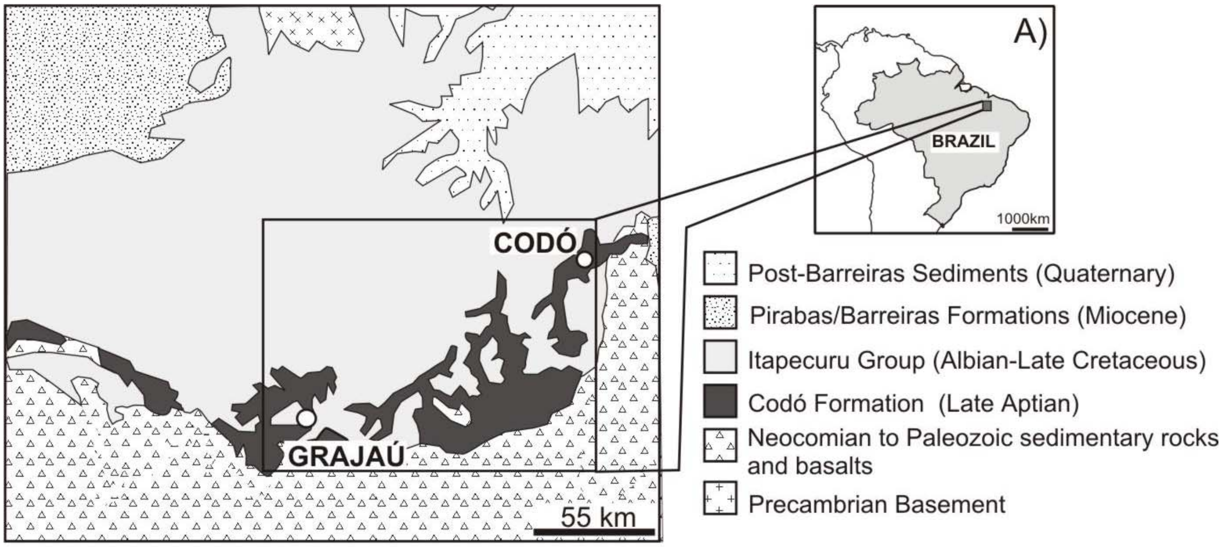

B) STRATIGRAPHY OF THE SÃO LUÍS- GRAJAÚ BASIN

AGE	DEPOSITIONAL SEQUENCE	STRATIGRAPHIC UNIT North	STRATIGRAPHIC UNIT South	TECTONIC STAGE
Quaternary		Post-Barreiras Sediments		Drift
Miocene		Pirabas/Barreiras Formations		
Lower Tertiary?/ Cenomanian	3	Itapecuru Group		
Albian	2			Rift
Late Aptian	1	Codó Formation	Grajaú Formation	Pre-rift

Fig . 4-1: A) Location and geological map of the study area in the north of Brazil. B) Stratigraphic framework of the São Luís-Grajaú Basin, with the depositional sequences discussed in the text.

The $^{87}Sr/^{86}Sr$ isotopic analyses were performed on mass spectrometers from the Geochronology Laboratory of the Universidade Federal do Para (Brazil). The ratios were normalized to $^{88}Sr/^{86}$=0.1194 in order to correct any mass discrimination, with results indicating mean values of 0.704120+-30x10^{-6} for the NBS 987 standard.

The second sample aliquot (circa 1.5 g) was used to quantify Rb by X-ray fluorescence (XRF), to analyse the contribution of ^{87}Rb to the $^{87}Sr/^{86}Sr$ ratio. Rb/Sr ratios vary between 0.01 and 0.02, indicating no need for corrections due to decay contribution (cf. Clauer, 1976).

The third sample aliquot (0.3 mg) was used for $\delta^{34}S$ determination carried out in the Iso-Analytical Ltd Laboratory, England. Vanadium pentoxide catalyst was added to the sample in a tin capsule, placed in an automatic sampler and combusted at up to 1700° C. The combusted gases were then swept in a helium stream over combustion catalysts (tungstic oxide/zirconium oxide) and through a reduction stage of high purity copper wires to produce SO_2, N_2, CO_2, and water. Water was removed using a Nafion™ membrane. Sulphur dioxide was resolved from N_2 and CO_2 on a packed GC column at a temperature of 30 °C. NBS-127 (barium sulphate, $\delta^{34}S_{V\text{-}CDT}$ = +20.3 ‰) distributed by the IAEA, Vienna. NBS-127, IAEA-S-1 (silver sulfide, $\delta^{34}S_{V\text{-}CDT}$ = -0.3 ‰) and Iso-Analytical IA-$BaSO_4$ (barium sulphate, $\delta^{34}S_{V\text{-}CDT}$ = +11.0 ‰) were used for calibration and correction.

Petrographic analysis of all evaporite samples and, whenever necessary, scanning electron microscopy were performed to provide the best constraints in the evaluation of possible diagenetic changes of the Sr and S values during burial, and thus decide on their potential use as paleohydrological indicators.

4.4. GEOLOGICAL FRAMEWORK AND PALEOENVIRONMENTAL CONTEXT

The sedimentary fill of the São Luís-Grajaú Basin consists of three 2nd-order sedimentary sequences (Fig. 4-1B) deposited from the Late Aptian to Quanternary (Rossetti, 2001). The Codó Formation developed during the lowstand stage of the oldest sequence. The prevalence of the polen *Sergipea variverrucata* in the deposits of the study area confirms their Late Aptian age (Batista, 1992; Antonioli, 2001; Rossetti *et al.*, 2001). This unit records the first deposits accumulated in a broad and shallow depression formed by mild tectonic stretching before the main Albian rifting stage. These Late Aptian deposits are represented throughout the basin by deltaic, eolian, lacustrine, as well as transitional to shallow marine deposits. A sharp discontinuity surface with a paleosol horizon occurs between the Late Aptian and the Albian deposits (Rossetti *et al.*, 2001; Fig. 4-2A).

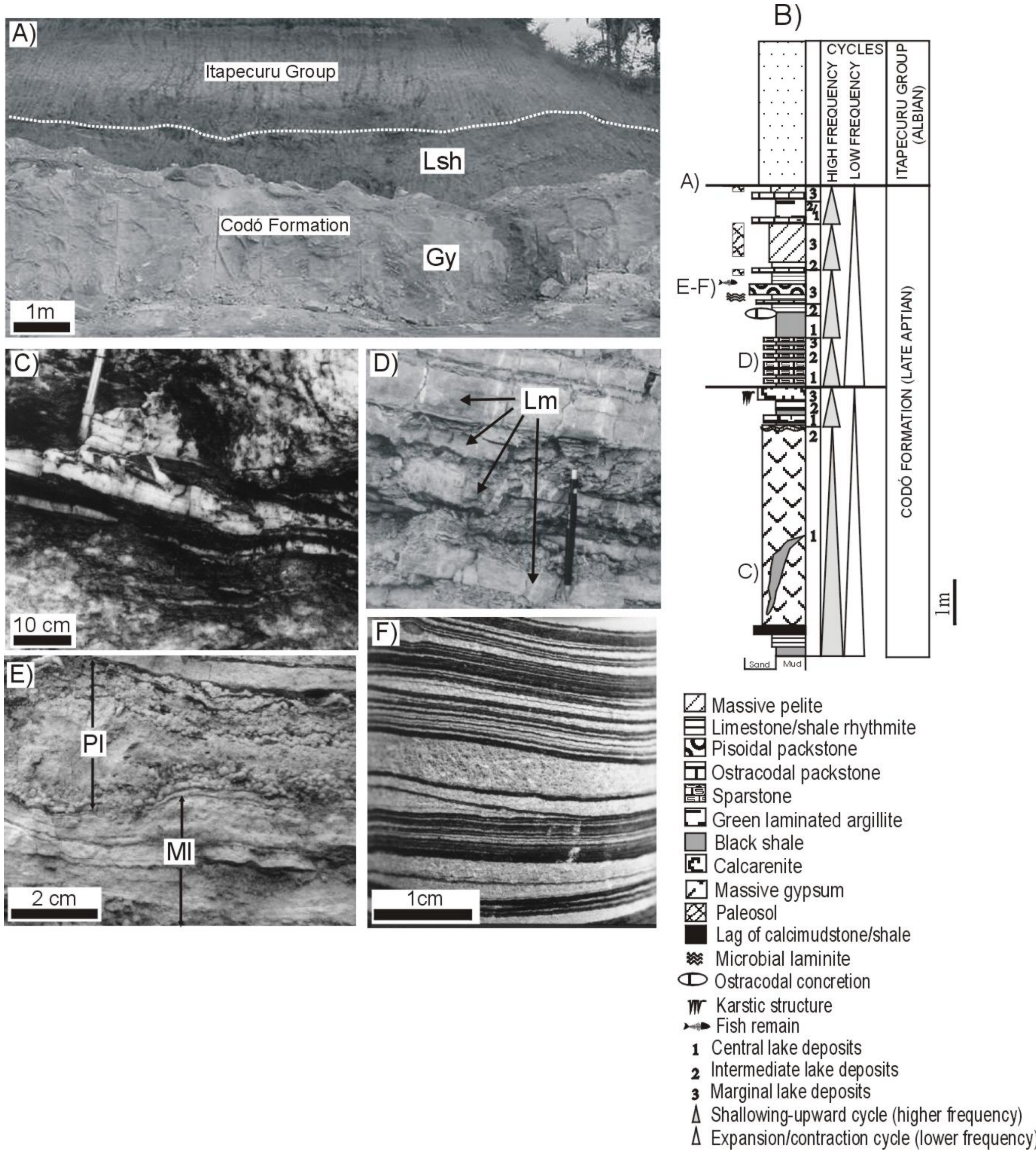

Fig . 4-2: A) A view of the unconformity between the Codó Formation and the overlying Albian deposits of the Itapecuru Group. (Gy= gypsum; Lsh=interbedded limestone and shale). B) Lithostratigraphic profile representative of the Codó Formation in the study area, with indication of the shallowing upward cycles formed by central lake (1), intermediate lake (2) and marginal lake (3) deposits. The letters to the left locate figures A-F. C) Bituminous shale (black areas) interbedded with evaporite (white areas) from central lake deposits. D) Interbedded limestones (lm) and shales (darker areas from intermediate lake deposits. E) Interbedded lime-mudstone (Ml) and pisoidal limestones (Pl) and F) Rhythmite of lime mudstone (white beds) and microbial mats (black beds) from marginal lake deposits.

In the study area, the Late Aptian Codó Formation consist ofs a 25 m-thick lacustrine prograding succession typically formed by shallowing-upward cycles (Fig. 4-2B). The base of these cycles includes evaporites and bituminous black shales attributed to central lake deposits (Fig. 4-2C). Pyrite and native sulphur are locally abundant in the shales. The central lake deposits progressively grade upward into laminated argillite interbedded with limestones (calcimudstone, laminated to massive peloidal wackestone to packstone and sparstone), attributed to intermediate lake environments (Fig. 4-2D). Bioturbation is locally present, as are symmetrical ripple marks. Ostracods represent circa 15-25% of the grains in the peloidal limestones, which may contain microbial mats. The top of the shoaling-upward cycles comprises a variety of intergrading lithofacies, including: 1) massive blocky pelite that varies upward from olive-green to brownish-red colors; 2) fenestral calcarenite formed by calcite grains; 3) ostracodal limestone (wackestone to grainstone); 4) pisoidal packstone (Fig. 4-2E) with elongated and agglutinating pisoids of various sizes interlaminated with microbial mats; 5) tufa; and 6) ostracodal limestone/shale rhythmite with abundant microbial mats (Fig. 4-2F). These deposits show an abundance of sedimentary features (i.e., paleosols, karstic surfaces, fenestrae, meteoric cements, vadose pisoids) typical of subaerial and/or meteoric exposure, consistent with their deposition in marginal lake environments. Most of the described sedimentary facies are also observed in the Grajaú area. However, in this locality evaporites dominate over the other facies, being represented by layered gypsum and gypsarenite.

The shallowing-upward cycles of the Codó Formation are arranged into a higher category of lower frequency cycles that are bounded by sharp discontinuity surfaces (Fig. 4-2B). At the base of these lower frequency cycles the superimposed shallowing-upward cycles are characterized by a higher volume of central lake deposits, while in its top shallowing-upward cycles with increased volume of marginal lake deposits dominate. It is noteworthy the presence of lags of intraformational calcimudstone and shales, clastic gypsum, as well as rhythmites with abundant microbial mats, at the base of the lower frequency cycles (Fig. 4-2B). The origin of these cycles is attributed to expansion and contraction of the lake system, probably related to syn-sedimentary seismic activity (Paz, 2000).

4.5. CHARACTERIZATION OF THE EVAPORITES

4.5.1. Description

The evaporites of the Codó Formation, represented by gypsum and locally anhydrite, occur as discontinuous lenses that are up to 4.5 m thick and circa 300 m long at the outcrop scale. In the Codó area, these deposits are interbedded with black shales, and exclusively occur in deeper central lake deposits, while in the Grajaú area they are linked to facies associations typical of shallower waters with evidence for exposure to meteoric and/or vadose conditions and pedogenesis.

The evaporites consist of three facies: layered gypsum, gypsarenite, and massive/macronodular gypsum. Layered gypsum dominates, and is comprised by laterally continuous, alternating dark/light horizontal beds that vary from few mm up to 10 cm thick (Fig. 4-3A-C). The dark beds are formed by either crystals or micronodules of gypsum less than 0.5 cm long distributed within a matrix of black shale. The light beds consist of upward-oriented fibrous gypsum crystals. The gypsarenite (Fig. 4-3C) is interbedded with the layered gypsum, forming layers few cm thick of moderate to poorly sorted, rounded to sub-rounded very coarse to pebbly gypsum grains. The massive/macronodular gypsum forms unstructured bodies (Fig. 4-3D) that are closely intergraded with macronodular gypsum consisting of centimeter-sized gypsum nodules, with or without a shale matrix. The gypsum nodules display an almond-like form defined by a web of undulating, horizontal to oblique fractures. Gypsum crystals up to 0.5 cm thick that grew perpendicularly to the fracture walls fill these fractures. Where fractures are several cm long, gypsum nodules replaced by anhydrite up to 3 cm in length are present (Fig. 4-3E). Rosettes of dark gypsum up to 5 cm in diameter are common in this facies. The massive/macronodular gypsum is in sharp contact with the layered gypsum, locally forming diapirs several meters long.

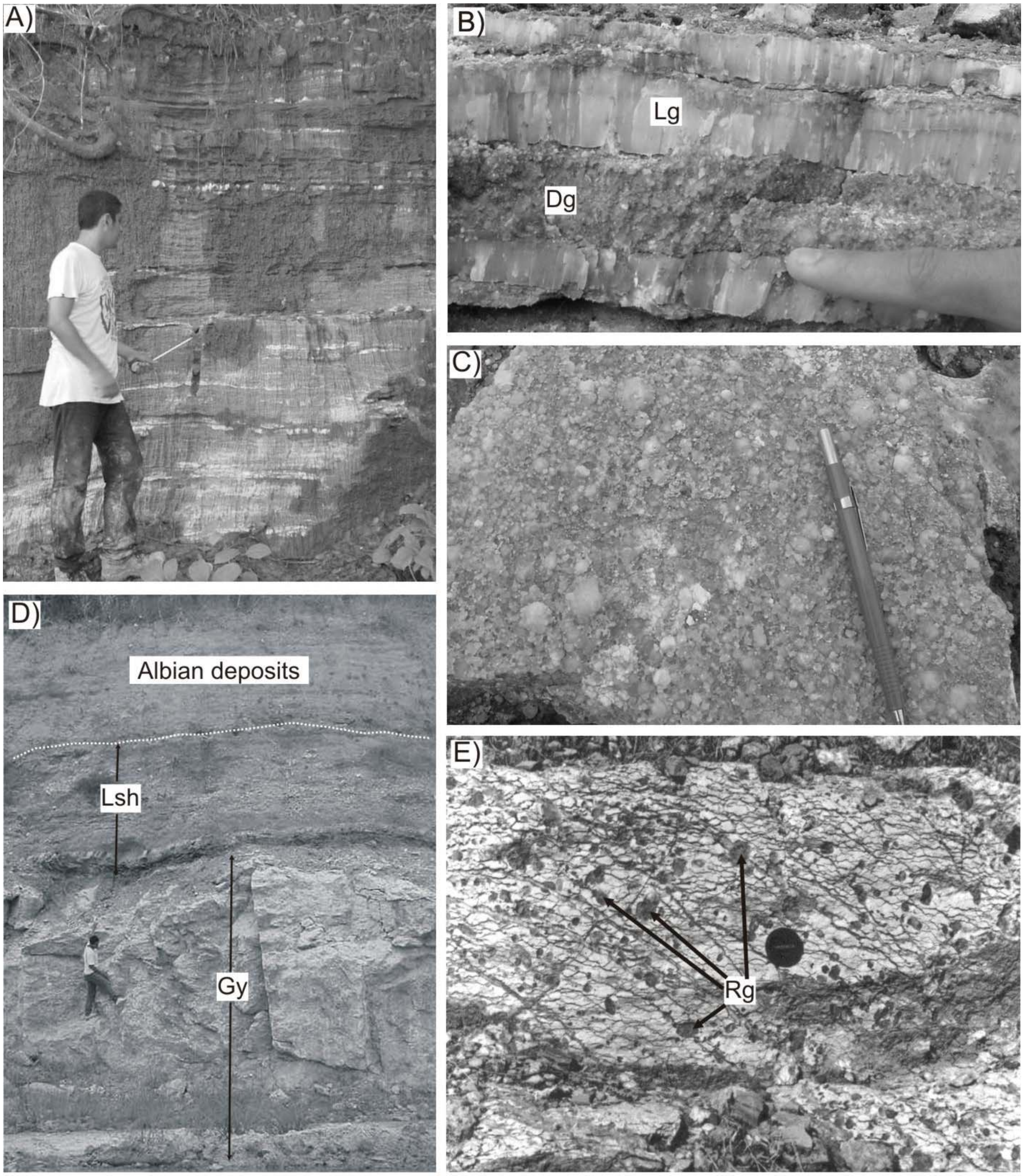

Fig . 4-3: Evaporite deposits from the Codó Formation. A) Layered gypsum. (Person for scale=1.68 m tall). B) Detail of the layered gypsum illustrating the alternating darker and lighter beds consisting of gypsum crystals or nodules within a matrix of black shale (Dg), and upward-oriented chevron/acicular gypsum crystals (Lg), respectively. C) A plan view of the gypsarenite facies (pen for scale=15 cm long). D) Massive/macronodular gypsum (Gy) underlying interbedded limestones and shales (Lsh). The white dotted line indicates the discontinuity surface between the Codó Formation and the Itapecuru Group (Albian). (Person for scale=1.68 m tall) E) A detail of the massive/macronodular gypsum strongly affected by fractures, resulting in almond-shaped anhydrite nodules. Note the abundant rosettes of gypsum (rg) that are disperse in this facies. (Lens cap for scale=10 cm in diameter).

Petrographic analysis of the evaporite facies showed that the darker beds are formed by nodular gypsum displaying laths up to 20 μm long of gypsum, and secondarily, by anhydrite, as well as by relics of calcite (Fig. 4-4A and B). The nodules were pervasively recrystallized to gypsum crystals averaging 200 μm long, internally displaying laths of gypsum and/or anhydrite, as well as relics of calcite. The volume of matrix is low in these nodules. The authigenic gypsum is in optical continuity beyond the nodule boundaries (Fig. 4-4C). The crystals from the lighter beds of the layered gypsum occur as aligned twin planes and superimposed growth faces with acute angles zig-zagging perpendicularly to the crystal long axes, and characterizes the chevron gypsum (Fig. 4-4D). These crystals are intergrown by acicular gypsum containing relics and/or ghosts of the chevron gypsum. In the gypsarenite facies (Fig. 4-4E), clasts were replaced by a mosaic of gypsum crystals varying from 100 μm to 2 mm in length. These display optical continuity beyond their boundaries and present abundant inclusions, similarly to the gypsum in the darker beds. The massive/macronodular gypsum is pervasively replaced by mosaics of either alabastrine gypsym (i.e., crystals up to 200 μm in diameter), or coarser crystals reaching up to 2 mm in diameter (Fig. 4-4F). As opposed to the previously described evaporite facies, the gypsum crystals in this facies lack inclusions, resulting in limpid mosaics. The anhydrite nodules are fine-grained to cryptocrystalline and internally display few tabular anhydrite crystals up to 250 μm. The nodules replace large (circa 8 mm) crystals of gypsum with well-preserved cleavage; they are, in turn, locally replaced by fine-grained gypsum.

4.5.2. Depositional setting

As previously stated, detailed facies analysis of the Codó Formation led to attribute it to a dominantly continental setting. This interpretation will be further supported by the isotope data presented in this paper. However, before going into that issue, it is important to detail the depositional setting of the evaporites as extracted from facies data, because both vertical and lateral variations in paleoenvironmental conditions seem to have affected the distribution of the isotope values in this instance.

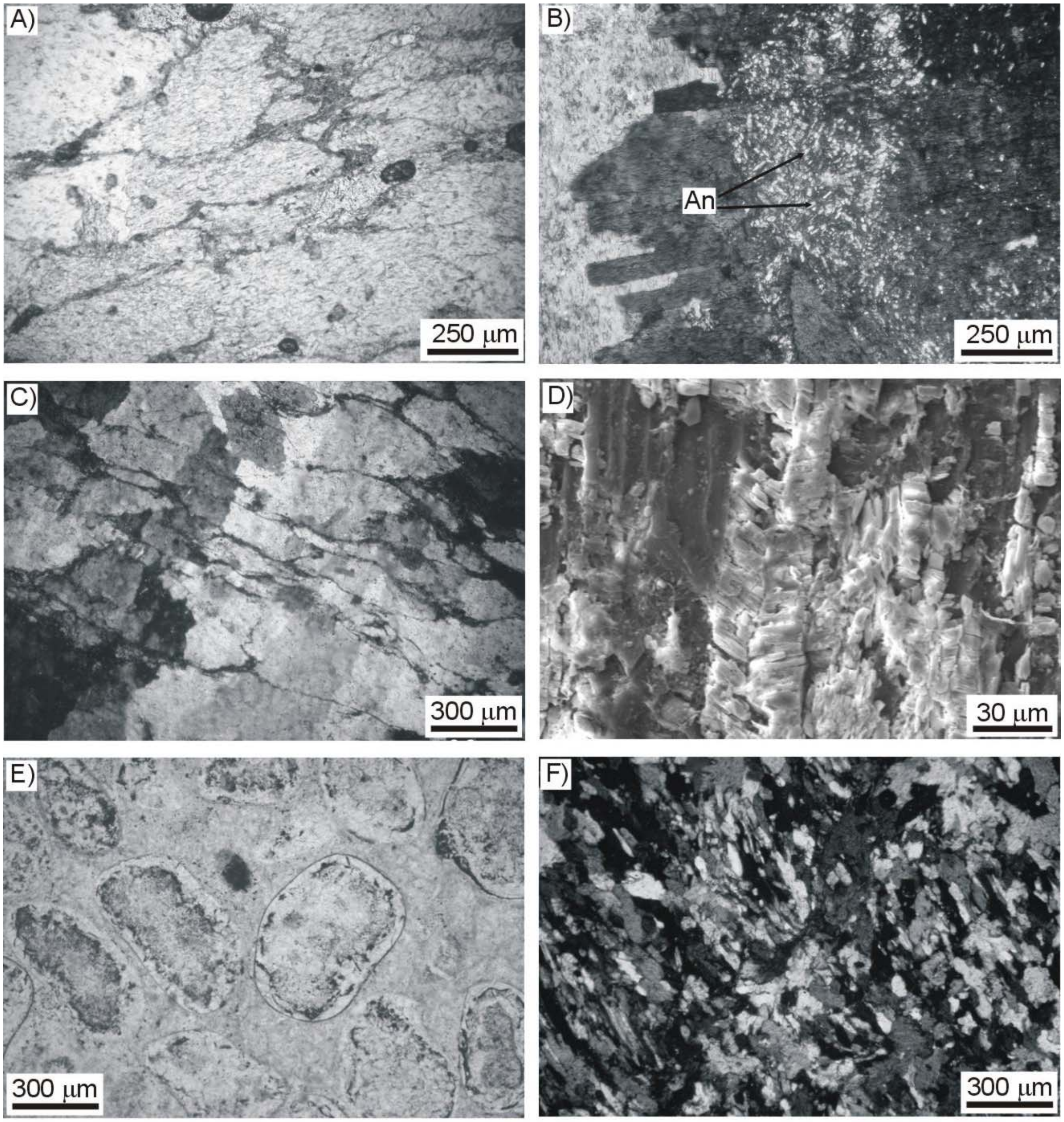

Fig . 4-4: Microscopy of the evaporites from the Codó Formation. A) Gypsum with nodular texture of the dark layered facies (parallel polarizers). B) Layered nodular gypsum with relics of anhydrite (=an; crossed polarizers). C) Recrystallized nodular gypsum displaying mosaic of gypsum crystals that grew beyond the nodule boundaries (crossed polarizers). D) Scanning electron photomicrography of the light beds in the layered gypsum, showing chevron gypsum locally replaced by acicular gypsum. E) A petrographic view of the gypsarenite formed by rounded gypsum grains after overgrowth. F) Alabastrine gypsum.

Stable and well-stratified hypersaline lakes with significant periods of anoxia and closure prevailed in the Codó area, which led to the preferential precipitation of salts in more saturated deeper central areas (Paz & Rossetti, 2001). Much more ephemeral conditions seem to have occurred in the Grajaú area, where more oxygenated water pans with evaporite precipitation in their margins and along surrounding mudflats prevailed (Fig. 4-5). This is demonstrated by the dominance of layered gypsum and gypsarenite in association with marginal and intermediate lake environments. In these facies, the chevron gypsum crystals of the light-layered gypsum attest to primary deposition on the floor of brine pools. Precipitation of similar features in many modern and ancient environments occurs when water depth is less than 2 m (e.g., Hovorka, 1987; Logan 1987; Handford, 1991; Smoot & Loweinstein, 1991). The darker layered gypsum is attributed to displacive intrasediment growth of crystals beneath the brine from groundwater brines in the capillary and/or upper phreatic zone, thus implying periods of eventual exposure (e.g., Kerr & Thomson, 1963; Southgate, 1982; Warren, 1999). The gypsarenite records periods when evaporite crystals were reworked. Therefore, the evaporites in the Grajaú area were dominantly formed in subaqueous, but shallower environments than in the Codó area, with better defined alternating periods of stable and ephemeral waters, a condition that led to envisage formation in a saline pan complex with widespread evaporitic mudflats.

Beside facies characteristics, a continental setting is also suggested by the abundance of ostracods mostly including the genus *Harbinia* and *Candona,* presence of charophytes, and absence of any marine tolerant fauna.

4.6. SR AND S ISOTOPES FROM THE EVAPORITES

Thirty-six samples were collected for Sr and S isotope analysis. However, only the results obtained from the layered gypsum and gypsarenite facies were used for paleoenvironmental purposes, because these lithologies showed the least degree of textural and/or mineralogical modification, while the massive/macronodular gypsum was strongly affected during burial, as discussed in the following section.

The results (Table 4-I; Fig. 4-6) for the layered gypsum and gypsarenite indicate variable $^{87}Sr/^{86}Sr$ ratios ranging from 0.708481 to 0.709280 in the Codó area and 0.708272 to 0.708935 in the Grajaú area, with only one sample displaying 0.708104 in the later. The massive/macronodular gypsum displayed the lowest values, ranging from 0.707824 to 0.708190. Discarding these values from our results, it is noteworthy that the $^{87}Sr/^{86}Sr$ ratios vary from higher to lower and then higher again upward within low frequency cycles. The Sr content ranges from 212 to 2051 ppm (mean value of 435 ppm). These values vary inversely to the Sr isotopes within individual cycles.

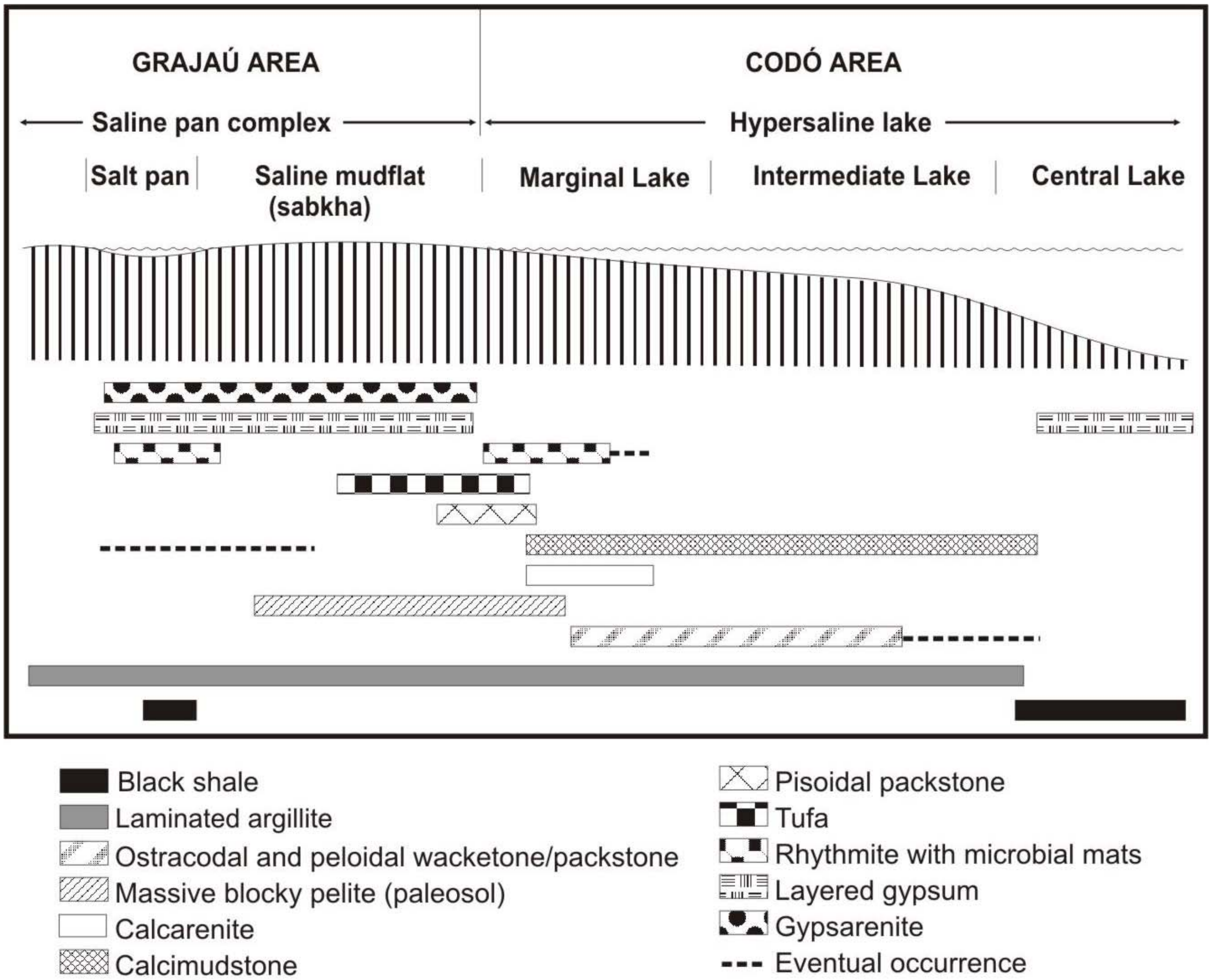

Fig . 4-5: A summary of facies distribution and depositional interpretation proposed for the Codó Formation in the study areas.

Table 4-I: Results of the strontium and sulphur isotope analyses from the evaporites of the Codó Formation in the study areas.

	Sample #	$^{87}Sr/^{86}Sr$	2σ	$\delta^{34}S$ (v-CDT)	Evaporite Facies
CODÓ	1	0.709280	18	16.59	Layered gypsum
	2	0.708901	15	17.09	
	3	0.708860	9	17.89	
	4	0.708558	15	17.47	
	5	0.708652	12	16.99	
	6	0.708481	14	-2.23	
	7	0.708675	53	16.12	
	8	0.708992	48	16.50	
	9	0.708116	17	15.85	Massive/ macronodular gypsum
	10	0.708153	14	15.66	
	11	0.708134	14	15.29	
	12	0.707824	46	15.21	
	13	0.707989	30	-	
	14	0.707960	34	-	
GRAJAÚ	15	-		-5.57	Layered gypsum
	16	0.708821	25	15.04	
	17	0.708831	24	15.15	
	18	0.708822	19	14.79	
	19	0.708754	29	15.34	
	20	0.708416	20	15.10	
	21	0.708561	15	15.06	
	22	0.708441	27	15.60	
	23	0.708413	59	15.35	
	24	0.708272	49	15.12	
	25	0.708442	27	15.30	
	26	0.708555	23	15.54	
	27	0.708935	28	15.29	
	28	0.708842	22	14.56	
	29	0.708758	26	14.60	
	30	0.708477	27	14.69	
	31	0.708443	25	14.75	
	32	0.708190	32	15.52	Massive/ macronodular gypsum
	33	0.708090	30	15.14	
	34	0.708138	55	15.24	
	35	0.708104	17	15.07	
	36	0.708104	11	14.60	

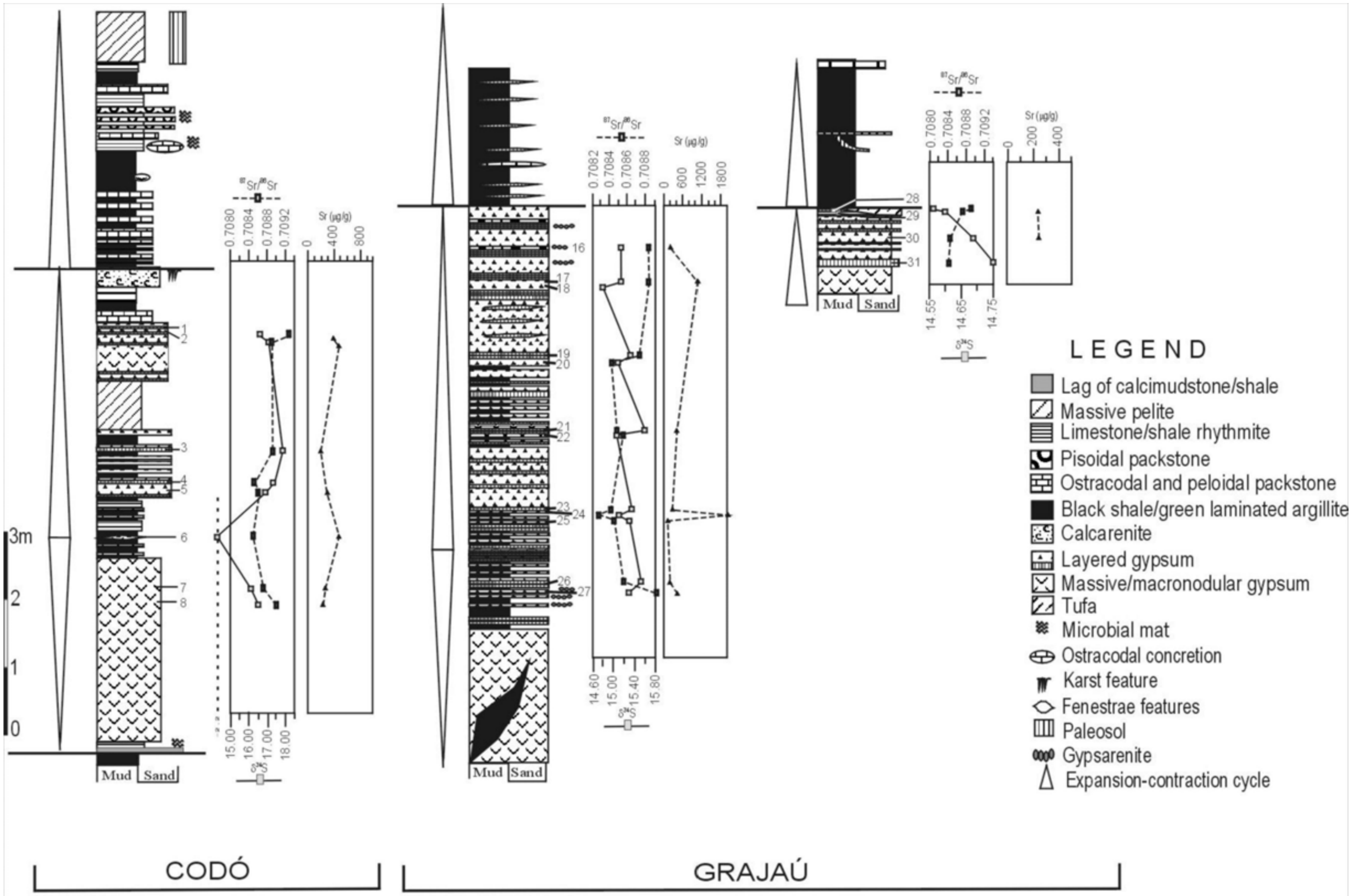

Fig . 4-6: Lithostratigraphic profiles representative of the Codó Formation in the study areas with the plot of $^{87}Sr/^{86}Sr$, Sr (ppm) and $\delta^{34}S$ isotope values.

The $^{34}S/^{32}S$ ratios from layered gypsum and gypsarenite in the Codó area varied from 16.12 to 17.89 ‰ $_{(V\text{-}CDT)}$, with only one sample having an anomalous value of –2.23 ‰ $_{(V\text{-}CDT)}$. The Grajaú area, in turn, showed distinctively lower values ranging from 14.79 to 15.60 ‰ $_{(V\text{-}CDT)}$, with one sample displaying a negative value of –5.57 ‰ $_{(V\text{-}CDT)}$. The distribution of S isotope within individual low frequency cycles changes following the same pattern shown by the Sr isotope data, except for local inverse covariance where marginal lake deposits dominate. The massive/macronodular gypsum in both areas showed S isotope values between 15.07 and 15.85 ‰ $_{(V\text{-}CDT)}$.

4.7. BURIAL OVERPRINT

An important step to consider, before analysing the significance of the Sr and S isotope data as potential paleoenvironmental indicators, is to eliminate diagenetic influences. A line of evidence suggests that, if the deposits were modified after deposition, diagenesis was not enough to cause any significant changes in the isotope values, which seems to rather reflect the primary water composition.

First, absence of significant diagenetic imprint is suggested by the overall wide dispersion of Sr and S isotope data within individual depositional cycles. Second, there is a consistent change in isotope values along the deposits formed during the expansion and contraction phases of the saline pan/lake systems, revealing a depositional, rather than a diagenetic signature. Third, petrographic and scanning electronic microscopic studies helped to select samples suitable for isotope investigation. In fact, most of the analyzed samples revealed at least a certain degree of replacement, recrystallization, cementation, neomorfism or dissolution. However, this study also led to conclude that the mineralogical modifications observed in the layered gypsum and gypsarenite, as explained in the following, were not enough to cause any significant change in the isotope signal, as opposed to the massive/macronodular gypsum that was pervasively modified during burial.

As previously discussed, the crevron crystals in the lighter portion of the layered gypsum record primary deposition on the floor of brine pools. The horizontal alternations of lighter and darker gypsum in this facies represent a product of sedimentary processes. The darker layered gypsum formed slightly after deposition, but still under strong influence of the depositional setting as precipitation took place within only a few milimeters below the depositional surface (cf. Warren, 1999). The chevron gypsum was in part replaced by acicular gypsum, as indicated by relic and ghost features of chevron gypsum. But even in this case the effects of diagenesis were rather mild, not disturbing bedding planes. Although ultimate evidence is lacking, the absence of other types of secondary gypsum in these beds suggests that such replacement took place also shortly after deposition, thus still under a strong influence of the primary brine. A second phase of gypsum would have affected this facies, as well as the gypsarenite, which locally resulted in gypsum crystals that grew beyond nodule or clast boundaries. However, this process was not extensive enough to replace the internal laths of anhydrite/gypsum and/or relics of calcite. This fact, added to isotope values similar to those from the layered gypsum, as will be shown in the following sections, led us to attribute an eodiagenetic origin for this second phase of gypsum formation. Gypsum crystals formed shortly after deposition will keep a primary isotope signature, because the precipitating fluids derive from dissolution of evaporites formed in the same depositional site (e.g., Denison *et al.*, 1998).

On the other hand, the massive/macronodular gypsum records salt replacement and recrystallization during deeper burial in association with halokinesis. As this process took place, the original structures were greatly obliterated, forming a dominantly massive deposit. The pervasive mosaics of limpid crystals typical of this facies might have required several phases of replacement, during which any primary sedimentary feature was lost. Although some of the macronodular texture might reflect relics of a primary nodulation, the majority of the macronodules originated by salt displacement, giving rise to fracturing and precipitation of bladed gypsum by introduction of sulphate-saturated intrastratal waters. The close association of anhydrite nodules with fractures points to their formation by local dewatering due to overpressure. In fact, these samples revealed anomalously the lowest isotope values, which is consistent with its distinct post-depositional evolution. Furthermore, samples with clay minerals, as revealed under the microscope, were not applied for analysis of geochemical tracers in order to avoid Sr contamination.

4.8. DISCUSSION

Considering that a significant diagenetic imprint was discarded in samples of layered gypsum and gypsarenite, the Sr and S isotopes could be used for paleoenviromental purposes. On the other hand, as expected, the values obtained for the massive/macronodular gypsum differed from the average strontium ratios. This is attributed to later growth of limpid gypsum crystals and secondary nodules of anhydrite, as characterized by petrographic studies. As a result, the isotope data from the massive/macronodular facies were discarded from our analysis. In addition, the sample from the Grajaú area that also showed an anomalously low Sr isotope value was also excluded, as this sample comes from a red-stained gypsum horizon only 0.2 m below a discontinuity surface probably related to prolonged subaerial exposure at the top of a shallowing-upward succession.

The $^{87}Sr/^{86}Sr$ and $^{34}S/^{32}S$ analyses have been successfully used to distinguish marine and non-marine brines throughout the world (Table 4-II). These methods have been increasingly applied in evaporites because: 1. evaporites are rich in strontium and sulphur; 2. evaporites are widespread in both marine and non-marine settings, and their distinction is very problematic where the associated deposits have no other diagnostic paleoenvironmental features, requiring more sophisticated geochemical procedures; 3. other geochemical tracers commonly used in paleoenvironmental reconstructions show many conflicting results (e.g., Hovorka *et al.*, 1993); 4. distribution of Sr and S ratios in seawater is well known for the Phanerozoic; 5. low permeability in evaporites difficults the introduction of external water carrying Sr and/or S that may modify their isotopic composition; and 6. Sr isotope is very sensible to detect the introduction of marine waters in continental settings.

Previous studies focusing on Sr isotopic composition of carbonates and evaporites, originated from marine-based brines, have established values between 0.70720 and 0.70735 for the Aptian (Bralower *et al.*, 1997; Jones & Jenkins, 2001; Fig. 4-7). The data generated here are much higher than expected for Late Aptian marine deposits, suggesting a continental brine source. The difference of the Sr isotope values from the Codó Formation relative to the Aptian seawater is at least of 0.00075. Similar variations of strontium isotope data relative to the seawater have also been measured from many other continental deposits recorded in the literature (e.g., Faure *et al.*, 1963; Jones & Faure, 1967, 1972; Faure & Barret, 1973; Denison *et al.*, 1998; Vonhof *et al.*, 1998; Playà *et al.*, 2000). Modern settings record even lower differences (i.e, 0, 00021) when continental and marine brines are compared, as measured for instance in the Abu Dhabi Sabhka (Müller *et al.*, 1990). Therefore, the high Sr isotope data from the layered gypsum and gypsarenite are related to a continental brine source, which is consistent with the proposed depositional model interpreted with basis on facies analysis.

Table 4-II: $^{87}Sr/^{86}Sr$ values of non-marine source brines and rocks.

Age ($^{87}Sr/^{86}Sr$ seawater)	Origin	Material	$^{87}Sr/^{86}Sr$	N*
Holocene (0.709173)	E. Great Salt Lake[2]	Brine	0.7167 to 0.7179	9
	W. Great Salt Lake[2]	Brine	0.7125 to 0.7139	4
	Lakes and rivers from Canadian Shield[3]	Brine	0.712 to 0.726	
	Lake Vanda (Antartida)[4]	Brine	0.7149	
	Lake George[2]	Brine	0.7184	
Miocene (0.7081 to 0.7089)	Pebas Formation[6]	Carbonate	0.708160 to 0.709051	10
	Eastern Betics[7]	Evaporite	0.70804 to 0.70888	
Jurassic (~0.7069) (~0.7073)	Todilto Formation[12]	Carbonate	0.707273 to 0.708673	40
		Gypsum	0.706873 to 0.708073	35
Permian	Beacon Supergroup[16]	Carbonate	0.7150 to 0.7280	12
	Salado-Tansill formations[9]	Evaporite	0.7069 to 0.7076	5
Devonian (~0.7077 to 0.7086)	Beacon Supergroup[16]	Carbonate	0.7260 to 0.7291	3

N*= number of samples.

[2]Jones and Faure (1972); [3]Faure et al. (1963); [4]Jones and Faure (1967); [6]Vonhof et al. (1998); [7]Playà et al. (2000); [12]Denison et al. (1998); [16]Faure and Barret (1973).

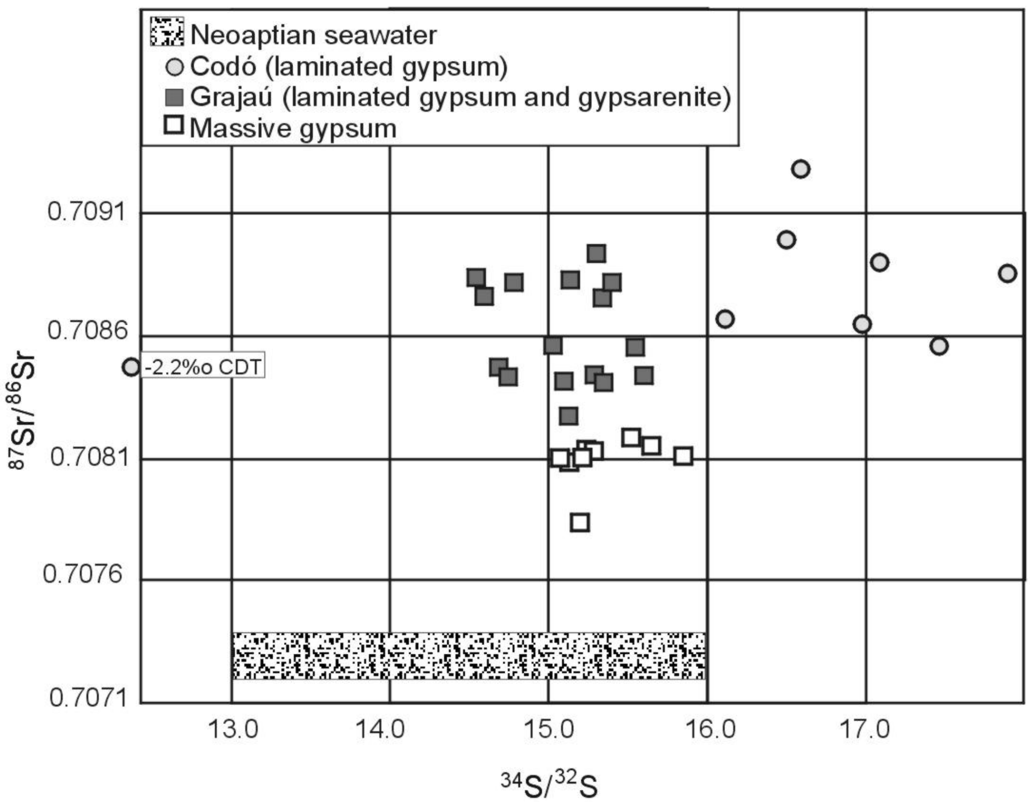

Fig . 4-7: $^{87}Sr/^{86}Sr$ and $\delta^{34}S$ values from the Codó Formation and comparison with the values from the Aptian seawater. Note that the strontium values for both of the study areas are much higher than those expected from Aptian seawaters, which support a continental-sourced brine for the evaporites. This interpretation is further supported by the higher values of S isotopes, and the scatter nature of both isotopes. The lower S values from the Grajaú area are interpreted to have a facies control, and probably respond to increased evaporation (see text for further discussion).

In addition to the high $^{87}Sr/^{86}Sr$ values, their wide distribution in a same section and between sections, with a standard deviation of 0.000262, conforms to the proposition of continental-derived brines (Playà *et al.*, 2000). Oceans favor geochemical homogenization, thus marine deposits should provide more consistent Sr isotope data during a given time interval (Denison *et al.*, 1998). For instance, studies in a modern sabkha from the Persian Gulf indicate a standard deviation of $^{87}Sr/^{86}Sr$ much higher (i.e., 0.000177) in continental brines than in marine brines (i.e., 0,000042) (Müller *et al.*, 1990). The standard deviation of the Sr isotope values in the Codó Formation is much higher than measured in this modern analog, reinforcing a continental origin for the brine.

The upward decrease, and then increase, in $^{87}Sr/^{86}Sr$ values within the low frequency depositional cycles in both of the study areas seem to be better explained by facies changes related to expansion and contraction of saline pan/lake systems (Fig. 4-8). Analysis of facies distribution within these cycles suggests either rapid or progressive expansion of the depositional system. Rapid expansion is recorded where central lake black shales and laminated argillites overlie directly the basal discontinuity surfaces at the base of the cycles. On the other hand, progressive expansion is suggested where this surface is overlain by clastic evaporites, rhythmites, and lags of intraformational calcimudstone/shales that grade upward into laminated argillites and black shales. Contraction of the depositional system is recorded by the increased dominance of marginal facies in the uppermost portions of the low frequency cycles.

The distribution of $^{87}Sr/^{86}Sr$ values according to the expansion and contraction phases of the saline pan/lake systems reinforces their primary nature. Hence, the progressive expansion of the depositional system gave rise to evaporitic precipitation. While evaporites precipitated in central environments, low lying marginal areas dominated by mud flats were exposed to substantial leaching due to weathering (Fig. 4-8). During this process, the draining of clay minerals might have released ^{87}Sr, increasing $^{87}Sr/^{86}Sr$ values of the evaporitic precipitating brines (cf. Hovorka *et al.*, 1993; Playà *et al.*, 2000). Similar facies control on the distribution of $^{87}Sr/^{86}Sr$ ratios has been documented in contraction/expansion cycles in the Eocene Green River Formation (cf. Rhodes *et al*., 2002).

Following initial expansion, increased contribution of external drainage resulted in a period of maximum expansion of the saline pan/lake systems. Flooding promoted water dilution, ending the evaporite precipitation. Increased inflow also resulted in the introduction of large volumes of muds in suspension, which were eventually settled down, forming the laminated argillites and black shales. Expansion caused flooding of widespread marginal mud flats and, as a consequence, the release of ^{87}Sr from clay minerals was cut off, resulting in relatively lower $^{87}Sr/^{86}Sr$ values.

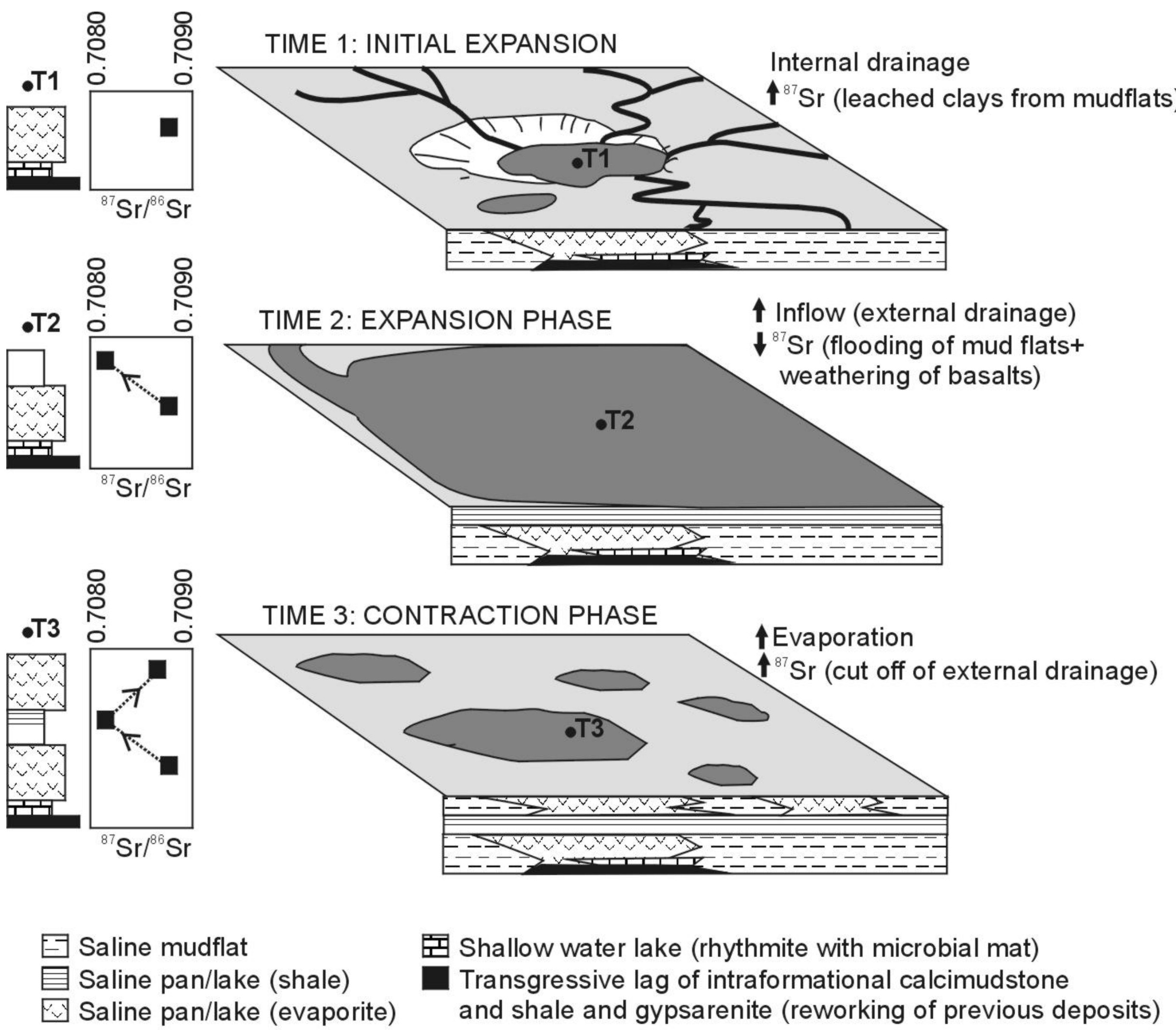

Fig . 4-8: Model to explain the distribution of ^{87}Sr/^{86}Sr according to the low frequency cycles of the Codó Formation. (Inspired on Rhodes *et al.*, 2002).

Additionally, the Sr isotope ratios might have decreased due to the contribution of Sr released from basaltic source rocks. This is suggested due to the fact that the study areas are located near Permian to Neocomian marine-derived limestones and evaporites from the intracratonic Parnaíba Basin, as well as Triassic to Neocomian basaltic rocks associated with the Xambioá-Teresina Arch (Fig. 4-1A). Weathering of these rocks might have contributed with significant amounts of ^{87}Sr-depleted waters into the evaporitic basin, resulting in relatively lower ^{87}Sr/^{86}Sr values. However, it is noteworthy that, even considering the influence of a basaltic sources, the ^{87}Sr/^{86}Sr values are still much higher than expected to Late

Aptian seawaters. Mixing of waters from both basaltic and sedimentary rocks might have provided continental brines with $^{87}Sr/^{86}Sr$ ratios comparable to the ones obtained for the study areas.

During a following stage, the inflow was interrupted and the saline pan/lake systems contracted. As the introduction of mud progressively reduced and evaporation increased, carbonates were formed and marginal facies became more widespread. As a consequence, the $^{87}Sr/^{86}Sr$ data increased.

Likewise the strontium, sulphur is also abundant and uniformly distributed in seawaters, and its isotope ratio changed through time, opening the possibility for its use to determine brine sources (Claypool *et al.*, 1980). During the Late Aptian, the $\delta^{34}S$ values ranged from 13 to 16 ‰$_{(V\text{-}CDT)}$ (Claypool *et al.*, 1980; Fig. 4-7). Similarly to strontium, the sulphur isotope values obtained in the Codó Formation are highly variable, as expected in continental-derived brines. In addition, the values from the Codó area are higher than 16 ‰$_{(V\text{-}CDT)}$, thus also conforming to continental-derived brines. However, values from the Grajaú area are lower, situating in the upper part of the range expected for marine waters. A marine contribution to the saline pan complex could explain these values, but this is not supported by the strontium nor by the facies data, as previously discussed. Therefore, if hybrid brine is to be considered in this instance, then the marine contribution was not enough to cause a significant geochemical imprint other than in the S isotope composition. Taking into account previous studies discussing this method, this interpretation is disregarded here because in general sulphur isotope is considered much less diagnostic of brine sources than strontium isotope (Chivas *et al.*, 1991; Denison *et al.*, 1998; Playà *et al.*, 2000). Considering the difference in facies patterns between the study areas, an alternative hypothesis is that the higher rates of evaporation in the Grajaú area, favored by the prevalence of shallower evaporitic environments, might have contributed to the depletion in ^{34}S. In seawaters, this process might account for about 2‰ of ^{34}S depletion (Hoefs, 1980), though there is no information available from lake systems, and the effect in the gypsum precipitate-brine relationship is an issue open for further research.

Considering a non-marine brine interpretation, then the changes in S isotope values between the Codó and Grajaú areas might have had a facies control. The increase in $\delta^{34}S$

values in the Codó area (Fig. 4-7) is attributed to a more restricted environment, resulting from the prevalence of a hydrologically closed lake system, as revealed by facies analysis (Paz and Rossetti, 2001). Under such conditions, the $\delta^{34}S$ tends to be increased due to the activity of sulphate-reducing bacteria, resulting in SO_4 depletion in the water and increasing the $\delta^{34}S$ (Hoefs, 1980). On the other hand, more oxygenated conditions would have prevailed in the Grajaú area, which led to a relative enrichment of sulphates and a consequent decrease in $\delta^{34}S$. The two anomalous negative sulphur isotope values obtained in the study area were derived from evaporite sampled from central lake black shales recording the beginning of flooding stages, and they may be related to recycling of underlying sulphides.

4.9. CONCLUSIONS

This study led to several conclusions: 1. when combined with facies analysis and optical (petrography and scanning electron microscopy), Sr isotope is a powerful tool for distinguishing evaporites derived from marine and non-marine brines. This effort led to the confirmation that the deposition of the Codó Formation in the southern and eastern margins of the Grajaú Basin, northern Brazil, took place dominantly in saline pan/lake depositional systems; 2. Sr isotopes revealed to be very sensible to detect hydrological changes in this type of environments; 3. however, fluctuations on the distribution of Sr values due to changes in sedimentary patterns are not enough to preclude distinguishing between marine and non-marine evaporites; 4. during initial expansion phases, the Sr isotopes in saline pan/lake environments tend to decrease due to leaching of ^{87}Sr from clay minerals of mud flats exposed to internal drainage; 5. during maximum expansion of this type of system, these values progressively decrease due to the cut off of this process, as the mud flats become flooded; 6, in the particular case of the study area, the lowering in Sr isotope values might have additionally caused the introduction of ^{87}Sr-depleted waters derived from weathering of older marine limestone and evaporites, as well as basaltic rocks; and 7. interruption of external drainage and contraction of the system caused increased carbonate precipitation, with consequent slight increase in Sr isotope values. The data from the study area allowed also to conclude that the application of sulphur isotope as a parameter to decipher brine sources is limited. This is because, even where strontium values and geochemical tracers indicate a non-marine brine source, the sulphur values might coincide with those from seawater for a given time interval, as observed in the Grajaú area. Hydrologically closed systems tend to develop anoxia, when the activity of sulphate-reducing bacteria results in SO_4 depletion in the water, with the consequent increase of $\delta^{34}S$. On the other hand, more oxygenated conditions lead to a relative enrichment of sulphates and a consequent decrease in $\delta^{34}S$. Therefore, significant fluctuations in sulphur isotope composition might take place due to changes in hydrological regime, and thus the use of this parameter alone is not recommended to decipher between marine/non-marine brines.

Acknowledgements. The Itapicuru Agroindustrial S/A is acknowledged for the permission to access the quarries with the exposures of the Codó Formation. This work was financed by the Brazilian Council for Research–CNPq (Project #460252/01).

REFERENCES

Antonioli, L. (2001) Estudo palino-estratigráfico da Formação Codó–Cretáceo Inferior do Nordeste brasileiro. Ph.D. Thesis, Universidade Federal do Rio de Janeiro, Rio de Janeiro, RJ, 265 pp.

Batista, A.M.N. (1992) Caracterização Paleoambiental dos sedimentos Codó-Grajau, Bacia de São Luís (MA). M.Sc. Thesis, Universidade Federal do Para, Belém, PA, 102 pp.

Bralower, T.J., Fullagar, P.D., Paul, C.K., Dwyer, G.S. and **Leckie, R.M.** (1997) Mid-Cretaceous strontium-isotope stratigraphy of deep-sea sections. *Geol. Soc. Am. Bull.* **109**, 1421-1442.

Brookins, D.G. (1988) Seawater $^{87}Sr/^{86}Sr$ for the Late Permian Delaware Basin evaporites (New México, U.S.A.). *Chem. Geol.*, **69**, 209-214.

Burke, W.H., Denison, R.E., Hetherington, E.A., Koepnick, R.B., Nelson and **H.F., Otto, J.B.** (1982) Variation of seawater $^{87}Sr/^{86}Sr$ throughout Phanerozoic time. *Geology,* **10**, 516-519.

Chivas, A.R., Andrew, A. S., Lyons, W.B., Bird, M.I. and **Donelly, T.H.** (1991) Isotopic constraints on the origin of salts in Australian playas. 1. Sulphur. *Palaeogeogr., Palaeoclimatol., Palaeoecol.*, **84**, 309-332.

Claudes, N. (1976) $^{87}Sr/^{86}Sr$ composition of evaporitic carbonates and sulphates from Miocene sediment cores in the Mediterranean sea (D.S.D.P., Leg 13). *Sedimentology*, **23**, 133-140.

Claypool, G.E., Holser, W.T., Kaplan, I.R., Sakai, H. and **Zak, I.** (1980) The age curves of sulphur and oxygen isotopes in marine sulphates and their mutual interpretation. *Chem. Geol.*, **28**, 199-260.

Denison, R.E., Kirkland, D.W. and **Evans, R.** (1998) Using strontium isotopes to determine the age and origin of gypsum and anhydrite beds. *J. Geol.*, **106**, 1-17.

Faure, G. and **Barrett, P.J.** (1973) Strontium isotope composition of non-marine carbonate rocks from the Beacon Supergroup of the Transantarctic Mountains. *J. Sedim. Petrol*., **43**, 447-457.

Faure, G., Hurley, P.M. and **Fairbairn, W.H.** (1963) An estimate of the isotopic composition of strontium in rocks of the Precambrian Shield of North America. *J. Geophys. Res.,* **68**, 2323-2329.

Handford, C.R. (1991) Marginal marine halite: sabhkas and salinas. In: *Evaporites, Petroleum and Mineral Resources* (Ed. J.D. Melvin), Developments in Sedimentology 50, pp.1-66. Elsevier, Amsterdam.

Hardie, L.A. (1984) Evaporites: Marine or non-marine?: *Am. J. Sci,* **87**, 193-240.

Hoefs, J. (1980) Stable isotope geochemistry. Springer-Verlag, Berlim, 208 pp.

Hovorka, S.D. (1987) Depositional environment of marine-dominated bedded halite, Permian Sant Andreas Formation, Texas. *Sedimentology*, **34**, 1029-1054.

Hovorka, S.D., Knauth, L.P., Fisher, R.S. and **Gao, G.** (1993) Marine to nonmarine facies transition in Permian evaporites of the Palo Duro basin, Texas: geochemical response. *Geol. Soc. Am. Bull.*, **105**, 1119-1134.

Jones, C.E. and **Jenkins, H.C.** (2001) Seawater strontium isotopes, oceanic anoxic events, and seafloor hydrothermal activity in the Jurassic and Cretaceous. *Am. J. Sci.* **301**, 112-149.

Jones, L.M. and **Faure, G.** (1967) Origin of the salts in Lake Vanda, Wright Valley, southern Victoria Land, Antarctica. *Earth Planet. Sci. Lett.*, **3**, 101-106.

Jones, L.M. and **Faure, G.** (1972) Strontium isotope geochemistry of Great Salt Lake, Utah. *Geol. Soc. Am. Bull.*, **83**, 1875-1880.

Kerr, S.D. and **Thompson, A.** (1963) Origin of nodular and bedded anhydrite in Permian shelf sdiments, Texas and New Mexico. *AAPG Bull.,* **47**, 1726-1732.

Logan, B.W. (1987) The Lake MacLeod Evaporite Basin, Western Australia–Holocene Environments, Sediments, and Geological Evolution. *AAPG Mem.,* 44, 140 pp.

Müller, D.W., McKenzie, J.A. and **Mueller, P.A.** (1990) Abu Dhabi Sabkha, Persian Gulf, revisited: application of strontium isotopes to test an early dolomitization model. *Geology,* **18**, 618-621.

Paz, J.D.S. (2000) Análise Faciológica da Formação Codó (Aptiano Superior), na Região de Codó (MA), Borda Leste da Bacia do Grajaú. M.Sc. Thesis, Universidade Federal do Pará, Belém, PA, 117 pp.

Paz, J.D.S. and **Rossetti, D.F.** (2001) Reconstrução paleoambiental da Formação Codó (Aptiano), borda leste da Bacia do Grajaú, MA. In: *O Cretáceo na Bacia de São Luís-Grajaú* (Eds. D.F. Rossetti., A.M. Góes and W. Truckenbrodt), pp. 77-101. Goeldi Press, Belém.

Playà, E., Ortí, F. and **Rosell, L.** (2000) Marine to non-marine sedimentation in the upper Miocene evaporites of the Eastern Betics, SE Spain: sedimentological and geochemical evidence. *Sed. Geol.*, **133**, 135-166.

Rhodes, M.K., Caroll, A.R., Pietras, J.T., Beard, B.L., and **Johnson, C.M.** (2002) Strontium isotope record of paleohydrology and continental weathering, Eocene Green River Formation, Wyoming. *Geology*, **30**, 167-170.

Rossetti, D. F. (2001) Depositional architecture of the São Luís-Grajaú Basin. In: *O Cretáceo na Bacia de São Luís-Grajaú* (Eds. D.F. Rossetti., A.M. Góes and W. Truckenbrodt), pp.31-46. Goeldi Press, Belém.

Rossetti, D.F., Góes, A.M. and **Arai, M**. (2001) A passagem Aptiano-Albiano na Bacia de São Luís-Grajaú, MA. In: *O Cretáceo na Bacia de São Luís-Grajaú* (Eds. D.F. Rossetti., A.M. Góes and W. Truckenbrodt), pp. 101-117. Goeldi Press, Belém.

Schreiber, B.C. and **El Tabakh, M.** (2000) Deposition and early alteration of evaporites. *Sedimentol.*, **47**, 215-238 (Supplement 1).

Smoot, J.P. and **Lowenstein, T.K.** (1991) Depositional environments of non-marine evaporites. In: *Evaporites, Petroleum and Mineral Resources* (Ed. J.D. Melvin). Developments in Sedimentology 50, 189-347. Elsevier, Amsterdam.

Southgate, P.N. (1982) Cambrial skeletal halite crystals and experimental analogues. *Sedimentol.*, **29**, 391-407.

Vonhof, H.B., Wesselingh, F.P. and **Ganssen, G.M.** (1998) Reconstruction of the Miocene western Amazonian aquatic system using molluscan isotopic signatures. *Palaeogeogr., Palaeoclim., Palaeoecol.*, **141**, 85-93.

Warren, J. (1999) *Evaporites: Their Evolution and Economics*. Blackwell Science, Oxford, 438 pp.

5. PALEOHYDROLOGY OF A LATE APTIAN LACUSTRINE SYSTEM FROM NORTHEASTERN BRAZIL WITH BASIS ON THE INTEGRATION OF FACIES AND ISOTOPIC GEOCHEMISTRY*

5.1. ABSTRACT

The Codó Formation records the initial evolutionary stages of an intracontinental rift system formed along the Brazilian equatorial margin in the Late Aptian. Deposits of this unit exposed in the eastern margin of the Grajaú Basin include evaporites, bituminous black shales and limestones. These lithologies were formed in a low energy, well stratified, predominantly anoxic and hypersaline lake system developed in a dominantly arid/semi-arid climate. This lacustrine succession is internally organized into three categories of shallowing-upward cycles, with the first- and second-order cycles being related to seismic activity associated with fault reactivations, and the third-order cycles recording seasonal fluctuations. Studies emphasizing petrography and analysis of the minor and trace elements Fe, Mg, Sr, Mn, and Na led to the evaluation that the Codó Formation was appropriate for isotopic investigations having paleoenvironmental and paleohydrologic purposes. The results of this study revealed a wide distribution of dominantly low $\delta^{13}C$ and $\delta^{18}O$ values, ranging from –5.69 ‰ to –13.02 $‰_{(PDB)}$ and from –2.71‰ to –10.80$‰_{(PDB)}$, respectively. This paper demonstrates that the

* Authors: J.D.S. Paz & D.F. Rossetti. Submitted to *Palaeogeography, Palaeoclimatology, Palaeoecology*

isotope ratios vary according to seismically-induced shallowing-upward cycles, in general becoming lighter in their bases, where central lake deposits dominate, and progressively heavier upward, where marginal lake deposits are more widespread. In addition, to confirm a depositional signature for the analysed samples, this behavior led to introduce a seismic-induced isotope model. Hence, lighter isotope ratios appear to be related with flooding events promoted by subsidence, which resulted in the development of a perennial lake system, while heavier isotope values are related to ephemeral lake phases favored through uplift and/or increased stability. Furthermore, the results show that a closed lake system dominated, as indicated by the overall good positive covariance (i.e., +0.42 to +0.43) between the carbon and oxygen isotopes, though open phases are also recorded by negative covariance values of –0.36. During closed phases, the $\delta^{18}O$ displayed the highest interval of variation (i.e., –3.63‰ to –4.89‰) due to the increased residence time, while this variation was low (i.e., –0.09‰ to -1.87 ‰) during open lake phases, when there was a balance in the water isotope composition caused by the continuous basin inflow.

5.2. INTRODUCTION

$\delta^{13}C$ and $\delta^{18}O$ records have been successfully applied for reconstructing the evolution and circulation patterns of oceanic basins throughout the geological time (e.g., Abell and Williams, 1986; Charisi & Schmitz, 1995; Hendry & Kalin, 1997). These studies are mostly based on the principle that the organic matter in marine sediments is characterized by extremely uniform isotopic compositions, which vary according to climate, as well as oceanic hydrology. The interpretation of these geochemical indicators in lacustrine settings is more complex, mostly because lake environments are more diversified, as evidenced by a wider distribution of carbon isotope ratios ranging from –25.9 to –10.5‰ (Bird *et al.*, 1991). Since the pioneer work of Stuiver (1970), several documentations on modern and Quaternary lake systems have provided the basis for an increased discussion on the many parameters that might influence the isotopic composition of the total inorganic carbon dissolved in lake waters (e.g., Fritz *et al.*, 1975; Katz *et al.*, 1977; Anderson & Arthur, 1983; MacKenzie, 1985; Hillaire-Marcel & Casanova, 1987; Bellanca *et al.*, 1989; Gasse *et al.*, 1989; Talbot & Kelts, 1990; Rosenmeier *et al.*, 2002; Herczeg *et al.*, 2003; Russell *et al.*, 2003). Despite these efforts, differentiation among the mechanisms that lead to variations in isotope composition of lake waters is not straightforward, as local causes might be mistaken by externally forced environmental changes (Talbot, 1990). In addition, in contrast to marine and modern lacustrine systems, the record of chemical changes in ancient lake deposits is yet very limited (Bird *et al.*, 1991; Lister *et al.*, 1991; Camoin *et al.*, 1997; In Sung & Kim, 2003), which have precluded a wider use of these geochemical tracers for paleoenvironmental purposes. Thereby, geochemical analysis of carbonate lacustrine deposits from a larger volume of analogs, where local causes can be distinguished from those of regional significance, are still needed in order to provide a full understanding of the mechanisms controlling lacustrine carbonate sedimentation.

In spite of the complex response, the available information concerning to carbon and oxygen isotope variations has arrived to some important generalizations. The most significant one for paleoenvironmental interpretation is the covariance of these geochemical tracers as an indicator of hydrologically closed lake systems, as opposed to the non-covariance in inlet lakes (e.g., Eicher & Siegnethaler, 1976; Gasse *et al.*, 1987, 1989; Talbot, 1990; Talbot & Kelts, 1990). Additionally, these isotopes have been applied for climate reconstructions of lake systems (e.g., Talbot & Keltz, 1990; Lister *et al*., 1991; Valero-Garcés *et al*., 1995). These applications are, however, highly dependent on the full understanding of facies distribution and of the possible modifications occurred during burial.

The goal of this paper is to contribute for the documentation of $\delta^{13}C$ and $\delta^{18}O$ values in ancient lacustrine systems, and discuss the causes of these variations analysing their relationship with shallowing-upward cycles within a Late Aptian succession formed during the early stages of a passive marginal rift. This unit, represented by the Codó Formation, is well exposed along several quarries in the eastern margin of the Grajaú Basin, where detailed studies focusing facies and facies architecture, stratigraphy, petrography, as well as Sr and S isotopes, have provided the basis to support deposition in a dominantly lacustrine setting (e.g., Rossetti *et al*., 2000; Paz and Rossetti, 2001). An integrated approach combining facies and isotope geochemistry provided the basis to analyze the distribution of carbon and oxygen isotopes in this ancient lake system, as well as to investigate the main parameters controlling its hydrology.

5.3. GEOLOGICAL SETTING

The Codó Formation records the first deposits accumulated within a broad and shallow depression formed by mild tectonic streching before the main rifting stage that culminated with the origin of the Equatorial South Atlantic Ocean during the Albian. These deposits are well represented in the Grajaú Basin (Fig. 5-1A), a semi-graben formed by the combination of pure shear stress and strike-slip deformation (Azevedo, 1991; Góes & Rossetti, 2001). This rift, which is connected with the São Luís Basin to the north, became an aborted intracontinental structure as the continental break up migrated northward.

The sedimentary fill of the São Luís-Grajaú Basin (Fig. 5-1B) reaches up to 4,000 m thick in the depocenters, and consists chiefly of Cretaceous deposits organized into three depositional sequences, i.e., S1, S2 and S3, formed during the Late Aptian/Early Albian, Early-Middle Albian and Middle Albian/Late Cretaceous, respectively (Rossetti 2001). The lowermost sequence S1 contains the Codó Formation, objective of this paper, and represents a succession up to 450 m thick of sandstones, evaporites, shales and limestones. This sequence displays a tripartite subdivision into systems tracts (Rossetti 2001), with the lowstand deposits grading progressively southward from shallow marine to continental (i.e., fluvial, deltaic, and lacustrine) in nature. The lowstand deposits are overlain by strata formed in the transgressive systems tract, and consist of a wedge of richly fossiliferous (mostly bryozoans, equinoderms, foraminifera and dinoflagellates) shales that pinches out to the basin margins. The highstand systems tract consists of shallow marine to continental deposits typically displaying stratal patterns varying upward from aggradational to progradational.

The maximum thickness of the Codó Formation in the Grajaú Basin is 150 m (Rezende & Pamplona, 1970). Its paleontological content mostly includes pollens, continental ostracods, insects, and fishes, which are all in agreement with a dominantly lacustrine interpretation for the depositional system. Additionally, pollen has been recovered from these deposits and allowed the establishment of a precise late Aptian age with basis on the presence of *Sergipea variverrucata* (Batista, 1992; Lima, 1982; Rossetti *et al*., 2001). The Codó Formation either grades downward into fluvial and deltaic deposits of the Grajaú Formation (e.g., Mesner & Wooldridge, 1964), or sharply overlies an unconformity over older Paleozoic and Triassic basement rocks. Its upper contact is an unconformity with Albian shallow marine, green to brownish-red mudstones interbedded with fine- to very fine-grained, cross-stratified sandstones of the Itapecuru Group (e.g., Rossetti & Truckenbrodt, 1997; Rossetti *et al*., 2001).

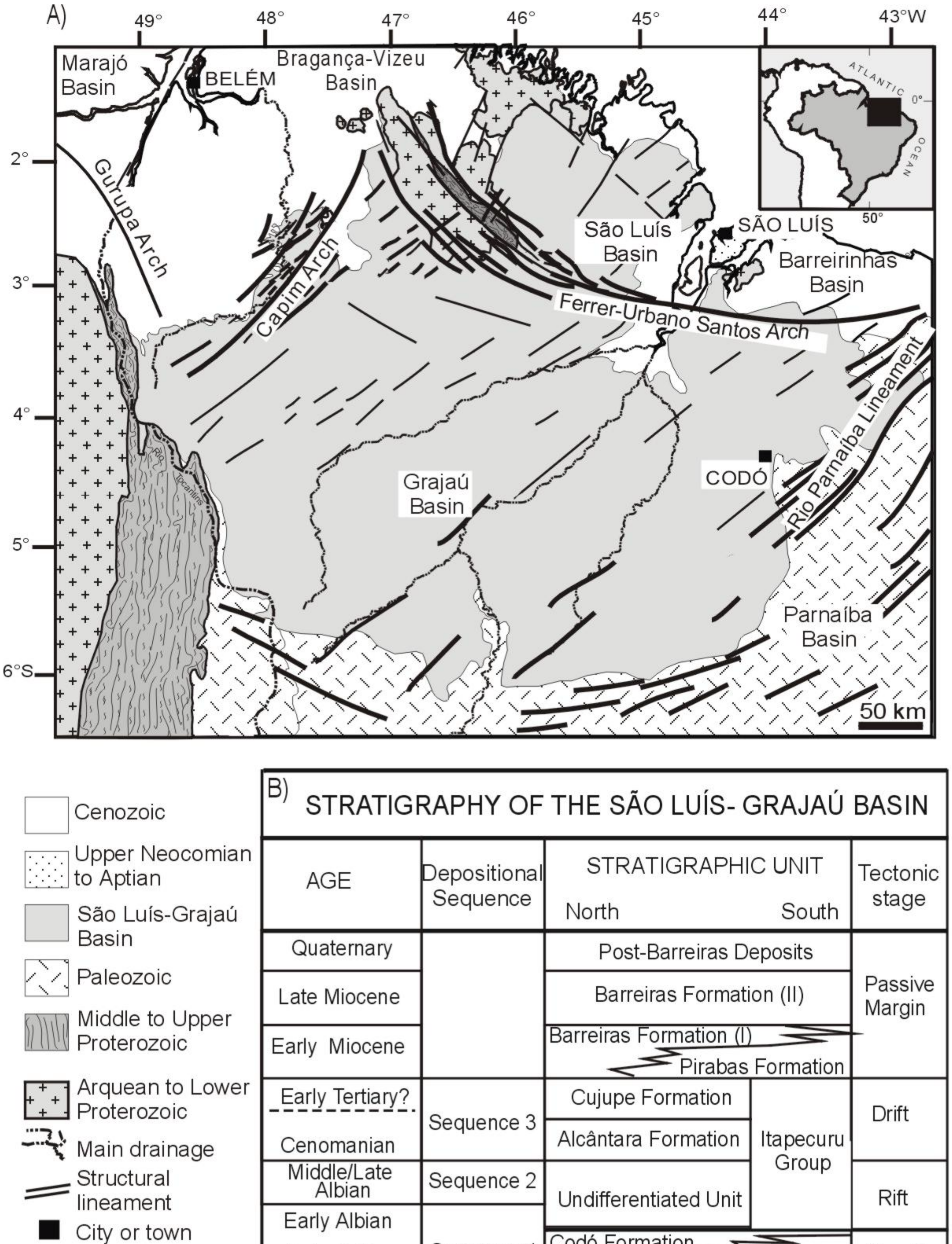

B) STRATIGRAPHY OF THE SÃO LUÍS- GRAJAÚ BASIN

AGE	Depositional Sequence	STRATIGRAPHIC UNIT North	STRATIGRAPHIC UNIT South	Tectonic stage
Quaternary		Post-Barreiras Deposits		Passive Margin
Late Miocene		Barreiras Formation (II)		
Early Miocene		Barreiras Formation (I) / Pirabas Formation		
Early Tertiary?	Sequence 3	Cujupe Formation	Itapecuru Group	Drift
Cenomanian		Alcântara Formation		
Middle/Late Albian	Sequence 2	Undifferentiated Unit		Rift
Early Albian / Late Aptian	Sequence 1	Codó Formation / Grajaú Formation		Pre-rift

Fig . 5-1: A) Location of the study area in the Codó region, eastern margin of the Grajaú Basin. B) Stratigraphy and main tectonic stages of the São Luís-Grajaú Basin.

5.4. FACIES ARCHITECTURE AND DEPOSITIONAL SYSTEM

5.4.1. Description

A detailed facies analysis of the Codó Formation exposed in the eastern margin of the Grajaú Basin was previously reported elsewhere (e.g., Paz and Rossetti, 2001). There, the Codó Formation consists of a lacustrine succession up to 25 m thick, attributed to three main sub-environments (Fig. 5-2): 1. central lake deposits, consisting of evaporites and bituminous black shales, locally with pyrite and native sulphur; 2. intermediate lake deposits, represented by laminated argillites and limestones; and 3. marginal lake deposits, including massive blocky pelites, fenestral calcarenites, ostracodal and pisoidal limestones, rhythmites of limestones and microbial mats, as well tufas. Paleosol, karstic feature, meteoric cement and vadose pisoid, typical of subaerial and/or meteoric exposures, are frequent features of the marginal lake deposits.

Three categories of cycles were recognized in the Codó Formation (Fig. 5-3). A detailed description of these cycles is presented in a separate paper (Paz and Rossetti, submitted), but a summary is included here as they are critical to help understanding the meaning of the isotope signals. Third-order cycles display regular thickness ranging from 5 to 10 cm, and consist of facies that vary according to the position in the lake setting. Hence, the central lake deposits show interbeddings either of bituminous black shales and evaporites, or bituminous black shales with streaks of calcimudstone and bituminous back shales with native sulphur. The intermediate lake deposits display bituminous black shale interbedded with peloidal limestone or green to gray laminated argillites interbedded either with calcimudstone or peloidal wackestone-packstone. The marginal lake deposits show either green to gray laminated argillites and ostracodal wackestone to grainstone, as well as alternations of ostracodal and/or lime mudstones, microbial mats and vadose pisoidal packstones.

The second-order cycles consist of either complete or incomplete successions with upward transitions from central to marginal lake deposits, with the latter displaying high internal facies variability when comparing one cycle to another. These cycles are characterized by limited lateral extension, as well as frequent and random thickness changes, which vary from few cm up to 5 m.

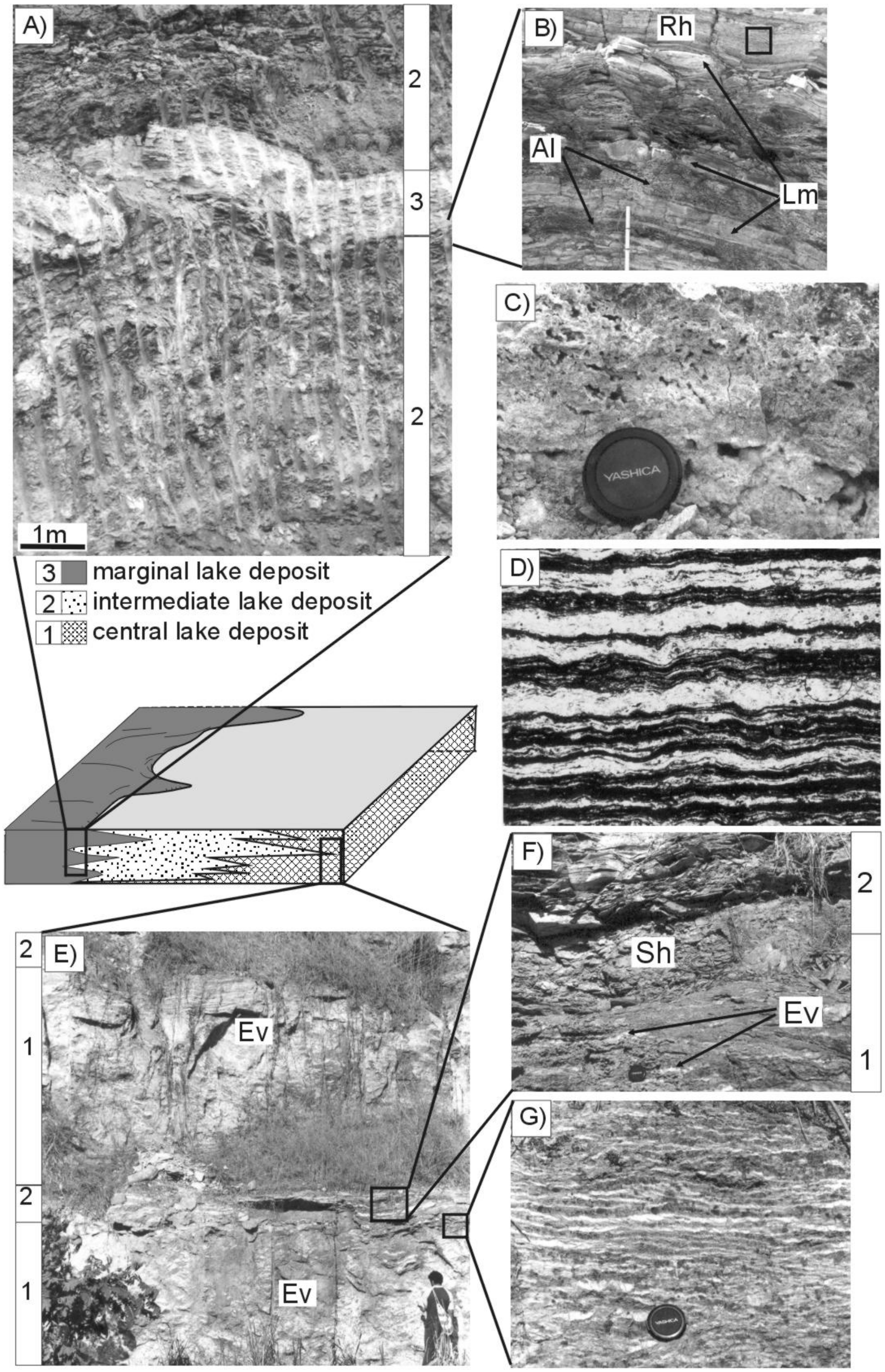

Fig . 5-2: Diagram illustrating the proposed lacustrine depositional model for the Codó Formation, characterized by central to marginal lake deposits. A) General view of marginal lake deposits between intermediate lake deposits. B) A detail showing the upward gradation from interbedded limestones (Lm) and laminated argillites (Al; intermediate lake) to rhythmites (Rh; marginal lake). C) Fenestral calcarenite from marginal lake deposits. D) Rhythmite of limestones (lighter color) and microbial mats (darker color) from marginal lake deposits. E) General view of central lake deposits (Ev=evaporite). F) Bituminous black shales (Sh) interbedded with evaporites (Ev). G) Layered gypsum.

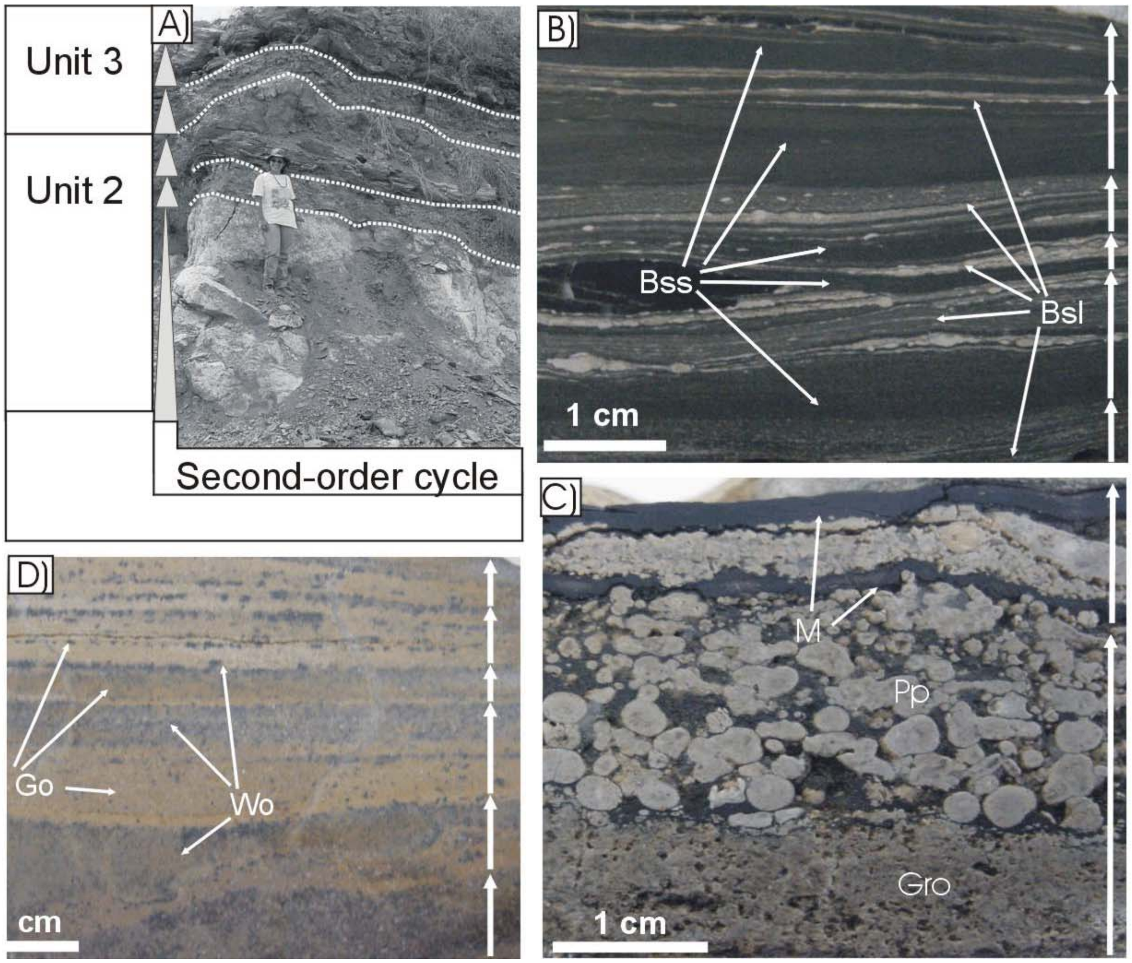

Fig . 5-3: Shallowing-upward cycles of the Codó Formation. A) Examples of first- and second-order cycles. B-D) Third-order cycles formed by alternations of bituminous black shale with streaks of lime-mudstone (Bsl) and bituminous black shales with native sulphur (Bss) (B), ostracodal grainstone (Gro) and vadose pisoidal packstone (Pp) with microbial mats (M) (C), ostracodal grainstone (Go) and wackestone (Wo) (D).

The first-order cycles define four episodes of shallowing (Fig. 5-4), organized from bottom to top as units 1 to 4. Unit 1 is only partly exposed at the base of the sections, consisting of bituminous black shales interbedded with calcimudstones, and are attributed to central and intermediate lake settings. Unit 2 reaches up to 8 m thick and contains, at the base, black bituminous shales interbedded with evaporites, which grade upward into limestones, laminated argillites and massive block pelites displaying a variety of features related to intermediate and marginal lake settings. Evaporites are, in general, absent or occur only as milimetric lenses or isolated crystals of gypsum. Unit 3 reaches up to 4 m thick and is constituted by intermediate and marginal lake deposits similarly to the underlying unit, but

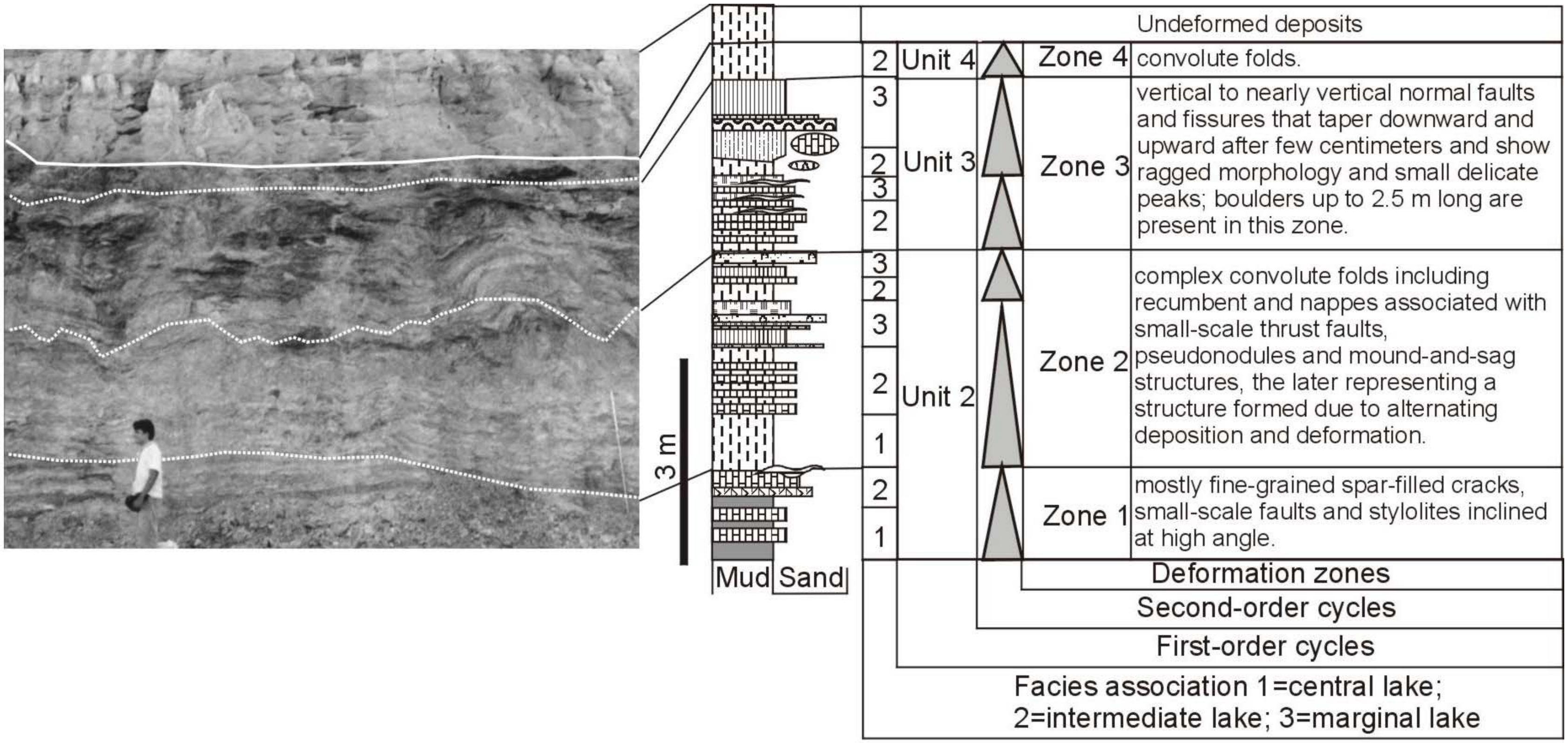

Fig . 5-4: First- and second-order cycles of the Codó Formation with relation to soft-sediment deformation zones attributed to syn-sedimentary seismic activity. (See Fig . 5-7 for legend).

with an increased frequency relative to the latter. A remarkable and exclusive feature of this unit 3 is the presence of oolites and calcareous (i.e., ostracodal packstone) concretions in its upper portion, which constitute important stratigraphic markers. The uppermost unit 4 is up to 5 m thick, being represented by laminated argillites containing only thin (<1 mm thick) laminae of gypsum or calcimudstone.

The first-order cycles closely match with stratigraphic horizons displaying syn-sedimentary soft sediment deformation that occur between undeformed deposits (Fig. 5-4), an observation that was crucial to reveal their genesis. Hence, units 1 and 2 correspond respectively to undeformed strata, and the deformation zones 1 and 2 described in Rossetti and Góes (2000). Deformation zone 1 consists of spar-filled cracks interconnected with small-scale faults, fissures and stylolites inclined at a high angle to bedding. Deformation zone 2 consists of strata with complex convolute folds associated with thrust faults, pseudonodules, and mound-and-sag structures, the latter correspond to synclines and anticlines mantled by sigmoidal laminations inclined toward the sag centres. Unit 3 corresponds to a deformed interval consisting of normal faults and fissures that are vertical to near vertical, present ragged morphologies with small, delicate edges, and taper both downward and upward after a few centimetres, being associated with intraformational boulders up to 2.5 m long. The uppermost unit 4 consists of shales with irregular convolute folds.

5.4.2. Interpretation

The facies present in the Codó Formation exposed in the eastern margin of the Grajaú Basin supports a low energy, well stratified, anoxic and hypersaline lake system developed under a dominantly arid/semi-arid climate (Paz and Rossetti, 2001).

The third-order cycles record minor changes in depositional conditions, attesting to alternations between mud settling and chemical precipitation of evaporites or limestones. This characteristic, added to the regular thickness variation, is consistent with seasonal fluctuations, with mud deposition and chemical precipitation taking place during less and more arid phases, respectively.

The higher-order cycles seem to have a different origin. The second-order cycles record successive episodes of upward gradation from deeper to relatively shallower lake environments, which resulted in the superposition of marginal lake deposits upon intermediate and/or central lake deposits. The high facies variability, when comparing one cycle to another, the limited lateral extension and the frequent and random thickness variations are attributes that match better with tectonically driven (e.g., Martel & Gibling, 1991; Benvenuti, 2003), rather than more symmetrical climatic cycles (e.g., Olsen, 1986; Goldhammer *et al.*, 1990; Smoot & Olsen, 1994; Steenbrinck *et al*., 2000).

The first-order cycles also appear to have resulted from syn-sedimentary tectonics (Fig. 5-4), as suggested by their good correlation with the deformation zones attributed to contemporaneous seismic activity related to fault reactivation (Rossetti and Góes, 2000). Based on this fact, it has been proposed that the Codó lake system was affected by alternating periods of distension and stability and even compression (Paz and Rossetti, chapter 2). The prevalence of central lake deposits at the base of the first-order cycles would have formed during higher subsidence, promoted by extension. On the other hand, the more widespread distribution of marginal lake deposits in the top of these cycles would record periods of higher stability or uplift. In addition to affect the development of the shallowing-upward cycles, these processes appear to have had a strong control on the isotope evolution of this lake system, as discussed in this paper.

5.5. GEOCHEMICAL TREATMENT

$\delta^{13}C$ and $\delta^{18}O$ data were analyzed from fresh samples in recently exposed quarries, to guarantee they were free from the influence of modern weathering. In this study, the analyses were performed using whole-rock limestone samples due to the fact that only ostracods are present in the studied deposits, and their distribution is not uniform to guarantee a good record of the individual cycles throughout the succession. Stable isotopic analysis has been successfully performed in whole-rock carbonates with the advantage of minimizing possible deviations related to vital effects, and even diagenesis (e.g., Urey, 1947; Camoin *et al*., 1997). Twenty milligrams of powered sample reacted in vacuum with 100% of orthophosphoric acid at 25^{o}C during 12 hours. The released CO_2 and H_2O were captured with liquid N_2. The CO_2 was separated from the water with a solution of alcohol and liquid N_2 in an off-line gas extraction line, and thereafter taken to the VG Isotech SIRA II mass spectrometer in the Stable Isotope Laboratory at the Universidade Federal de Pernambuco (LABISE/UFPE). The results are reported in δ notation, which is defined as the per mil deviation from a standard. The Peedee Belemnite Standard (‰ PDB) were used to the notation of both isotopes. Replicate analysis gave a standard deviation (2σ) lower than 0.02 %o for $\delta^{13}C$ and 0.03 %o for $\delta^{18}O$.

The isotopic analyses were run using samples selected after their study under the microscope to assure a primary signature. In addition, a double check on the diagenetic influence was made through the analysis of Fe, Sr, Mg, Mn and Ca. The procedure consisted in drying 1.5 g of sample at 1000°C for 2 hours. Samples were then fused using lithium tetraborate and lithium fluorite, and analysed in the X-Ray Fluorescence Spectrometer of the Stable Isotope Laboratory at the Universidade Federal de Pernambuco (LABISE/UFPE).

5.6. EVALUATION OF DIAGENETIC IMPRINT

The petrographic analysis of 83 limestone samples from the Codó Formation allowed to evaluate its diagenetic signature, observing the amount of lime mud, recrystallization, replacement, cementation, and fracturing. Several authigenic processes were observed, the most important ones including recrystallization of calcite, cementation and filling of fractures and secondary porosity by mosaics of calcite, replacement of micrite and ostracod shells by chert and chalcedony, and pyrite formation within ostracod shells and dispersed in calcimudstones. Despite these modifications, it was possible to select 53 samples consisting of microfacies either not affected or only mildly affected by diagenesis, which enhanced their potential to preserve the carbon and oxygen composition as a reflex of the depositional record. The samples used in this study included mostly calcimudstone (36%) and ostracodal wackestone to grainstone (45%; Fig. 5-5), and subordinately fenestral calcarenite (8%), pisoidal packstone (6%), and peloidal packstone to grainstone (6%).

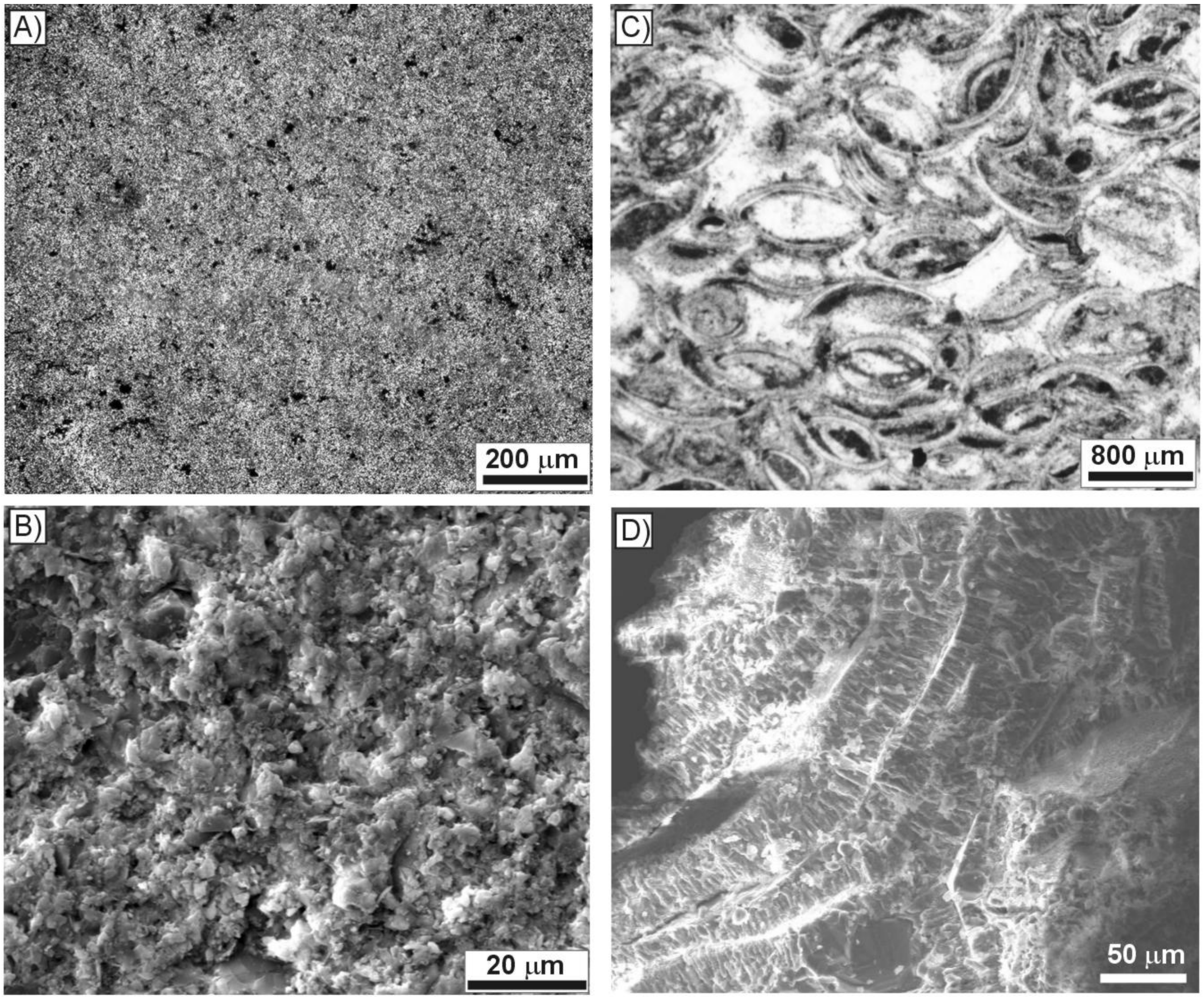

Fig . 5-5: Photomicrographies of biogenetically not affected facies utilized for the isotopic analysis. A,B) Calcimudstone (A=crossed nichols; B=scanning electron microscopy). C) Ostracodal grainstone (crossed nichols). D) Electron photomicrography illustrating ostracode shells of ostracodal grainstone, formed by densely packed, columnar calcite crystals attributed to primary origin.

After the petrographic studies, samples were additionally investigated using geochemical analysis of Fe, Sr, Mn, and Mg to help detecting diagenetic modification at a higher degree of reliability. These elements are the principal trace consituents in the calcite structure of both marine and non-marine limestones. Considering that their values remained constant through time, which seems to have been the case at least for most of the Phanerozoic (Holland, 1978), a comparison among values commonly expected from stratal waters provides information to detect potentially significant diagenetic influences. The results (Fig. 5-6) show that, in general, all the samples that appeared to be petrographically suitable for isotope analysis contain minor and trace elements as expected for continental deposits not affected by diagenesis. Exceptions are samples with high Fe content, which is due either to high volume of organic matter or pyritization. However, these samples were also included in the isotope analysis presented here, considering that: 1. the other geochemical tracers are within the range expected for diagenetically non-affected rocks; 2. the isotope values do not show any divergence with respect to the other samples; and 3. they derive from facies with pedogenetic influence associated with marginal lake deposits, a situation that favours an increased Fe and Mn circulation.

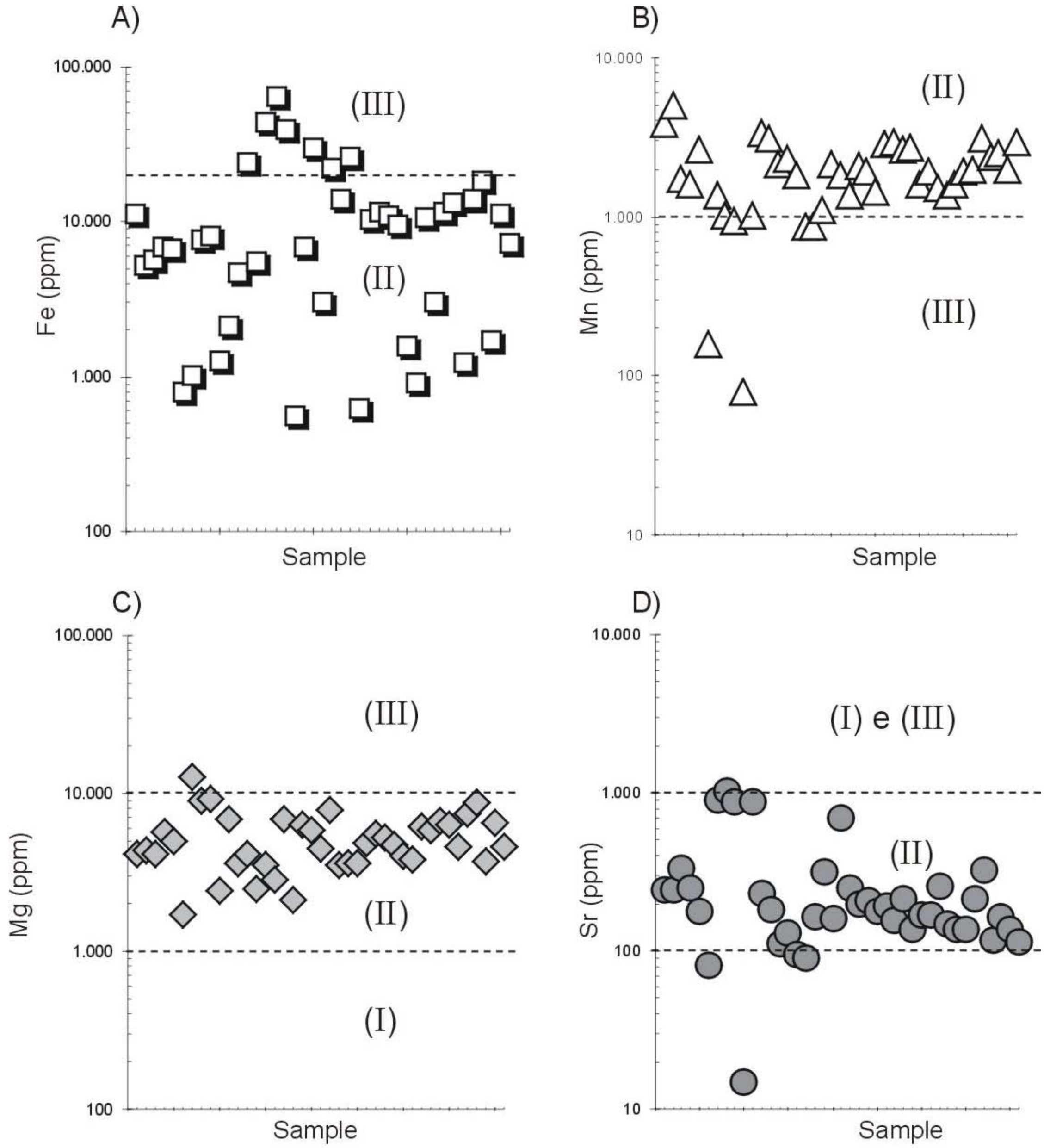

Fig . 5-6: Distribution of the trace elements Fe (A), Mn (B), Mg (C) and Sr (D) from samples used in the isotopic analysis presented herein (I=meteoric calcite; II=marine calcite; III=diagenetic calcite). (After Tucker and Wright, 1990).

5.7. STABLE ISOTOPES

The $\delta^{13}C$ isotope curves show an overall similar pattern in all the studied profiles, with ratios ranging from –5.69 ‰ to –13.02 ‰ (Table 5-I). In general, two short intervals with higher values at the base and top of the profiles are separated by a large interval with depleted values (Fig. 5-7). The behavior of the isotope curves reflects the position of the first-order. For instance, unit 2 displays increasing values at the bottom, followed by a short negative excursion to ultimately oscillate toward heavier and, in more rarely, lighter values at the top. The values in unit 3 are more regularly distributed, varying upward from lighter to heavier.

Table 5-I: $\delta^{13}C_{(‰\ PDB)}$ and $\delta^{18}O_{(‰\ PDB)}$ values observed in the study area. A, B and C mean the vertical profiles showed in the Fig. 5-7.

Prof	Sample		$\delta^{18}O$	$\delta^{13}C$
A	01	pisoidal packstone	-5,49	-10,10
	02	ostracodal packstone	-7.24	-11.80
	03	Calcimudstone	-8.91	-10.03
	04	Calcimudstone	-9.17	-9.13
	05	Calcimudstone	-9.15	-8.96
	06	fenestral calcarenite	-8.36	-6.65
	07	ostracodal packstone	-8.45	-9.92
	08	ostracodal packstone	-8.36	-10.92
	09	Calcimudstone	-7.22	-9.26
	10	Calcimudstone	-8.92	-5.15
	11	Calcimudstone	-8.16	-6.09
	12	Calcimudstone	-8.62	-6.31
	13	ostracodal packstone	-8.28	-8.50
B	14	ostracodal packstone	-6.05	-11.99
	15	ostracodal packstone	-7.02	-12.67
	16	ostracodal packstone	-3.39	-7.98
	17	ostracodal packstone	-4.75	-9.6
	18	pisoidal packstone	-4.28	-10.8
	19	ostracodal packstone	-6.62	-10.48
	20	ostracodal packstone	-6.51	-10.71
	21	ostracodal packstone	-5.27	-12.39
	22	Calcimudstone	-10.8	-11.47
	23	Calcimudstone	-10.36	-11.27
	24	Calcimudstone	-10.44	-11.14
	25	Calcimudstone	-7.58	-11.89
	26	ostracodal packstone	-7.6	-12.56
	27	ostracodal packstone	-4.77	-12.16
	28	ostracodal packstone	-3.01	-6.81
	29	ostracodal packstone	-2.71	-7.55
	30	Calcimudstone	-4.80	-9.04
C	31	ostracodal packstone	-6,87	-10,96
	32	ostracodal packstone	-5.32	-9.30
	33	ostracodal packstone	-7.69	-10.95
	34	pisoidal packstone	-7.62	-11.51
	35	ostracodal packstone	-8.38	-11.00
	36	ostracodal packstone	-7.83	-11.87
	37	Calcimudstone	-8.69	-11.72
	38	Calcimudstone	-9.41	-11.03
	39	peloidal packstone	-9.36	-10.89
	40	peloidal packstone	-9.15	-12.38
	41	fenestral calcarenite	-9.83	-10.70
	42	fenestral calcarenite	-8.00	-10.00
	43	ostracodal packstone	-8.64	-12.12
	44	fenestral calcarenite	-9.94	-11.80
	45	Calcimudstone	-8.83	-11.74
	46	ostracodal packstone	-8.18	-11.57
	47	Calcimudstone	-8.99	-12.12
	48	Calcimudstone	-9.24	-13.02
	49	Calcimudstone	-8.62	-11.23
	50	Calcimudstone	-9.29	-11.18
	51	peloidal packstone	-8.06	-6.10
	52	ostracodal packstone	-6.65	-10.14
	53	ostracodal packstone	-7.42	-5.69

The fluctuation in carbon isotope ratios is fairly comparable within individual second-order cycles, particularly in the intermediate and upper portions of the successions, where values, in general, increase, or less commonly, remain constant. Downward in the cycles, the carbon ratios oscillate slightly between lighter and heavier. A change in pattern occurs in the lower portions of the profiles (Fig. 5-7), where there is an upward trend to lower values.

Similarly to the carbon, the oxygen isotope ratios obtained for the Codó Formation are dominantly low, ranging from –2.71‰ to –10.80‰. The behavior of the curves along the profiles, as well as within the first- and second-order cycles, also shows patterns that are very similar to the ones described for the carbon, but with oscillations toward lighter values in the lower and intermediate portions of the cycles. Exception is an increased value in the second-order cycles located at the lower portions of profiles A and C, where the oxygen isotope values increase.

Comparisons of the carbon and oxygen curves reveal a positive covariance in profiles B and C, with values ranging from +0.42 to +0.43, while profile A shows a negative covariance of –0.36 (Fig. 5-8). This behavior is reflected in both the first- and second-order cycles. The only exception is the second-order cycle at the base of profile C, which displays an inverse covariance.

5.8. ISOTOPIC CHARACTERIZATION OF THE LACUSTRINE SYSTEM

The carbon and oxygen data presented here have valuable application for further support the lacustrine signature of the Codó Formation, as well as reconstruct its paleohydrology and evolution through time. This procedure was made possible only considering the primary signature of these data, as confirmed by the petrographic and minor and trace elements discussed earlier in this paper. In addition, the wide distribution of the carbon and oxygen values throughout the analysed profiles, their overall good covariance, and pulsating oscillations according to the first- and second-order shallowing-upward cycles, as described above, led to exclude a significant diagenetic influence.

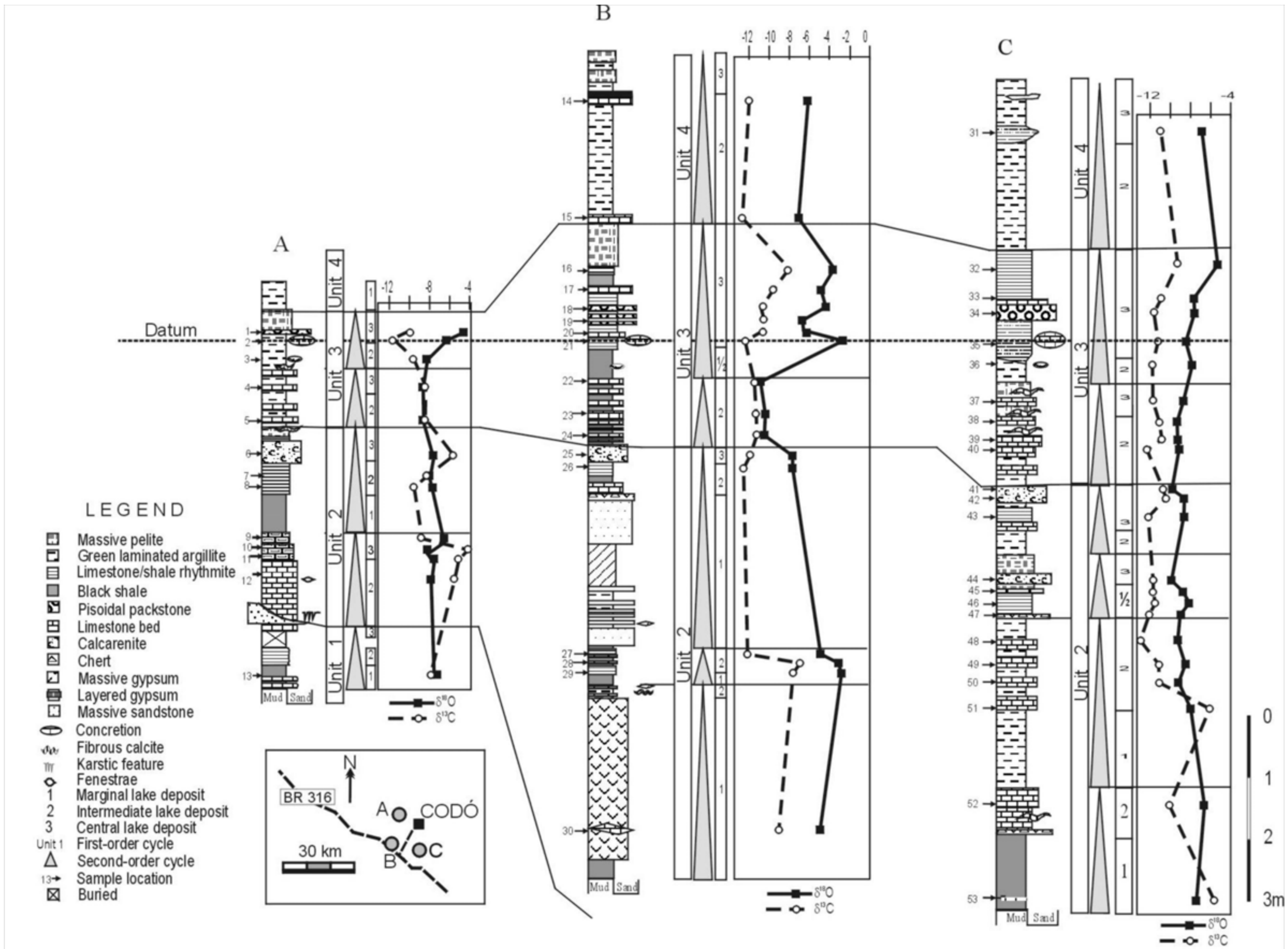

Fig . 5-7: Lithostratigraphic profiles representative of the Codó Formation exposed in the study area, with the stratigraphic distribution of facies associations, first- and second-order cycles, and $\delta^{18}O_{(‰ PDB)}$ and $\delta^{13}C_{(‰ PDB)}$ values.

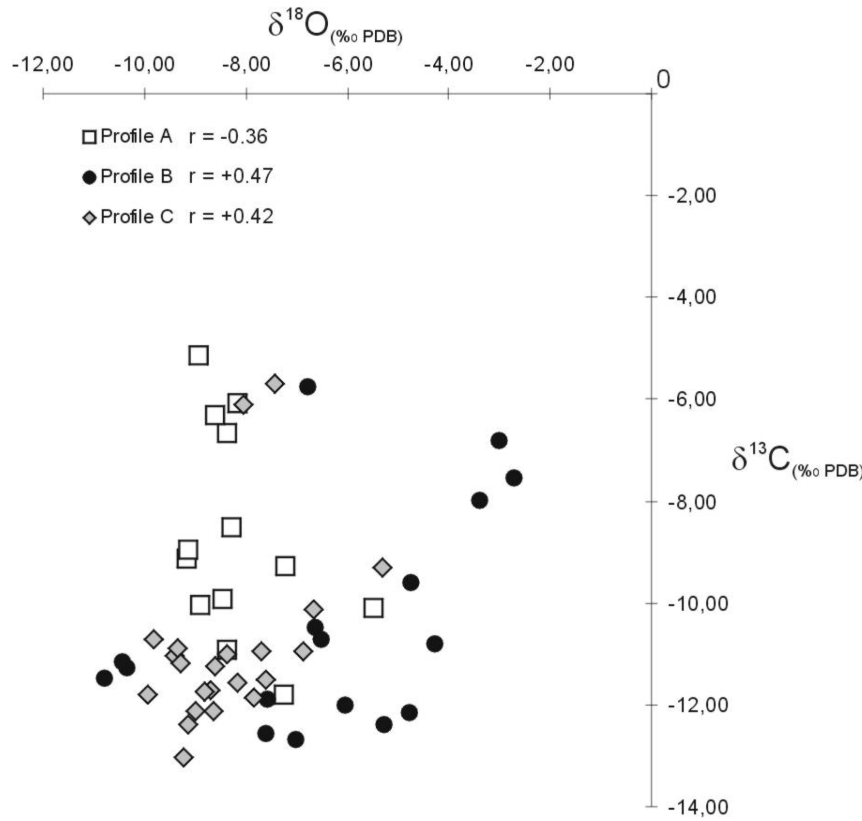

Fig . 5-8: Plot and correlation of carbon and oxygen isotope data from the Codó Formation in the eastern Grajaú Basin. The positive correlation in profiles B and C is attributed to episodes of dominantly closed lake system, while the negative correlation in profile A records lake opening.

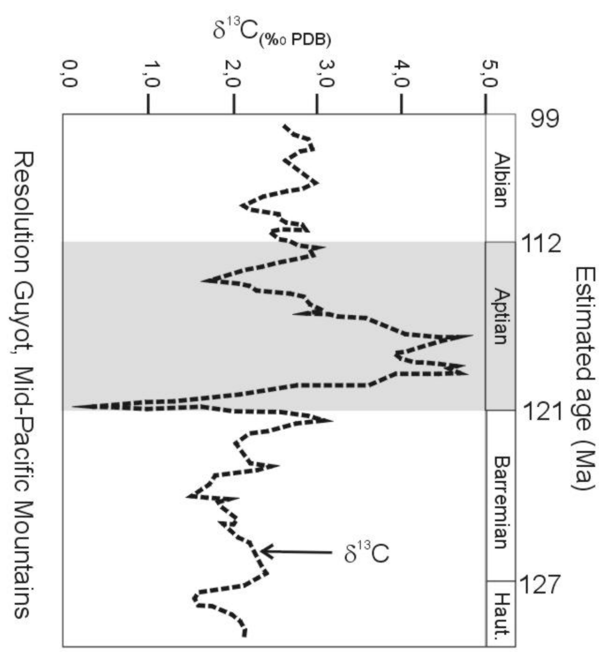

Fig . 5-9: $\delta^{13}C$ trend of marine-bearing Aptian carbonates (Modified from Jones and Jenkins, 2001).

The results of the isotope analysis are in agreement with a lacustrine interpretation for the Codó Formation exposed in the eastern margin of the Grajaú Basin, as proposed in previous publications (e.g., Campbell *et al*., 1949; Aranha *et al*., 1991; Rossetti *et al*., 2000; Paz & Rossetti, 2001). Several observations related to the carbon and oxygen isotope data support this interpretation. First, a non-marine setting is indicated by the exclusive occurrence of values lighter than –5.15 ‰ for the carbon, which is well below the range of about –2‰ and +5‰ expected for marine limestones (e.g., Deines, 1980; Hoefs, 1980). Second, the carbon values obtained in the study area are consistent with Late Aptian continental deposits, since marine limestones of this age display values ranging from +2%o to +4%o (Jones & Jenkins, 2001; Fig. 5-9). Third, the ratios –2.71‰ to -10.80 ‰ for the oxygen isotopes are also consistent with a continental setting (Talbot, 1990; Bird *et al*., 1991). A marine-influenced continental environment might show lighter values of up to –5‰ (e.g., Ingram *et al*., 1996; Hendry & Kalin, 1997; Fig. 5-10), but this hypothesis is very unlikely in this instance because 91% of the analysed samples are below this value. Fourth, the overall wide range of both $\delta^{13}C$ and $\delta^{18}O$ values, is typical of continental-derived waters, as considered in a number of works (e.g., Talbot & Kelts, 1990; Casanova & Hillaire-Marcel, 1993; Camoin *et al*., 1997; Fig. 5-10). Fifth, the good covariance between the oxygen and carbon isotope data (Fig. 5-8), although not exclusive to, is more consistent with a non-marine setting (Turner *et al*., 1983; Gasse *et al*., 1987; Talbot, 1990; Talbot & Kelts, 1990; Charisi & Schmitz, 1995).

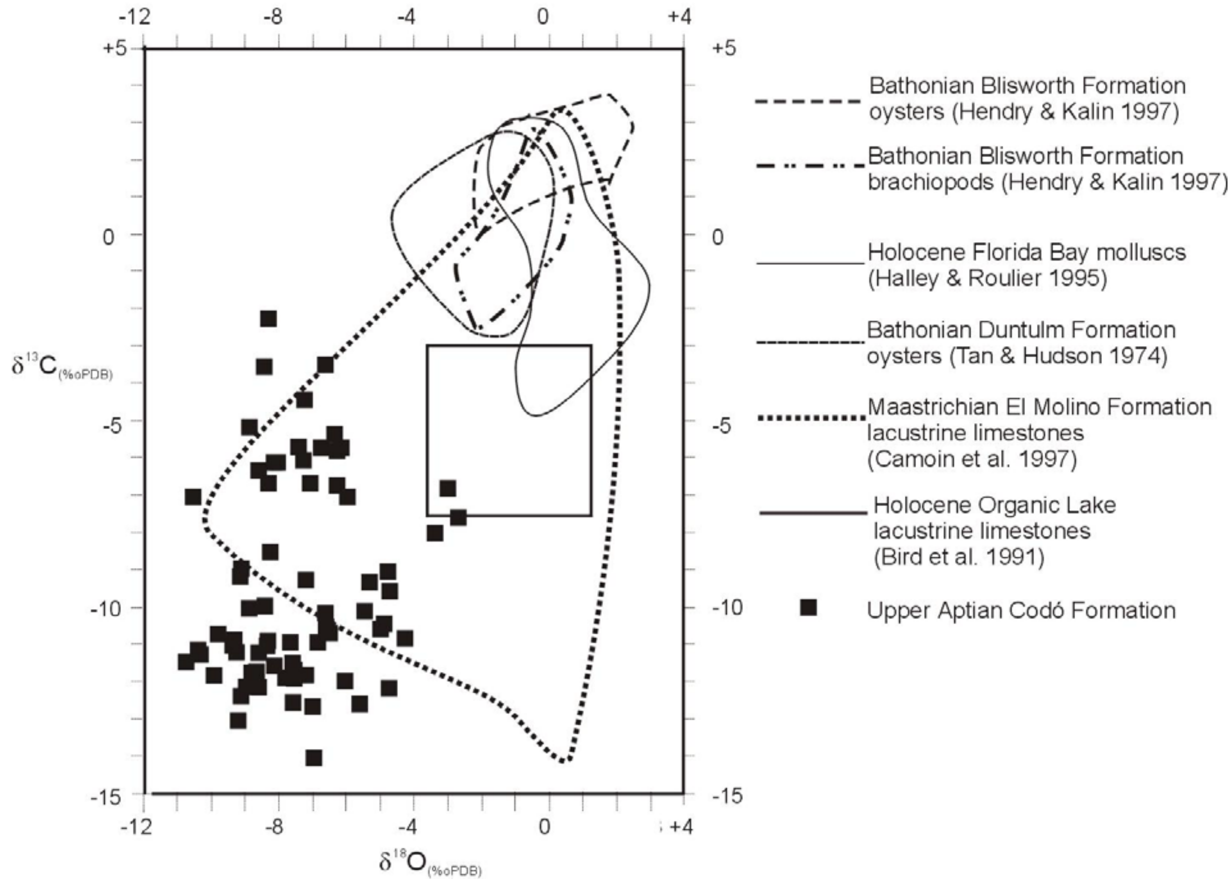

Fig . 5-10: Plots of carbon and oxygen stable isotope data from several marine and lacustrine deposits throughout the world (Modified from Hendry and Kalin, 1997), and their comparison with data obtained in the Codó Formation. This diagram shows that the isotopic composition of the Codó Formation is in conformity with isotope data from lacustrine limestones.

In addition to support a non-marine deposition, the carbon and oxygen isotope data revealed to be valuable for reconstructing lake paleohydrology. Both of these isotopes have been used directly or indirectly to interpret climate (Fig. 5-11). In fact, temperature and hydrological balance are the main controllers of isotopic composition in lake systems (Kelts & Talbot, 1990; Lister *et al.*, 1991). It is well known from studies of modern settings that temperature causes fractionation of the oxygen in a constant ratio of 0.26 ‰/^{o}C in the bicarbonate-water-carbonate system (cf. Craig, 1965; Friedman & O'Neill, 1977). However, the wide range of $\delta^{18}O$ values observed in the Codó Formation would require a temperature gradient equivalent to about 40^{o}C, not expected considering a low paleolatitudinal location (>10^{o}) of the study area during the Late Aptian (Scotese *et al.*, 1989). On the other hand, the balance between influx and evaporation causes drastic changes in lake isotopic composition

(Talbot, 1990; Lister *et al*., 1991). Evaporation leads to enriched ^{18}O, as lighter ^{16}O escape to the atmosphere. Conversely, high water inflow results in the return of ^{16}O from the atmosphere, causing depletion in $\delta^{18}O$ values. Thus, low $\delta^{18}O$ values have been related to higher lake levels, while high $\delta^{18}O$ are attributed to lower lake levels, parameters that have been indirectly related to climate (e.g., Talbot, 1990; Caimon *et al*., 1997; Lister *et al*., 1991).

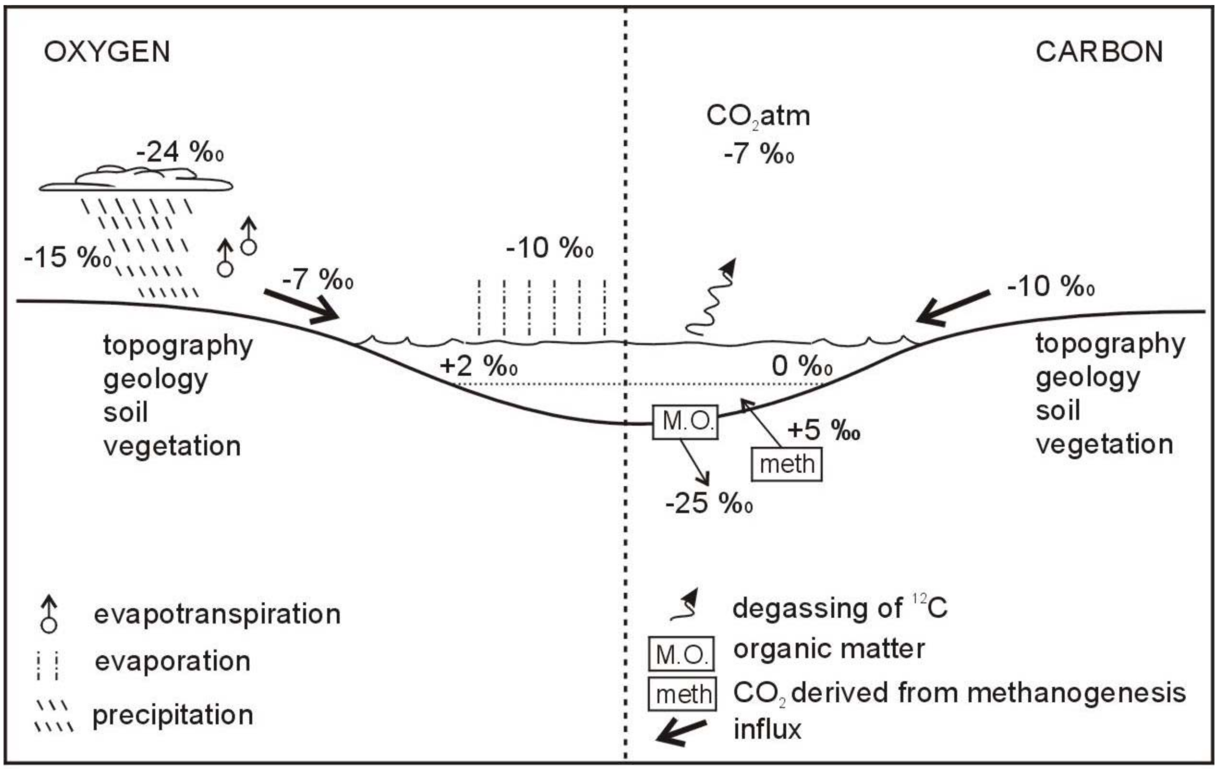

Fig . 5-11: Schematic diagram illustrating the main mechanisms that contribute to modify $\delta^{13}C_{(‰ PDB)}$ and $\delta^{18}O_{(‰ PDB)}$ of the carbonates in a lake system.

Carbon isotope ratios also have a direct relation to climate. Hence, higher $\delta^{13}C$ values have been associated with aridity, while lower $\delta^{13}C$ values indicate relatively more humid climates (e.g., Talbot & Keltz, 1990; Valero-Garcés *et al*., 1995). This interpretation is based on the fact that dry climates favour evaporation, increased influence of C4-path vegetation type, lower influx, and lake stratification, which ultimately lead to organic matter preservation with the consequent output of ^{12}C from the lake water.

A close relationship between the carbon and oxygen isotope ratios and the first- and second-order shallowing-upward cycles is recorded in the study area. These changes are analysed in the following in terms of facies development, which is not necessarily related to climate changes, as widely applied in the literature (e.g., Olsen, 1986; Smoot & Olsen, 1994; Goldhammer *et al*., 1990; Steenbrick *et al*., 2000; Hofmann *et al*., 2000; Aziz *et al*., 2000). In this instance, the variation in both isotopes from lighter to heavier values along individual second-order cycles follows upward gradations from central to marginal facies deposits, which are related to changes in subsidence rates, as previously discussed (Fig. 5-12). Such facies stacking requires alternating episodes of lake deepening and shallowing, which is associated with increased subsidence and the return to relative stability or even uplift, respectively. Extreme shallowing might have culminated with periods of desiccation, as indicated by deposits with paleosols. Heavier isotope values recorded during these situations could be attributed to a significant enhancement of the isotopic exchange with the atmosphere. This is because as the water became extremely shallow, evaporation increased significantly due to heating (Fig. 5-12). Differences in carbon values according to location in the lake system, with marginal areas displaying higher values, have been also noted by other authors (e.g., Camoin *et al*., 1997; Casanova & Hillaire-Marcel, 1993). The loss of ^{12}C to the atmosphere as a cause to enrich the ^{13}C in the dissolved inorganic carbonate appears to be an active process in the epilimnion of lakes with low water inflow (Stiller *et al*., 1985; Talbot, 1990; Talbot & Kelts, 1990).

The upward lighter trends of carbon and oxygen isotope values observed in the lower portions of the studied successions is related to lake stratification and bottom anoxia, as suggested by the prevalence of central lake deposits consisting of evaporites and bituminous black shales. Such situation leads to ^{12}C burial, increasing the amount of ^{13}C dissolved in the central lake waters (Herczeg, 1988; Talbot & Kelts, 1990). The subtle upward decrease in isotope values would record the transition to intermediate lake environments, where this effect was less significant. In addition, as opposed to the shallowing-upward cycles located upward in the studied succession, marginal lake deposits that could contribute to increase the isotope values through atmosphere exchange, as proposed above, are in general lacking in the upper portions of these cycles.

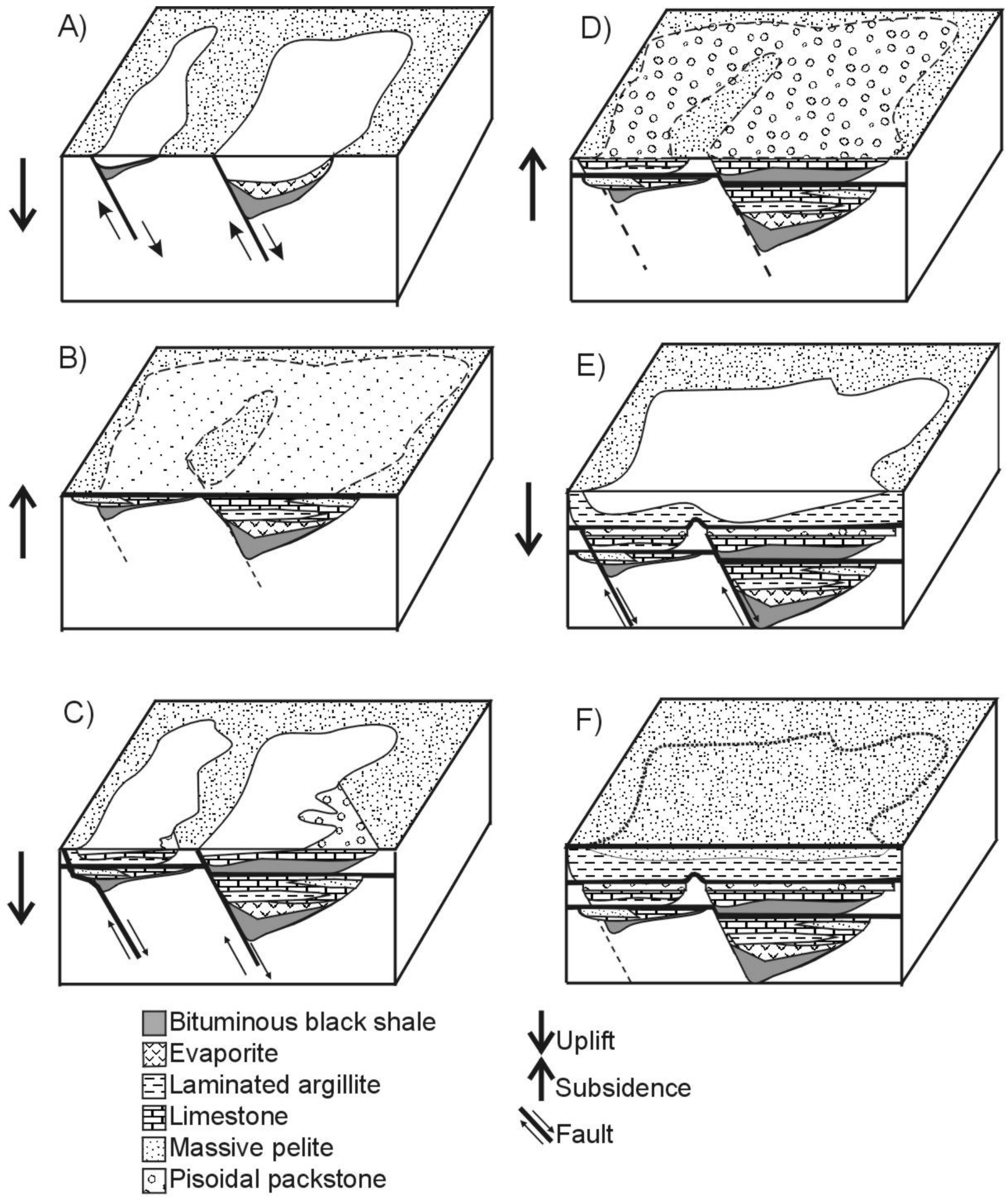

Fig . 5-12: Summary of the depositional model proposed for the origin of the Codó lake system in the eastern of the Grajaú Basin, illustrating the close relationship of facies development, and thus the distribution of oxygen and carbon isotopes, with alternation between syn-sedimentary fault displacement and uplift. A) Offset of few meters along faults displaced along the basin margins resulted in the creation of accommodation space along subsiding areas, where the lake system developed, giving rise to first-order cycle represented by unit 2. B) Uplift contributed to decrease the lake level with the consequent spread out of marginal deposits at the top of unit 2, culminating with lake dryness and formation of a discontinuity surface with paleosols. C) Fault reactivation resulted in a renewed phase of lake deepening, with deposition of central and intermediate facies deposits recorded by unit 3. D) Renewed uplift promoted the fall in lake level and widespread formation of marginal deposits represented by pisoidal packstone to grainstone and rhythmite, which culminated with lake exposure and soil development at the top of unit 3. E) Fault reactivation with renewed deposition of laminated argillites, recorded by unit 4. F) Increasing stability led to progressive decrease in water level resulting from the abandonment of the lacustrine deposition in the study area, with subaerial exposure and formation of an unconformity at the top of the Codó Formation.

The overall upward high-low-high trend of the isotope values coincides with the position of the first-order cycles. As presented earlier, these cycles record main episodes of lake desiccation superposed upon second-order cycles. The lightest values in the lower portions of the first-order cycles is related to periods of maximum flooding, when the lake was established and deeper water levels prevailed, as reflected by the better development of central lake deposits. As the lake evolved, increased evaporation led to a lower water level, progressively enhancing the isotope values and ultimately culminating with lake desiccation, when the isotope values reached the heaviest ratios. This trend, well documented in unit 3, is a little modified in the lower portions of unit 2, where the heaviest ratios were recorded as a result of lake stratification and anoxia, as this time coincides with the maximum development of evaporites and/or bituminous black shales in this lacustrine basin. The abundance of these lithologies in unit 2, where relatively deeper water facies prevail, lead to propose that, rather than evaporation, lake stratification and anoxia were crucial to form the evaporites (e.g., Warren, 1999). As the lake evolved through time, shallower water conditions became progressively better developed and evaporation increased, but with restrict or no precipitation of evaporative minerals.

The overall moderate positive covariance between the carbon and oxygen isotope curves shown in profiles B and C is attributed to the prevalence of a closed lake environment, a pattern that have been noticed in many other ancient and modern lake systems throughout the world (e.g., Eicher & Siegenthaler, 1976; Gat, 1981; McKenzie, 1985; Gasse *et al*., 1987; Janaway & Parnell, 1989; Talbot, 1990; Talbot & Kelts, 1990; Lister *et al*., 1991). It is interesting to note that unit 2 of profile C coincides with a period of high covariance. This is consistent with the presence of evaporites in these beds, typical of closed basins (Warren, 1999). In spite the evidences for lake closure, a comparison between the isotope curves shows alternating phases of higher and relatively lower covariance, attributed to episodes of lake opening. This can be particularly seen in profile A (Fig. 5-7), where the overall covariance between carbon and oxygen isotopes is negative.

It is interesting to observe that the $\delta^{18}O$ displayed the highest interval of variation during closed phases, which ranged from -3.63‰ to –4.89‰, against the interval of variation of –0.09‰ to -1.87 ‰ that characterizes open phases. This is because closed lakes have better chances to show oscillations in water levels as the residence time increases, which lead to enhance the $\delta^{18}O$. Conversely, the isotopic composition of open lakes is more stable due to the balance caused by the continuous basin inflow, as recorded in several lake systems, such as Lake Henderson (Stuiver, 1970), Lake Huleh (Stiller & Hutchinson, 1980) and Greifensee (McKenzie, 1985).

5.9. FINAL REMARKS

The carbon and oxygen isotopic composition of the Codó Formation in the eastern Grajaú Basin can be directly related to facies changes, as revealed by the good correspondence between the isotope values and the shallowing-upward cycles. Deciphering the causes of these changes through time, whether related to climate fluctuation or to any other variation in the basin, such as subsidence or sediment inflow, is not so straightforward. There has been an agreement among the authors in relating carbon and oxygen isotopes with lake hydrology, which is often used directly or indirectly to make inferences about climate (e.g., Smoot & Olsen, 1994; Steenbrick *et al*., 2000; Hofmann *et al*., 2000; Aziz *et al*., 2000). However, this study shows that significant changes in carbon and oxygen isotope composition of lake waters, resembling climatic cycles, can be also related to fluctuations in subsidence rates caused by syn-sedimentary seismic activity. In this case, combination of isotope and sedimentological data provided the key for distinguishing which of these factors left the most significant imprint in the sedimentary record.

We have shown in this paper the close relationship of both carbon and oxygen isotopes with the first- and second-order shallowing-upward cycles that characterize the studied unit. The dominant asymmetric nature of these cycles, inferred with basis on the high facies variability when comparing one cycle to another, the limited lateral extension, as well as the frequent and random thickness changes, led to propose that climate was not their primordial controlling factor. On the other hand, sedimentological data favour to attribute these cycles to syn-sedimentary seismic activity associated with the early tectonic evolution of the São Luís-Grajaú Basin during the Late Aptian. The Codó Formation was deposited just prior to the main rifting that culminated with the process of opening of the South Atlantic Equatorial Ocean. During this initial time, there was the development of a shallow, but extensive subsiding intracontinental basin (Azevedo, 1991; Góes & Rossetti, 2001). This characteristic matches well with the presence of shallow lakes in marginal areas of the basin, where faults with reduced offsets are expected to have prevailed. Subsidence gave rise to local water accumulation, forming closed and perennial lake systems, but as compression took place, and the area was uplifted, the development of ephemeral lakes appears to have been favoured. This situation is recorded in the studied profiles by a change from shallowing-upward cycles with dominance of central and intermediate lake deposits, to cycles with well-developed marginal lake deposits, as occurs in the lower and upper portions of the first-order cycles, respectively. Such facies arrangement records the upward transition from periods of maximum flooding to periods when the lake level fell to lower levels. The carbon and oxygen isotopic composition of such lake basins is expected to be characterized initially by light values, but as the residence time increases due to shallowing, heavier values are reached due to the high evaporation-inflow budget provided by the progressive decrease in water level.

Because arid climate prevailed along the Brazilian equatorial margin during the Late Aptian (Lima *et al*., 1980; Lima, 1982; Batista, 1992; Rodrigues, 1995; Rossetti *et al*., 2001), evaporite precipitation took place in central lake areas, induced by water stratification and bottom anoxia (Kirkland & Evans, 1981). The highest value of carbon isotope coinciding with the moment of maximum formation of evaporites and bituminous black shales is consistent with this interpretation.

Therefore, different styles and/or intensities of seismic pulses alternating with sediment deposition might cause changes in the lake level, promoting alternating periods of flooding and fall in the lake level, and resulting in well-developed asymmetric shallowing-upward cycles. Such scenario will ultimately affect the overall isotope composition of lake waters.

Acknowledgments. The Itapicuru Agroindustrial S/A is acknowledged for the permission to access the quarries with the exposures of the Codó Formation. This work was financed by the Brazilian Council for Research–CNPq (Project #460252/01). The authors are grateful to Dr. Alcides Sial e Dr. Valderez Ferreira for helping with the geochemical analyses.

REFERENCES

Abell, P.I., Williams, M.A.J., 1986. Sedimentary carbonates as isotopic marker horizons at Lake Turkana, Kenya. In: Frostick, L.E., Renaut, R.W. Reid, I., Tiercelin, J.-J. (Eds.), Sedimentation in the African Rifts. Spec. Publ., Geol. Soc. Am. 25, 153-158.

Anderson, F.W., Arthur, M.A., 1983. Stable isotopes of oxygen and carbon and their application to sedimentologic and paleoenvironmental problems. Short Course Notes, SEPM, 10, 151 p.

Aranha, L.G., Lima, H.P., Makino, R.K., Souza, J.M., 1991. Origem e evolução das bacias de Bragança-Viseu, São Luís e Ilha Nova. In: Milani, E.J., Raja Gabaglia, G.P. (Eds.), Origem e Evolução das Bacias Sedimentares. PETROBRAS, Rio de Janeiro, pp. 221-234.

Azevedo R.P., 1991. Tectonic evolution of Brazilian Equatorial Continental Margin Basins. Doctoral Thesis, University of London, London, 455 p.

Aziz, H.A., Hilgen, F., Krijgsman, W., Sanz, E., Calvo, J.P., 2000. Astronomical forcing of sedimentary cycles in the middle to late Miocene continental Catalayud Basin (NE Spain). Earth Planet. Sci. Lett. 177, 9-22.

Batista, A.M.N., 1992. Caracterização Paleoambiental dos sedimentos Codó-Grajaú, Bacia de São Luís (MA). M.Sc.Thesis, Universidade Federal do Pará, Belém, 102 p.

Bellanca, A., Calvo, J.P., Censi, P., Elizaga, E., Neri, R., 1989. Evolution of lacustrine diatomite carbonate cycles of Miocene age, southeastern Spain: petrology and isotope geochemistry. J. Sediment. Petrol. 59, 45-52.

Benvenuti, M., 2003. Facies analysis and tectonic significance of lacustrine fan-deltaic successions in the Pliocene-Pleistocene Mugello Basin, Central Italy. Sediment. Geol. 157, 197-203.

Bird, M.I., Chivas, A.R., Radnell, C.J., Burton, H.R., 1991. Sedimentological and stable isotope evolution of lakes in the Vestfold Hills, Antarctica. Palaeogeog., Palaeoclim., Palaeoecol. 84, 109-130.

Botz, R., Stoffers, P., Faber, E., Tietze, K., 1988. Isotope geochemistry of carbonate sediments from Lake Kivu (East Central Africa). Chem. Geol. 69, 299-308.

Camoin, G., Casanova, J., Rouchy, J.M., Blanc-Valleron, M.M, Deconinck, J.F. 1997. Environmental controls on perennial and ephemeral carbonate lakes: the Central Palaeo-

Andean Basin of Bolivia during Late Cretaceous to early Tertiary times. Sediment. Geol. 113, 1-26.

Campbell, D.F., Almeida, L.A., Silva, S.O., 1949. Relatório preliminar sobre a geologia da Bacia do Maranhão. Boletim do Conselho Nacional do Petróleo 1, 1-160.

Casanova, J., Hillaire-Marcell, C., 1993. Carbon and oxygen isotopes in African lacustrine stromatolites: palaeohydrological interpretation. In: Swart, P.K., Lohmann, K.C., McKenzie, J., Savin, S. (Eds.), Climate Change in Continental Isotopic Record. Geophys. Monogr., Am. Geophys. Union, 94, 123-133.

Craig, H., 1965. The measurement of oxygen isotope palaeotemperatures. In: Tongiorgi (Ed), Stable Isotopes in Oceanographic Studies and Palaeotemperatures. Cons. Naz. Rich. Lab. Geol. Nucl., Pisa, pp. 9-130.

Charisi, S.D., Schmitz, B., 1995. Stable (^{13}C, ^{18}O) and strontium (^{87}Sr/^{86}Sr) isotopes through the Paleocene et Gebel Aweina, eastern Tethyan region. Palaeogeog., Palaeoclim., Palaeoecol. 116, 103-129.

Deines, P., 1980. The isotopic composition of reduced organic carbon. In: Fritz, P.J., Fontes, J. (Eds.), Handbook of Environmental Isotope Geochemistry: v.1, Terrestrial Environment. Elsevier, Amsterdam, pp. 329-406.

Eicher, U., Siegenthaler, U., 1976. Palynological and oxygen isotope investigations on Late-Glacial sediment cores from Switzerland. Boreas 5, 109-117.

Friedman, I., O'Neill, J.R., 1977. Compilation of stable isotope fractionation factors of geochemical interest. In: Fleischer, M. (Ed.), Data of Geochemistry. Geological survey Prof. Paper 440-KK, U.S. Gov. Print. Office, Washington, pp. 1-12.

Fritz, P., Anderson, T.W., Leqis, C.F.M., 1975. Late Quaternary trends and history of Lake Erie from stable isotope studies. Science 190, 267-269.

Gasse, F., Fontes, J.C., Plaziat, J.C., Carbonel, P., Kaczmarska, I., De Decker, P., Soulié-Marsche, I., Callot, Y., Depeuble, P.A., 1987. Biological remains, geochemistry and stable isotopes for the reconstruction of environmental and hydrological changes in the Holocene lakes from north Sahara. Palaeogeog., Palaeoclim., Palaeoecol. 60, 1-46.

Gasse, F., Lédée, V., Massault, M., Fontes, J.C., 1989. Water-level fluctuations of Lake Tanganyika in phase with the oceanic changes during the last glaciation and deglaciation. Nature 342, 57-59.

Gat, J.R., 1980. The isotopes of hydrogen and oxygen in precipitation. In: Fritz, P.J., Fontes, J. (Eds.), Handbook of Environmental Isotope Geochemistry: v.1, Terrestrial Environment. Elsevier, Amsterdam, pp. 21-47.

Gat, J.R., 1984. The stable isotope composition of Dead Sea waters. Earth Planet. Sci. Lett. 71, 361-376.

Góes, A.M., Rossetti, D.F., 2001. Gênese da Bacia de São Luís-Grajaú. In: Rossetti, D.F., Góes, A.M., Truckenbrodt, W. (Eds.), O Cretáceo na Bacia de São Luís Grajaú. Museu Paraense Emilio Goeldi, Coleção Friedrich Katzer, Belém, pp. 15-29.

Goldhammer, R.K., Dunn, P.A., Hardie, L.A., 1990. Depositional cycles, composite sea-level changes cycle stacking patterns, and hierarchy of stratigraphic forcing: examples from Alpine Triassic platform carbonates. Geol. Soc. Am. Bull. 102, 535-562.

Hendry, J.P., Kalin, R.M., 1997. Are oxygen and carbon isotopes of mollusc shells reliable palaeosalinity indicators in marginal marine environments? A case study from Middle Jurassic of England. J. Geol. Soc. London 154, 321-333.

Herczeg, A.L., 1988. Early diagenesis of organic matter in lakes sediments: a stable carbon isotope study of pore waters. Chem. Geol. 72, 199-209.

Herczeg, A.L, Leaney, F.W., Dighton, J.C., Lamontagne, S., Schiff, S.L., Telfer, A.L., English, M.C., 2003. A modern isotope record of changes in water and carbon budgets in a groundwater-fed lake: Blue Lake, South Australia. Limnol. Oceanogr. 48, 2093-2105.

Hillaire-Marcell, C., Casanova, J., 1987. Isotopic hydrology and paleohydrology of the Magadi (Kenya)-Natron (Tanzania) basin during Late Quaternary. Paleogeog., Paleoclim., Paleoecol. 58, 155-181.

Hoefs, J., 1980. Stable Isotope Geochemistry. 2nd Ed. Springer-Verlag, Berlim, 208 pp.

Hofmann, A., Tourani, A., Gaupp, R., 2000. Cyclicity of Triassic to lower Jurassic continental red beds of the Argana Valley, Morocco: implications for paleoclimate and basin evolution. Palaeogeogeog., Palaeoclim., Palaeoecol. 161, 229-266.

Holland, H.D., 1978. The Chemistry of the Atmosphere and Oceans. Wiley-Interscience, New York, 351 pp.

Holmes, J.A., Street-Perrott, F.A., Allen, M.J., Fothergill, P.A., Harkness, D.D., Kroon, D., Perrott, R.A., 1997. Holocene palaeolimnology of Kajemarum Oasis, Northern Nigeria: an isotopic study of ostracodes, bulk carbonate and organic carbon. J. Geol. Soc. London 154, 311-319.

Ingram, B.L., Ingle, J.C., Conrad, M.E., 1996. A 2000-yr record of Sacaramento-San Joaquin River inflow to the San Francisco Bay estuary, California. Geology 24, 331-334.

In Sung, P., Kim, H.J., 2003. Palustrine calcretes of the Cretaceous Gyeongsang Supergroup, Korea: Variation and paleoenvironmental implications. The Island Arc 12, 110-124.

Janaway, T.M., Parnell, J., 1989. Carbonate production within the Orcadian Basin, northern Scotlabd: a petrographic and geochemical study. In: Talbot, M.R., Kelts, K (Eds.), The Phanerozoic Record of Lacustrine Basins and their Environmental Signals. Palaeogeogr. Palaeoclimatol. Palalaeoecol. 70, 89-105.

Johnson, T.C., Halfman, J.D., Showers, W.J., 1991. Paleoclimate of the past 4000 years at Lake Turkana, Kenya, based on the isotopic composition of authigenic calcite. Palaeogeog., Palaeoclim., Palaeoecol. 85, 189-198.

Jones, C.E., Jenkins, H.C., 2001. Seawater strontium isotopes, oceanic anoxic events, and seafloor hydrothermal activity in the Jurassic and Cretaceous. Am. J. Sci. 301, 112-149.

Katz, A., Y. Kolodny, A. Nissenbaum, 1977. The geochemical evolution of Lake Lisan– Dead Sea system: Geochim. Cosmochim. Acta 41, 1609-1626.

Kirkland, D.W., Evans, R., 1981. Source-rock potential of evaporitic environment. AAPG Bull. 65, 181-190.

Kelts, K., Talbot, M., 1990. Lacustrine carbonates as geochemical archives of environmental change and biotic/abiotic interactions. In: Tilzer, M.M., Serruya, C. (Eds.), Large lakes: Ecological Structure and Function. Brock/Springer Series in Contemporary Bioscience, Springer-Verlag, pp. 288-315.

Lima, M.R., 1982. Palinologia da Formação Codó, Maranhão. Boletim do Instituto de Geociências-USP 13, 116-128.

Lima, M.R., Fulfaro, V.J., Bartorelli, A., 1980. Análise palinológica de sedimentos cretáceos da região de Marabá, Estado do Pará. Boletim do Instituto de Geociências, USP 11, 55-161.

Lister, G.S., Kelts, K., Chen, K.Z., Yu, J.-Q., Niessen, F., 1991. Lake Qingai, China: closed-lake basin levels and the oxigen isotope record for ostracoda since the latest Pleistocene. Palaeogeogr., Palaeoclimatol., Palaeoecol. 84, 141-162.

Martel, A.T., Gibling, M.R., 1991. Wave-dominated lacustrine facies and tectonically controlled cyclicity in the Lower Carboniferous Horton Bluff Formation, Nova Scotia Canada. In: Anadón, P., Cabrera, Ll., Kelts, K. (Eds.), Lacustrine Facies Analysis. Int. Ass. Sediment. Spec. Publ. 13, 223-244.

McKenzie, J.A., 1985. Carbon isotopes and productivity in the lacustrine and marine enviroment. In: Stumm, W. (Ed.), Chemical Processes in Lakes. Wiley, New York, pp. 99-118.

Mesner, J.C., Wooldrigde, L.C.P., 1964. Maranhão Paleozoic Basin and Cretaceous coastal basins, north Brazil. AAPG Bull. 48,1475-1512.

Olsen, P.E., 1986. A 40-million-year lake record of Early Mesozoic orbital climatic forcing. Science 234, 842-848.

Olsen, P.E., Kent, D.V., 1996. Milankovitch climate forcing in the tropics of Pangea during the Late Triassic. Palaeogeog., Palaeoclim., Palaeoecol. 122, 1-26.

Paz, J.D.S., Rossetti, D.F., 2001. Reconstrução paleoambiental da Formação Codó (Aptiano), borda leste da Bacia do Grajaú, MA. In: Rossetti, D.F., Góes, A.M., Truckenbrodt, W. (Eds.), O Cretáceo na Bacia de São Luís-Grajaú. Museu Paraense Emilio Goeldi, Coleção Friedrich Katzer, Belém, pp. 77-101.

Paz, J.D.S., Rossetti, D.F., submitted. Tectonically-driven lacustrine cycles: an example from the Codó Formation (Late Aptian), northeastern Brazil. Geol. Mag.

Rezende, W.M., Pamplona, A.H.R.P., 1970. Estudo do desenvolvimento do Arco Ferrer-Urbano Santos. PETROBRAS, Boletim Técnico 13, 5-14.

Rodrigues, R., 1995. A geoquímica Orgânica na Bacia do Parnaíba. Doctoral Thesis, Universidade Federal do Rio Grande do Sul, Porto Alegre, 225 p.

Rosenmeier, M.F., Hodell, D.A., Brenner, M., Curtis, J.H., Guilderson, T.P., 2002. A 4000-year lacustrine record of environmental change in the Southern Maya Lowlands, Petén, Guatemala. Quaternary Res. 57, 183-190.

Rossetti, D.F., 2001. Arquitetura deposicional da Bacia de São Luís-Grajaú, meio norte do Brasil. In: Rossetti, D.F., Góes, A.M., Truckenbrodt, W. (Eds.), O Cretáceo na Bacia de São Luís Grajaú. Museu Paraense Emilio Goeldi, Coleção Friedrich Katzer, Belém, pp. 31-46.

Rossetti, D.F., Góes, A.M., 2000. Deciphering the sedimentological imprints of paleoseismic events: an example from the Codó Formation, northern Brazil. Sediment. Geol. 135, 137-156.

Rossetti, D.F., Truckenbrodt, W., 1997. Classificação estratigráfica para o Albiano-Terciário Inferior (?) na Bacia de São Luís, MA. Boletim do Museu Paraense Emílio Goeldi (Série Ciências da Terra) 9, 31-43.

Rossetti, D.F., Paz, J.D., Góes, A.M., in press. Facies analysis of the Codó Formation (Late Aptian) in the Grajaú area, southern São Luís-Grajaú Basin. An. Acad. Bras. Cien.

Rossetti, D.F., Truckenbrodt, W., Santos-Júnior, A.E., 2001. Clima do Cretáceo no Meio-Norte brasileiro. In: Rossetti, D.F., Góes, A.M., Truckenbrodt, W. (Eds.), O Cretáceo na Bacia de São Luís Grajaú. Museu Paraense Emilio Goeldi, Coleção Friedrich Katzer, Belém, pp. 67-76.

Rossetti, D.F., Paz, J.D., Góes, A.M., Macambira, M., 2000. A marine versus non-marine origin for the Aptian-Albian evaporites of the São Luís and Grajaú basins, Maranhão state (Brazil) based on sequential analysis. Rev. Bras. Geoc. 30, 642-645.

Russell, J.M., Johnson, T.C., Talbot, M.R. 2003. A 725-yr cycle in the climate of Central Africa during the Late Holocene. Geology 31, 677-680.

Scotese, C.R., Gahagan, L.M., Larson, R.L., 1989. Plate tectonic reconstructions of the Cretaceous and Cenozoic ocean basins. In: Scotese, C.R., Sager, W.W. (Eds.), Mesozoic and Cenozoic Plate Reconstructions, Elsevier, Amsterdam, pp. 22-48.

Smoot, J.P., Olsen, P.E., 1994. Climatic cycles as sedimentary controls of rift-basin lacustrine deposits in the Early Mesozoic Newark Basin based on continuous core. In: Lomando, A.J., Schreiber, B.C., Harris, P.M. (Eds.) Lacustrine Reservoirs and Depositional Systems. SEPM Core Workshop, 19, 239-295.

Steenbrink, J., Van Vugt, N, Kloosterboer-Van Hoeve, M.L., Hilgen, F.J., 2000. Refinement of the Messinian APTS from sedimentary cycle patterns in the lacustrine Lava section (Servia Basin, NW Greece). Earth Planet. Sci. Lett. 181, 161-173.

Stiller, M., Hutchinson, G.E., 1980. The waters of Meron: a study of Lake Huleh, 1. Stable isotopic composition of carbonates of 54 m core: paleoclimatic and paleotrophic implications. Arch. Hydrobiol. 89, 275-302.

Stiller, M., Rounick, J.S., Shasha, S., 1985. Extreme carbon-isotope enrichments in evaporating brines. Nature 316, 434-435.

Stuiver, M., 1970. Oxygen and carbon isotope ratios of fresh-water carbonates as climatic indicator. J. Geophys. Res. 75, 5247-5257.

Tan, F.C., Hudson, J.D.,1974. Isotopic studies on the palaeoecology and diagenesis of the Great Estuarine Series (Jurassic) of Scotland. Scottish J. Geol. 10, 91-128.

Talbot, M.R., 1990. A review of the paleohydrological interpreatation of carbon and oxygen isotopic ratios in primary lacustrine carbonates. Chem. Geol. 80, 261-279.

Talbot, M.R., Kelts, K., 1990. Paleolimnological signatures from carbon and oxygen isotopic ratios in carbonates from organic carbon-rich lacustrine sediments. In: Katz, B.J. (Ed.), Lacustrine Basin Exploration: Case Studies and Modern Analogs. AAPG Memoir 50, 99-112.

Tucker, M.E., Wright, V.P., 1990. Carbonate Sedimentology. Blackwell Science, Oxford, 482 pp.

Turner, J.V., Fritz, P., Karrow, P.F., Warner, B.G., 1983. Isotopic and geochemical composition of marl lake waters and implications for radiocarbon dating of marl lake sediments. Can. J. Earth Sci. 20, 599-615.

Urey, H.C. 1947. The thermodynamic properties of isotopic substance. Geochim. Cosmochim. Acta 48, 562-581.

Valero-Garcés, B.L., Kelts, K., Ito, E., 1995. Oxigen and carbon isotopes trends and sedimentological evolution of a meromictic and saline lacustrine system: the Holocene Medicine Lake basin, North American Great Plains, USA. Palaeogeogr., Palaeoclimatol., Palaeoecol. 177, 253-278.

Warren, J. K., 1999. Evaporites: Their Evolution and Economics: Blackwell Scientific, Oxford, 438 pp.

6. CONCLUSÕES GERAIS

1. A Formação Codó consiste em depósitos dominantemente continentais nas áreas estudadas, onde se distinguem dois contextos deposicionais: a) lagos estáveis, bem estratificados e salinos, com períodos de fechamento e conseqüente anoxia do sistema prevalecendo na margem leste da Bacia de São Luís-Grajaú, com evaporitos restritos à porção central nas partes mais profundas da bacia lacustre; e b) complexos de *sabkha/saline pan* na porção sul da Bacia de São Luís-Grajaú, onde as condições climáticas e/ou tectônicas favoreceram o desenvolvimento de lagos efêmeros, com a formação de extensas planícies de lama contendo abundante precipitação de evaporitos centrada nas partes marginais do sistema;

2. A Formação Codó na área de estudo depositou-se de forma cíclica, formando ciclos de arrasamento ascendente, interpretados como registro de períodos de expansão e contração do sistema lacustre-sabkha-*saline pan*, gerados por flutuações climáticas e tectônicas;

3. Ciclos climáticos foram revelados por diversos pares milimétricos de fácies deposicionais, arranjados em estilo semelhante a varves;

4. Ciclos tectônicos foram revelados por: a) alta variabilidade de fácies; b) limitada extensão lateral dos ciclos; c) mudanças aleatórias na espessura e freqüência dos ciclos; e d) correspondência com zonas de deformação sísmica sindeposicional;

5. O Sr mostrou-se como um parâmetro paleoambiental sensível, registrando valores muito distintos daqueles esperados para águas marinhas neoaptianas;

6. Os valores de Sr também tiveram boa correlação com os ciclos deposicionais de menor freqüência (i.e., ciclos de ordem superior), sendo sua variação atribuída a períodos de contração e expansão da bacia lacustre;

7. O S mostrou-se menos sensível como indicador paleoambiental. Embora os valores sejam condizentes com salmoura de origem continental na área de Codó, isto não se repetiu na área de Grajaú, onde os valores diferem em uma faixa mais ampla do que aquela esperada em ambientes com influência continental. É possível que os valores de S distintos entre as duas áreas estudadas estejam refletindo variações nas condições de oxigenação do sistema deposicional, com valores maiores na área de Codó, onde condições anóxicas prevaleceram, incentivando a proliferação de bactérias sulfato-redutoras que influenciaram fortemente o fracionamento do S e deixaram o sulfato residual da água do lago enriquecido preferencialmente em ^{34}S.

8. Este trabalho demonstrou que flutuações nas taxas de subsidência, causadas por atividade sísmica sin-sedimentar pode responder por variações nos valores dos isótopos de C e O muito semelhantes àquelas observadas em sucessões resultantes formadas por flutuações de ordem climática;

9. Diferentes estilos e/ou intensidades de pulsos sísmicos, alternados com deposição sedimentar, causam mudanças no nível do lago e promovem períodos de inundação e dessecação do sistema deposicional durante episódios de estiramento e compressão, respectivamente. A deposição de carbonatos com valores de $\delta^{13}C$ e $\delta^{18}O$ preferencialmente mais leves, associada com a instalação preferencial de lagos perenes na fase de inundação, e de valores de $\delta^{13}C$ e $\delta^{18}O$ mais pesados, associados com a instalação de lagos efêmeros durante dessecação, foram bem marcantes no ciclos de ordens intermediária e superior.

10. A análise de fácies detalhada e o mapeamento de padrões de empilhamento estratal são a chave para a interpretação de sucessões progradantes como no caso da Formação Codó. A combinação deste tipo de informações com dados isotópicos de C, O, Sr e S propicia interpretações mais refinadas de sistemas deposicionais continentais onde ocorrem depósitos de evaporitos e calcários. Além disto, este tipo de integração possibilita a disponibilização de informações visando-se reconstituir condições paleohidrológicas do sistema deposicional e dos fatores controladores de sua evolução.